Application of Strain Gage Technology in Low Flow Stream Monitoring

By

Kevin L. Boerma

A Thesis Submitted to the Faculty of the

DEPARTMENT OF CHEMICAL AND ENVIRONMENTAL ENGINEERING

In Partial Fulfillment of the Requirements
For the Degree of

MASTER OF SCIENCE
WITH A MAJOR IN ENVIRONMENTAL ENGINEERING

In the Graduate College

THE UNIVERSITY OF ARIZONA

2000

20000627 141

STATEMENT BY AUTHOR

This thesis has been submitted in partial fulfillment of requirements for an advanced degree at The University of Arizona and is deposited in the University Library to be made available to borrowers under rules of the Library.

Brief quotations from this thesis are allowable without special permission, provided that accurate acknowledgment of source is made. Requests for permission for extended quotation from or reproduction of this manuscript in whole or in part may be granted by the head of the major department or the Dean of the Graduate College when in his or her judgment the proposed use of the material is in the interests of scholarship. In all other instances, however, permission must be obtained from the author,

SIGNED: _____

APPROVAL BY THESIS DIRECTOR

This thesis has been approved on the date shown below:
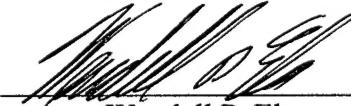
_____   05/11/00
Wendell P. Ela   Date
Assistant Professor of
Environmental Engineering

ACKNOWLEDGMENTS

I would like to take an opportunity to thank all those that have made this possible. Your hard work and dedication are greatly appreciated. I could not have done it without you. I'd like to especially thank Jen Hafer for her mentoring during the first term to help bring me up to speed. Also special thanks to Elaine, Mark, Chad, Matt, Karen, Sunil, Krista, Mike, Jiahan, Tim, Roger, Dr. Conklin and others for their support during the past two years at the University of Arizona.

I would also like to especially thank my advisor, Dr. Wendell Ela. He made this journey as enjoyable as possible with his dedication and encouragement. His assistance and patience were critical in the success of this project. I couldn't imagine a better advisor to work with than him. Thank you very much!

Last but not least, I owe my wife, Melissa, a tremendous amount of love and gratitude. She supported me though the stressful times at school, which seemed almost constant during the past two years. She worked diligently on getting our house ready for sale while I was finishing up this project and the Air Force was moving us to a new location. She is special and I am lucky to have her in my life. I love you!!!

TABLE OF CONTENTS

LIST OF ILLUSTRATIONS

LIST OF TABLES

ABSTRACT

Streamflow in natural channels is commonly studied for reasons varying from quantifying available water resources to ascertaining the impact of pollution on riparian systems. The accurate knowledge of flow rates with high temporal resolution is particularly important in environmental engineering studies so that mass balances can be determined for geochemical monitoring and modeling. Such studies, as well as beneficial use studies, require an understanding of the stream's hydrological changes on time scales from minutes to years. However, these studies in low velocity (<1.5 ft/s) streams are severely limited due to the lack of available flow meter technology. Currently, there is no low cost, portable, low flow meter available. This project involves the design, construction, and testing of two flow meter designs (a surface and subsurface design) which address this deficiency. The meters use strain gage technology to measure the velocity variation across a cross-sectional stream profile. Field and calibration experiments were conducted to determine the best design and also to evaluate the flow meters' accuracy, repeatability, usability, and range. The study found that the surface velocity meter design was much easier to use, but the subsurface design, which measured velocity at various depths, was considered to have better repeatability and accuracy. The results of this study show flow meters based on strain gage technology may provide an inexpensive, accurate and simple means to monitor flow rates in low velocity streams.

CHAPTER 1. INTRODUCTION

One of the fundamental parameters characterizing a stream or river is the measurement of its flow. Stream flow is defined as the amount of water that moves past a reference point in a given amount of time. It is usually expressed in units of m^3/sec or ft^3/sec.

There are several reasons why it is often important to quantify the amount of water flowing in a stream. It is significant in determining mass balances for general water quality, including pollution discharge effects. Since nearly all chemical testing measures the concentration of a pollutant species, it is only by combination of this measurement with a flow rate measurement that a knowledge of the actual mass of pollutant can be ascertained. For example, a low flow stream may be uninhabitable for living organisms due to higher contaminant concentrations than if a similar source discharged into a high flow stream. Knowledge of flow rate and velocity are also important in understanding the potential to keep suspended contaminants mobile in a waterway and, therefore, to estimate the contaminant transport to downstream lakes and larger rivers. Flow measurements are also important in determining hydrological changes. The measurements can verify gaining and losing regions of a stream and assist in the general understanding of a stream's dynamics. The other obvious need for flow measurements is to quantify the amount of water available for irrigation or drinking water use.

The flow in a stream is affected by several factors. Rainstorms, irrigation systems, dams, evaporation and water removal by adjacent vegetation can influence stream flows over daily, monthly and even annual periods. Flow variations on a daily scale can occur due to evapotranspiration and daily temperature fluctuations. The variations on the

monthly scale are usually related to seasonal variations, and flow rates on annual timescales vary due to major storm and flood events.

Flow is a function of the stream's cross-sectional area and its velocity. To obtain quality flow measurements in a stream is a challenging task. Streams have widely varying characteristics, many which make measurement very difficult. They can be heavily vegetated, have varying depths, be located in remote areas, have significantly unique cross-sectional areas and flow variations, etc.

Traditional flow meters and flow meter methods often provide minimal assistance in studying remote areas. Current meters and techniques are often not practical or are inaccurate due to low flows, inadequate for multiple stream placement and non-continuous readings, too expensive, or require significant alteration of the natural stream flow for their operation and installation.

The limitations of the available flow monitors become apparent when studying mining-contaminated streams in Arizona. Mining has been a major industry in several areas of Arizona. The mine tailings are still a significant pollution source for many of the streams that transverse the countryside. These streams are often considered low flow, and thus, the mining waste, which is high in metals and acidic, can significantly alter a stream's natural state. These stream waters often carry high metals concentration from direct and indirect contact with the mining wastes. Metals are deposited in the stream sediments causing a real and potential source of long term contamination. There is also a significant potential for these streams to provide toxic metals to the larger downstream

lakes and rivers that they feed. Therefore, studies of the flows and pollution levels in these streams are of important concern to our environment.

In order to quantify the environmental impact of the surface water contamination, a knowledge of the temporal variation of both stream flow rate and chemical composition is required. If either of these measurements is missing, then the actual pollutant flux can not be determined. However, typically the flow rate can only be determined at a few, widely spaced positions or by estimation from spot main channel velocity measurements without correlation to changing bed form and vegetation impacts.

CHAPTER 2. BACKGROUND AND LITERATURE REVIEW

2.1 Current Technology and Limitations

Current technology includes two basic types of flow meter devices. There are meters that measure pressure (or head) and meters that measure velocity to determine flows. Examples of pressure (or head) measuring devices are weirs, flumes, orifices and venturi meters. Velocity measuring devices include a float and stopwatch, anemometer and propeller meters, Doppler velocity meters, and optical strobe velocity meters. These devices are often limited in stream studies due to low flows, high cost, or when implemented, they significantly disturb a stream bed or natural stream pathway. Some are limited by the frequency of measurements over a given time period. Others must apply one velocity measurement across a stream's cross-sectional area.

There are several important factors in determining if a device is the best for a particular site. Factors to consider include a flow meter's accuracy and repeatability, its portability, its initial, operational, and maintenance costs, and its range. For example, a site located on a mountainside and a few miles from accessible vehicle paths with no electrical power source would need a meter that was lightweight and powered by long life batteries. The meter might also need to measure large variations in flow rates and be adequately protected to operate effectively during a monsoon storm event or on days when mountain snows are melting creating significant stream flow. Another type of meter might be chosen for an area with consistently steady high flows in a channel that is

well defined without vegetation. A third meter would be chosen for a site that required very accurate measurements and could be permanently stationed in a narrow channel.

Accuracy is one of the most important factors when choosing a flow meter device. It is the ability of a meter to provide values that are within a close range of the true value. Different flow monitoring situations vary in accuracy requirements. For example, a water utility company requires accurate measurements prior to billing its customers for their usage. In stream monitoring, acceptable accuracy may be +/- 20% or higher (1) due to the potential complexities of this system. Also note that different meters are accurate over different flow ranges. A weir can be designed to be accurate over a large flow range depending on the size of the weir design. Certain velocity meters are only accurate for higher flow conditions due to measurement interference noise at low flows. Along with accuracy, repeatability is important over a reasonable service life. A meter needs to be able to repeat its performance within a specific error percentage.

Depending on the application, the meter's monitoring range is important. The ability of a meter to monitor a large range of flow rates can be extremely useful in situations where several streams are being studied or if wide variations of flow rates occur in a particular stream. During a storm event, a significant flow variation in a stream can occur. If a study involves the effects of these events on a stream, an optimal flow meter would need a large flow range to cover both the periods of lower flow and of the storm event flow.

Of course, comparative cost is important. Depending on whether a meter is portable or fixed, the cost can vary tremendously. Often battery-powered equipment is required in

remote areas, but if it is not, electric powered may be easier and cheaper to implement. Installation, maintenance and operating costs are all factors that need to be analyzed. Meters are usually considered more favorably if they have few or no moving parts. Fewer moving parts often implies that the meter is more rugged and has a longer service life.

Often in environmental flow monitoring applications, the flow meter has to be approved by a governing body, i.e. the EPA (2). The main reasons that this is required are to ensure that the monitoring device does not change or damage the basic environmental conditions of a system and that the device produces consistent results. An example of a device changing a natural stream system is a weir since it would reduce the stream's naturally occurring flow movement. It would also create a ponding effect immediately behind the structure. These situations could lead to results in studies (i.e., of bed form, vegetation type) that would not naturally take place (3, 4 and 5).

2.2 Head (or pressure) Monitoring Devices

Head (or pressure) monitoring equipment generally require more permanent structures and, in a stream, often alter the natural condition of the stream. The siting for these types of devices needs to be located in a constricted section of the stream since the water usually needs to flow across or through the monitoring device structure. These meters are variable in cost and ease of installation based on the control requirements for this constriction. They are almost impractical for very remote locations due to construction requirements. The measuring gages can usually be continuous and electrical or battery-powered depending on the requirement. Several of these flow meters are

usually considered very accurate over a wide flow range when correctly designed and implemented (6).

2.3 Velocity Measuring Devices

The velocity meter requires knowledge of the cross-sectional area of the water that is monitored. The flow is simply equal to the velocity multiplied by the cross-sectional area over which it acts. In a stream, it is often more complicated than just one velocity over the entire cross-sectional area. Depending on its depth, vegetation, and base surface, a stream's velocity rate can vary widely across its cross-sectional area (7). It has always been important in flow monitoring to minimize these effects by selecting the best monitoring locations along a stream path.

2.3.1 Types of Velocity Measuring Devices and Selection Criteria

Current velocity meters vary significantly in portability, accuracy, range, and cost. The simplest flow method is the float and stopwatch method. The EPA volunteer flow monitoring program uses this method (8). The method is simple and cheap. An orange, or similar object, is dropped into a stream and timed over a specific distance. Distances of 20 feet or greater are recommended. A minimum of repeating this task at least three times is also recommended to obtain an average surface velocity. The surface velocity is then multiplied by a coefficient to estimate an average cross-sectional area velocity. The coefficient takes into account that the surface velocity travels faster than near the stream bottom and gives an overall average velocity. A coefficient of 0.8 is recommended for rocky-bottom stream beds and 0.9 for muddy-bottom stream beds. This method has some drawbacks when studying a stream. It is not easy to continually monitor the flow without

significant disturbance of the stream and significant manpower. Vegetation can also play a significant role in the ease of monitoring and the availability of a 20-foot stream length to monitor. This method also estimates one flow over the entire cross-sectional area, which is often inaccurate, if the stream's bed, depth, or vegetation density varies significantly over its cross-section.

Another type of velocity measurement meter includes the anemometer and propeller meters. These meters use cup wheels or propellers to sense velocity. This technique has been shown to be accurate to within +/- 5% in flows (9). It is also very portable and could be used to estimate separate flows across a cross-sectional area. A major drawback with this meter is that it is not accurate in flows less than 1.5 ft/sec in open channels (10). Streams, which are open channels, often have flow rates of less than 1.0 ft/sec. The use of this type of meter would be impractical if separate flow measurements are taken across the cross-sectional area of a low flow stream, especially with vegetation effects. The propeller-type meters are prone to inaccuracy and damage by suspended debris and vegetation and must be frequently inspected to maintain operation.

There are other flow meters that can be used but portability, cost, and limited multiple cross-sectional velocity measurements are significant drawbacks. The meters include an electromagnetic current meter, which creates voltages proportional to the flow velocity (11). These could provide continual readings but are not extremely reliable with current technology and are primarily suited to pipe or constricted channel flow. The Doppler type current meter can measure the change of source light or sound frequency from the frequency of reflections from moving particles in the stream to calculate a velocity. An

optical strobe velocity meter is also being used. It uses a strobe effect. Light reflected from the water surface is reflected into a series of lenses and focused through a lens piece. A rotating drum in the system can be adjusted so that the image appears steady. Based on this rotation, the surface velocity of the stream can be obtained. All of these meters are expensive and typically unsuitable for normal natural stream application due to extremely limited portability.

There are other factors that could determine if a flow meter is suitable for a task. The meter may need to easily pass sediment and debris depending on a stream's natural state. The flow might be significantly restricted by the meter's operation, which could decrease the sensitivity of the meter at low flow rates. Also, calibration must be easily achieved and standardization of the calibration is very useful.

2.3.2 Application of Velocity Measuring Devices

The vertical velocity profile changes in a stream spatially. The surface velocity is faster than the velocity near the bottom of the stream. This is due to the surface resistance of the stream bed. The resistance can vary depending on the roughness of the stream bed and various coefficients are applied to obtain an average velocity over an applicable cross-sectional stream area per the EPA method. Vegetation can also provide resistance and slow down the velocity, which increases the potential error in assigning coefficients under this condition.

There are several techniques to obtain average vertical velocity; not all include a coefficient multiplied by the surface velocity. The techniques include a two-point method, a sixth-tenths depth method, a vertical velocity-curve method, a subsurface

method, a depth integration method, a two-tenths method, a three-point method and a one-point continuous method (12). These methods are discussed below.

- Two-point method: Measure the velocity at 0.2 and at 0.8 of the water depth and use the average of these two measurements as the average velocity. It is considered highly accurate for stream depths greater than or equal to 2 feet.

- Six-tenths depth method: Measure the velocity at 0.6 of the water depth and use this as the average velocity. Its accuracy is considered satisfactory and can be used in shallow streams.

- Vertical velocity-curve method: Measure the velocity at multiple vertical depths to obtain a profile to determine the mean velocity. It is considered very accurate but it takes a significant amount of time and therefore cost.

- Subsurface method: Measure the velocity just below the water surface and multiply it by a coefficient ranging from 0.85 to 0.95 depending on the water depth, velocity, and bed surface characteristics. No further reference or assistance was referenced on assigning this coefficient, but the reference did state that the coefficient determination limits the accuracy and usefulness of this method.

- Depth integration method: Observe the velocity along a vertical line in the stream by raising a velocity meter to obtain two or more readings and average the recorded velocities. This method is not considered accurate and is only used for rough, quick velocity estimates.

- The two-tenths, three-point and one-point continuous methods: These methods require previously established relationships between true flow rates and the velocities

obtained by the method. These are accurate assuming no change from established relationship such as erosion or sedimentation. Storm events would eliminate these methods from effectively being used in many streams until the relationship between flow rate and the velocity at a fixed depth is reestablished.

There are several features of a stream that can significantly impact a meter's response. These need to be addressed when determining the location to set up the monitoring stations. The approach flow just upstream of the monitoring location needs to be as smooth as possible. The longer and straighter that the channel is ensures the measured results are accurate. Turbulence, rough water surface and poor flow patterns may significantly impair the measurement's accuracy. The stream bed and vegetation influence these parameters greatly. The effects of these need to be minimized to the maximum extent possible when choosing the location.

2.3.3 Basic Theory of Strain Gages

Strain gages have been used for several years to relate strain to stress on a material. Figure 2.1 shows a typical strain gage. It can be used to measure a normal stress (force applied in the same direction as the material changes) or a shear stress (force applied at a 90 degree angle to change the material). For the purposes of this topic, normal stress is applicable.

A strain gage consists of a pattern of wire lengths in one direction embedded in a thin flat mounting material. As the mounting material bends in the established direction, the wires are stretched or compressed in proportion to the amount of bending. The electrical resistance of the patterned strain gage wire changes in proportion to the degree of tension

(stretching) or compression. Thus, the stress of the gage is measurable as the resistance of the embedded wire pattern to electrical current.
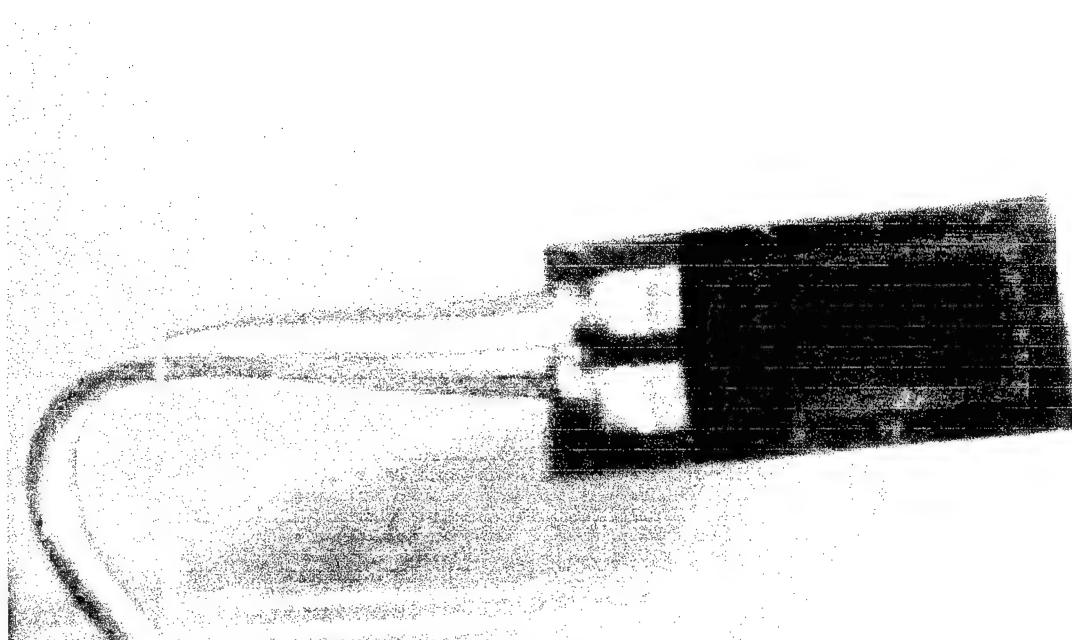
Figure 2.1 A Typical Strain Gage (approximate scale 13:1)

Strain gages are often connected in a full wheatstone bridge circuit to increase the gage's overall sensitivity. This means that four strain gages are attached to the material that is subjected to a normal stress. Two of the strain gages are attached to the backside of the bending material so they are in compression. The other two gages are attached to the front side of the material and are in tension when the material bends. Quarter and half wheatstone bridge circuits can be used but are not as sensitive as the full bridge. Figures 2.2 shows diagrams of a wheatstone bridge circuit and the front and back sides of the

neck of a meter with strain gages attached. It also shows a side view of the neck bending

under an applied force.

A generic wheatstone bridge circuit output voltage, E_o, can be expressed as:

$$E_o = E (R_1/(R_1+R_2) - R_4/(R_3+R_4)), \qquad \text{(Eqn 2-1)}$$

where E is the input voltage and R_1-R_4 are gage resistances as shown in Fig 2.

The equation is often written as:

$$E_o/E = R_1/(R_1+R_2) - R_4/(R_3+R_4). \qquad \text{(Eqn 2-2)}$$

If the bridge is balanced and no output voltage is produced,

$$R_1/(R_1+R_2) = R_4/(R_3+R_4). \qquad \text{(Eqn 2-3)}$$

Altering resistances from the zero state will produce corresponding output voltages.

For measuring stream velocity, the strain gages are attached in a wheatstone bridge

pattern to a frame (neck/paddle combination) that would bend under the force caused by a

stream's velocity. The strain gages would then measure this force by changing their

resistance proportional to the bending of the neck portion of the frame. The motivation

for this project is that the resistance change can be monitored and calibrated to provide

useful data on a stream's velocity via the bending produced in a submerged paddle.

This work is not the first use of strain gage technology for environmental flow

measurements. Paul A. Roland (1996) developed a strain gage based device to measure

very low flows, three-dimensionally in a lake (13). His work indicated that monitoring

low flows using strain gages was possible and this work extends and modifies that effort

to application in low velocity stream flows.

Wheatstone Bridge Circuit

Front View   Back View   Side View
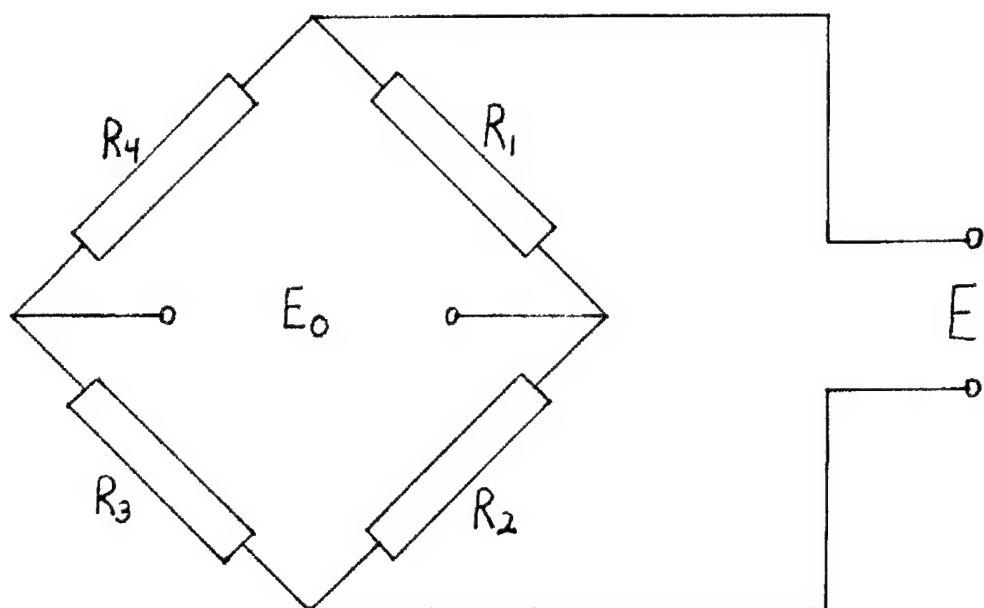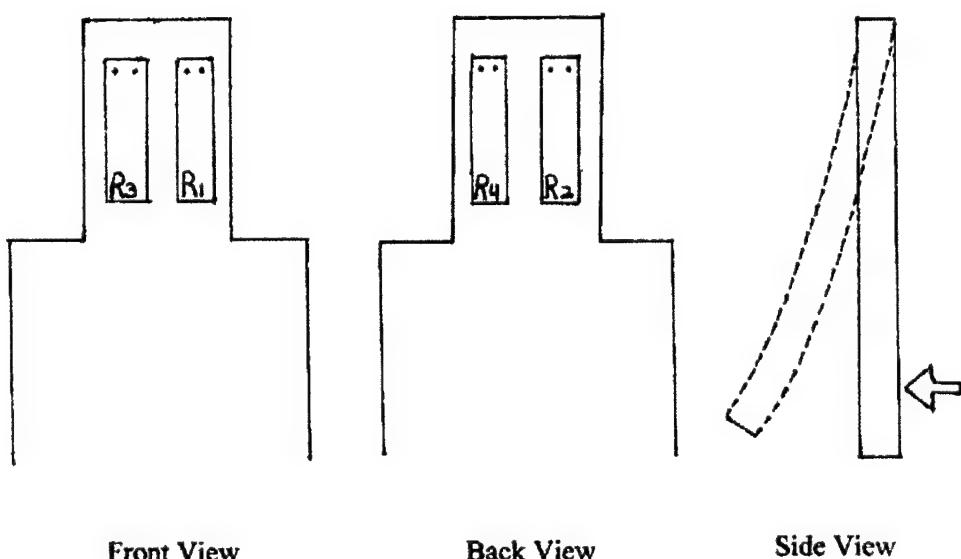
Figure 2.2 Diagram of Wheatstone Bridge Circuit and Diagram of Meter's Neck Region
Showing Strain Gage Locations and Neck Deformation.

CHAPTER 3. METHODS AND MATERIALS

3.1 Design #1 Meter
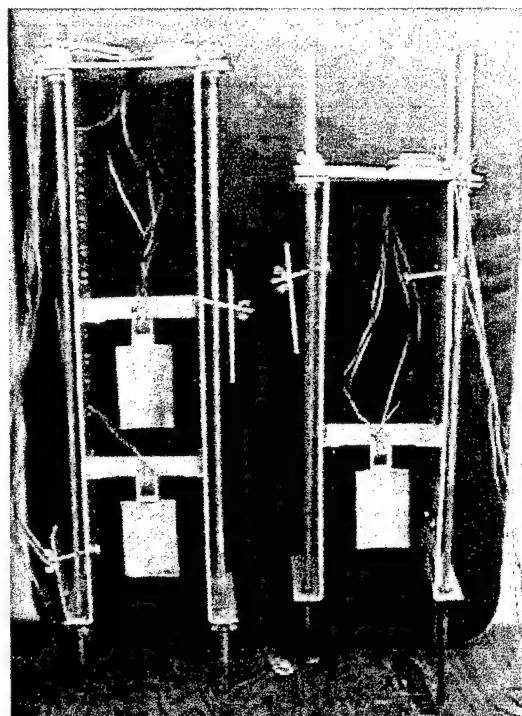
Figure 3.1 Double and Single Strain Gage Meters: Design #1

The initial low flow strain gage meter design (see Figure 3.1 for a picture of the design

#1 meters) included a paddle attached to a rigid frame by a narrow neck extension. The

strain gages were attached to this extension. The purpose of the neck extension was to be

the primary focal point of the material bending from the force of the water flow.

Aluminum was chosen for its flexibility as the paddle and neck material. The early

versions of this design used a paddle thicker than the neck. This was done to ensure that

the bending occurred primarily in the neck area instead of both the neck and paddle

regions. The efforts were intended to ensure that the strain gages attached to the

aluminum in the neck area would be under the maximum strain from the force of the low stream flows. From experimental observations, the extra thickness did not create significantly more bending in the neck. In addition, it appeared that increased amounts of extra weight on the paddle could eventually reduce the effect of the force of the water flow and, consequently, decrease the meter's sensitivity due to inertial effects. Thickness of the paddle and neck were varied to determine the most usable design. The variations included thicknesses of 0.016", 0.006", and 0.003" (For this and subsequent design measurements, English units rather than metric units have been utilized to maintain consistency with the units in the purchase of materials for meter fabrication). The 0.016" thickness definitely presented too much resistance with little sensitivity to the flows below 1.0 ft/sec but the 0.006" and 0.003" were quite sensitive to the low flows. The major problem with the 0.003" thickness was that the neck extension deformed quickly and eventually separated from the paddle base after minimal usage and handling. The 0.006" thickness was the choice for the future versions. In the July field experiment mentioned later, the neck on the bottom paddle of strain gage meter 1 was kept at 0.003" thick to test sensitivity and its environmental field response as a function of material thickness.

The final design #1 meter (see Figure 3.2 for diagram) included an aluminum paddle and neck of 0.006" thickness cut entirely from a single piece of aluminum sheet. The final dimensions of the bendable region of the neck were ¾" width x 1" height. An additional top 1/4" edge was attached to the bottom edge of the L-shaped mounting crossbar of the support structure. The paddle's dimensions were 2" width x 3" height.

Front View of
Paddle/Neck
Mount

Side View of
Paddle/Neck
Mount
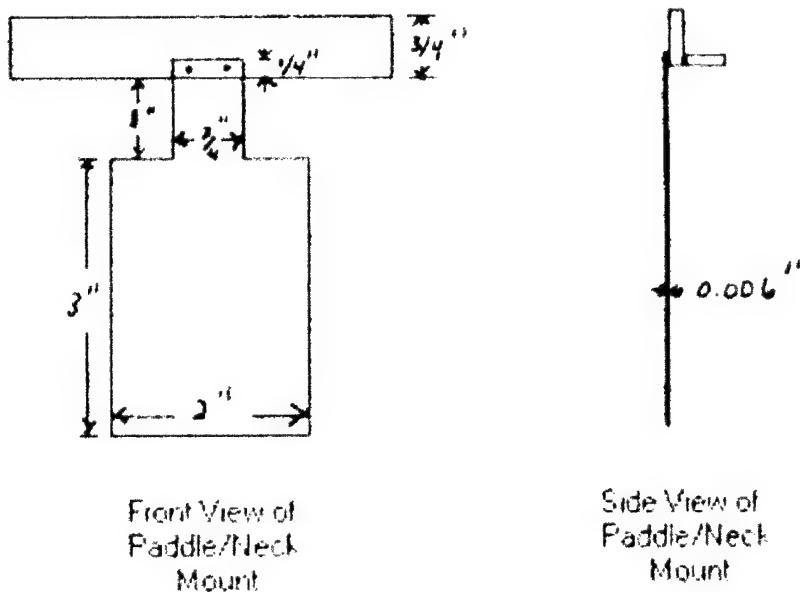
Figure 3.2 Diagram of Design #1 Meter Paddle/Neck Mounting Region

Two mounting structures of similar design were developed to allow for varying water depths measurements at Pinal Creek. Each included two aluminum sides of 4" width and 1/8" thickness. The larger structure was 20.5" high and supported two paddles by L-shaped mounting crossbars that could be placed at varying heights. The smaller structure supported one paddle and was 15" high. The length of the L-shaped mounting crossbars was 4.25" which allowed water flow around the 2" wide paddle. The extensions of the L-shaped crossbar were 0.75" long and 1/16" thick. The sides were used to help protect the paddle from large debris in the river flow and allowed for paddle height adjustment.

3.2 Strain Gage Selection and Mounting

Strain gage selection included evaluating temperature, size, orientation, accuracy, stability, and environment to determine the gage series, gage length, pattern, resistance,

leadwire options and the STC (Self Temperature Compensation) number. An A-alloy for the temperature range used (10-30°C) and the aluminum backing material was recommended via personal communications during April 1999 with representatives from Measurement Group, Inc., a major strain gage manufacturer. The strain gage parameters chosen were the CEA gage series, single-grid gage pattern and STC number 13.

A gage length was also needed. Based on the Measurement Group, Inc.'s recommendations during the April 1999 discussion and the design neck sizes, the chosen gage length for design 1 was 0.125" and, mainly due to availability, was 0.25" for design 2. The overall lengths of the two different gages were 0.35" and 0.45", respectively. Either was satisfactory for placement on the neck design but the gage length of 0.25", the longer overall length, provided greater neck area coverage.

Both gages are considered larger type gages by the manufacturer. The larger gage lengths are easier to handle during installation, and preattached leadwires (option P2 for Measurement Group CEA-series gages) were available from the company in these sizes. The fatigue life for the larger gages is longer than for the smaller ones under similar strains. The gage's life expectancy is decreased depending on duration and the magnitude of the strain. No fatigue in the strain gages was noted during these experiments.

There was also a choice in the gage resistance – 120 ohms or 350 ohms. The 350 ohm resistance gage decreases the leadwire effects and their associated temperature fluctuations more than the 120 ohm resistance gages. The 350 ohm gage was chosen to maximize the output signal-to-noise ratio.

Bonding of the selected strain gages to the aluminum also requires some choices. For this project involving testing of the flow meter, M-Bond 200 adhesive was used. This adhesive life expectancy is considered temporary, approximately a year, and is effected by moisture. Due to the limitations and extensive handling, strain gages were reattached occasionally. No reattachment was done between field use and calibration on any of the meters. The gages were inadvertently pulled off one meter during the December field trip after tripping on the attached wires, accentuating the fragile nature of the adhesive bond. Adhesives with longer life expectancy are available and should be used for future research in which a longer instrument lifespan is required.

The strain gages were mounted in a vertical orientation with two on the frontside in tension and two on the backside in compression of the neck to complete a full wheatstone bridge circuit as shown earlier in Figure 2.2. The strain gages were mounted using a prescribed kit, part no. GAK-2-200, and the technique prescribed by Micro-Measurements Division, Measurements Group, Inc.

The method included surface preparation of the aluminum, layout of gage location, and bonding of the strain gages to the aluminum. The surface preparation included a process of degreasing, sanding, wet sanding, acid conditioning and neutralizing. The gage location layout was lightly etched in the neck area. The gages were bonded using a two-part adhesive, M-Bond 200, to the aluminum.

After the strain gage was bonded to the aluminum, a coating was required to protect it from the water. The engineers, at Measurement Group, Inc., recommended a layer of

microcrystalline wax followed by a coating of silicone rubber. This coating was used on all of the strain gages utilized in this project.

3.3 Computer Hardware and Accessories

In addition to the design of a strain gage meter, a choice between options had to be made for supplying the input voltage, signal conditioning, and retrieving and recording the output voltage from the strain gage circuit. Portable machines dedicated to use for multi-strain gage operations were available. A second option was to purchase a strain gage board and connect it to a portable laptop computer. Based on price and future use considerations, the laptop computer option was considered the best.

An eight-channel strain gage board, model no. SC-2043-SG from National Instruments, was chosen to connect to a laptop computer via a DAQCard E Series I/O card from National Instruments Corporation. A laptop computer with 64 MB RAM, a Pentium II processor, and two PC Card slots was purchased from Gateway. Two long-life batteries were also purchased initially to allow flexible, extended field operations.

The strain gage board, powered by the laptop, supplied the strain gage input voltage. The strain gage board circuitry also conditioned the output voltage from the strain gage wheatstone bridge circuit to minimize noise effects. It also allowed the user to adjust each individual, at rest, meter's circuit to zero. The board can operate up to eight meters (with full wheatstone bridge circuits). The strain gage board was also used in a limited set of experiments by completing a wheatstone half bridge circuit with only two strain gages attached. In this case, only eight meters could still potentially be attached

simultaneously. The strain gages for both designs were connected to the strain gage board by 50 foot leadwire cables to allow for cross-sectional coverage of the stream.

The multi-meter network system was operated by LabVIEW software by National Instruments Corporation. A system operation file was initially established using this software package to initialize the strain gage board to provide input voltages to the strain gage circuit and to monitor the output voltage. For easy control of the individual strain gage meters via the strain gage board, a LabVIEW system operation program file was set up to control each individual meter's operation. With assistance from Mark Poppe, a graduate student in the Environmental Engineering program at the University of Arizona, a strain gage control and monitoring virtual instrument was created as a LabVIEW system operation file. The program captured a reading every 1.0 seconds and output the running average of the last 60 readings to obtain an average output voltage. This averaged output voltage once stabilized (typically after about 2 minutes) was recorded as a single experimental data point.

3.4 Meter Design #2

The paddle centroid in the design #1 format was adjusted to measure the appropriate mid-depth velocity so that established coefficients could be applied to calculate the mean velocity (see section 2.3.2 discussion). For the double paddle configuration, the upper and lower centroids had to be adjusted to the 0.8 and 0.2 fractional stream depths, respectively, before placement of the meters in the waterway. For the single paddle configuration, the paddle centroid was set to access the 0.6 fractional depth prior to meter placement. In both cases, if the stream stage (depth) changed significantly during a

monitoring period, the paddle heights were adjusted accordingly. In order to avoid this necessity, a second major design was developed (see Figure 3.3). This meter was
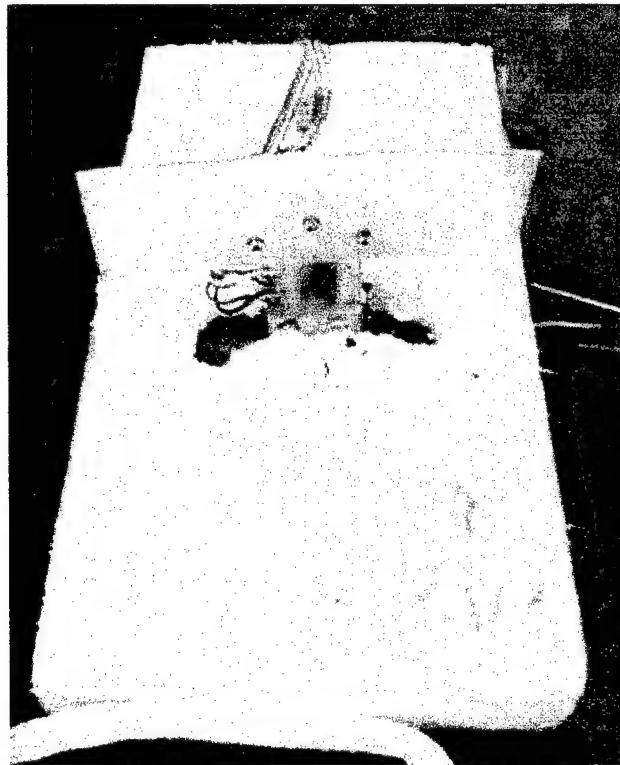
Figure 3.3 Meter Design #2 in Inverted Position

designed to measure the velocity just below the water's surface where according to the EPA method and others, a single characteristic coefficient will apply (assuming bed form, vegetation, etc. remain relatively constant). The design #2 meter (see Figure 3.4) was built using the paddle and neck design of design #1, but the paddle was made to be interchangeable. This refinement was made to increase sensitivity in a particular velocity range and to widen the total accessible range by varying the paddle size. For example, to provide access to high flows a small paddle size may be used, while for measurement of

low flows a larger paddle may be installed. All paddles were constructed of 0.016"

aluminum. The neck was mounted in a floating support device and the flexing portion of

the neck was again 1" height by ¾" width. There were 4 main paddle sizes for

theoretical and field experiments. The paddle was mounted to the neck by three screws

for easy field changes.

The overall structure was a styrofoam block (5"x 8" x 1") in which the neck and its

support device were placed. The placement allowed for the bottom edge of the attached

paddle to be 0.5" below the styrofoam base. When floating, the paddle was submerged

slightly more than 0.5" depth. A rope was used to tie the floating styrofoam platform to

two support rods inserted in the stream bed. During the field experiments, no side

protection was used but later experiments were conducted to determine their effects.

Front View of
Paddle/Neck
Mount

Side View of
Paddle/Neck
Mount
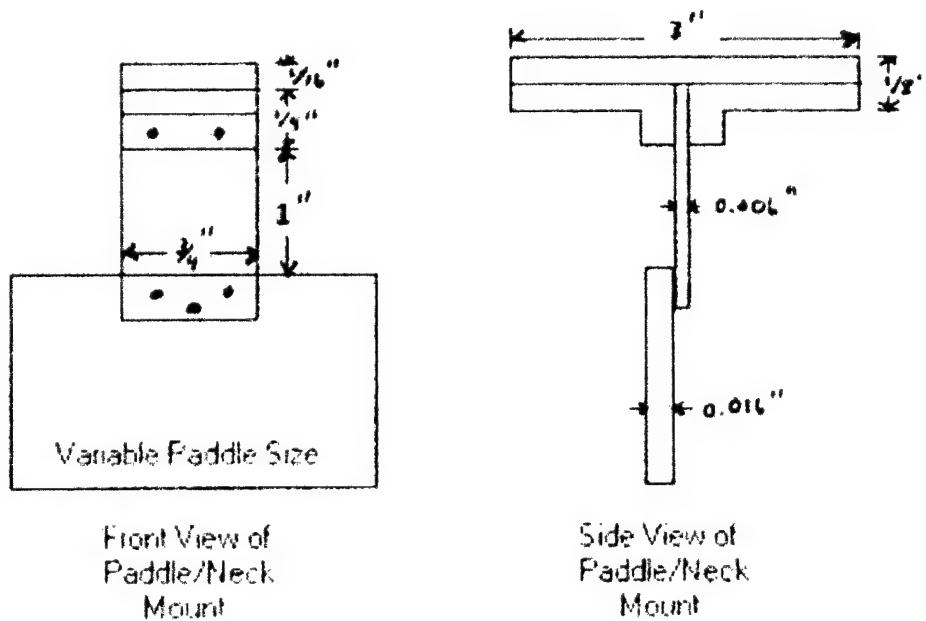
Figure 3.4 Diagram of Design #2 Meter Paddle/Neck Mounting Region

3.5 Calibration in Flume

The calibration procedure was basically the same for both designs. We used an outside flume system that consisted of a water basin, a pump, an above ground tank and a channel. The channel flow was gravity fed from the above ground tank and adjusted by varying a gate valve. There were no flow measurement capabilities already installed on the structure.

To measure the flow in the calibration channel, we measured the surface velocity. This was done by the float and stopwatch method (see section 2.3.1). A golf ball was wrapped with bubble wrap to enable it to float near the surface level of the water. It was then timed over a 4-foot length. This was done 6 times for each strain gage meter output voltage calibration reading and the arithmetic mean was taken as the average velocity.

A zero reading was normally taken before and after the velocity (voltage) reading during both field and calibration experiments. The zero readings are averaged and subtracted from the output reading to obtain an actual output voltage for the comparison graphs. For the design #1 graphs and the July field trial (described later), a zero reading was taken before and after each reading. For the design #2 graphs and the December field trial, a zero reading was normally taken initially and then at the end of the set of experiments.

The main analytical difference between the two designs was that the second design used a direct correlation between the gage reading and the surface velocity measurement obtained by the float and stopwatch method. For the first design, a coefficient is required to relate the subsurface (paddle) velocity to the near surface velocity measured by the

float and stopwatch method. Since the calibration channel bottom and sides were relatively smooth and free of vegetation, a coefficient of 0.9 (14) was multiplied against the surface velocity to obtain an average velocity for the design 1 meters.

If equipment is available, future calibrations, especially for the first design, should be done with a calibrated flume, which incorporates a built-in flow monitoring device. This would simplify calibrations considerably by eliminating the errors in using the float and stopwatch method over the relatively short four-foot length. A flume capable of greater range in flow rates would also be very useful.

The graphs were plotted using a polynomial fit, forcing a zero intercept. This method was used to standardize the graphing and gave the best response incorporating the higher voltage vs flow points. There were at least two design #1 meters whose graphs did not work well with the polynomial fit. There is potential that the alignment of the gages or the bond between the gage and the aluminum was different from the majority and therefore provided different results. These meters fit better with a polynomial fit not through zero, and it was used for their calibration curve fitting and for subsequent calculations using their output.

3.6 Field Test Site Location

Pinal Creek in Globe, AZ, was chosen as the test field site. Members of the University of Arizona's Hydrology Department were currently conducting research on this stream. Two locations were primary sites for their study and were considered the best sites for field testing the meters. The locations' names were $J^2 7.5$ and $J^2 8$.

This stream had characteristics that were similar to other mining contaminated streams across Arizona. It had varying levels of vegetation density across its cross-sectional area, and the open channel depth, bed character, and width varied considerably along the stream's length. Therefore, the flow rate would vary significantly across its cross-sectional area. Due to storm events, the stream bed profile was expected to change significantly during a year time period.

The USGS currently has a continuous readout, flow monitoring station on Pinal Creek at Inspiration Dam. Historical and real time data can be accessed from the USGS website. The current address for Inspiration Dam is 'http://waterdata.usgs.gov/nwis-w/AZ/index.cgi?statnum=09498400'. The dam is located ~3 km further downstream of the monitoring points chosen in this study. Due to this stream having a variety of gaining and losing regions, the data from Inspiration Dam is noted but not relied upon for comparing results.

This site had several advantages/disadvantages for this study. The field site constantly changed throughout the experiments. The flow rate significantly changed from the July to the December field experiments due to the addition of an upstream water treatment plant. This provided a larger range of flow rates for the stream but limited any comparisons between the two field studies. The stream bed also changed due to the increased flow rate and seasonal storm events that occurred. This altered sampling locations between the two studies. The site's only comparison flow rate was the bromide tracer study and this was not continuous which limited comparisons of any diurnal flow rate changes. The cross-sectional stream bed was very wide with a relatively narrow

main channel, and the water level was very shallow at the wide edges. Increases in water height provided significant changes in total water area, but most of the increased area was located in the stagnant edges of the stream. This effect creates tremendous difficulties in meter placement across the stream. The meters assigned to the stagnant region of the stream require placement in a representative region for the entire stagnant area. This placement was usually in a vegetative zone, which could interfere with the meter's response. If the vegetation was cleared and flow resistance decreased, the water flow rate tends to be greater than the actual amount and creates a higher meter response. This gives the meter a high erroneous response, which is magnified by the vast area that it was applied.

CHAPTER 4. RESULTS AND DISCUSSION

4.1 Design #1 Meter

4.1.1 Meter Calibration

The design #1 meters were calibrated in the calibration flume and the results of the calibration experiments are listed in Appendix A. The meters were calibrated over velocity ranges that represented their flow range during the July field trial. The neck on the bottom paddle of strain gage meter 1 was kept at 0.003" thick for sensitivity and field environment comparisons. Only the bottom meters where calibrated for Meters 1 and 2 since the top meters were not used in the July field experiment. Figures 4.1 and 4.2 provide examples of representative calibration curves for meters with 0.003" and 0.006" neck thicknesses, respectively.

Since standardization is desired, the calibration graphs were examined for regularities. A polynomial fit with a zero intercept was used since the majority of graphs exhibit good R^2 values with this fit. Meter 8 is an exception. This meter had a much better fit with a polynomial fit not through zero. Table 4.1 indicates that a calibration curve, using current construction methods and materials, cannot be standardized by a single set of parameters for use between strain gages. Reasons for this include varying adhesive thickness, strain gage alignment, and thickness of the wax and silicon rubber protective coatings.

Figure 4.1 Design #1 Double Strain Gage Meter 1, Bottom Paddle Calibration Graph w/ Error Bars for Both X- and Y- Axes; Velocity error bars shown and voltage error bars within data symbol

Figure 4.2 Design #1 Double Strain Gage Meter 2, Bottom Paddle Calibration Graph w/ Error Bars for Both X- and Y- Axes; Velocity error bars shown and voltage error bars within data symbol
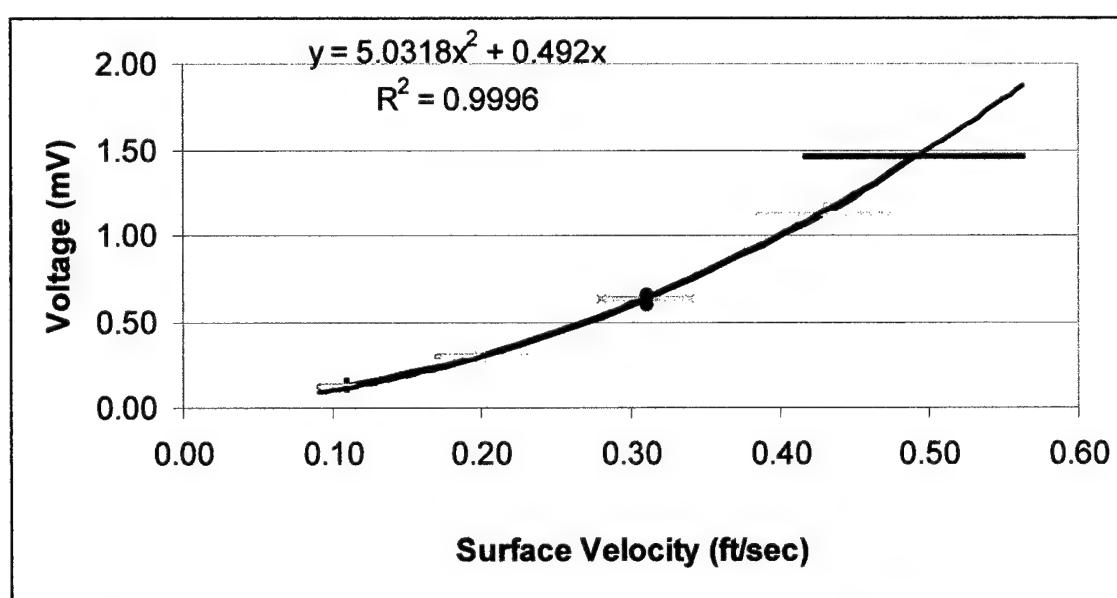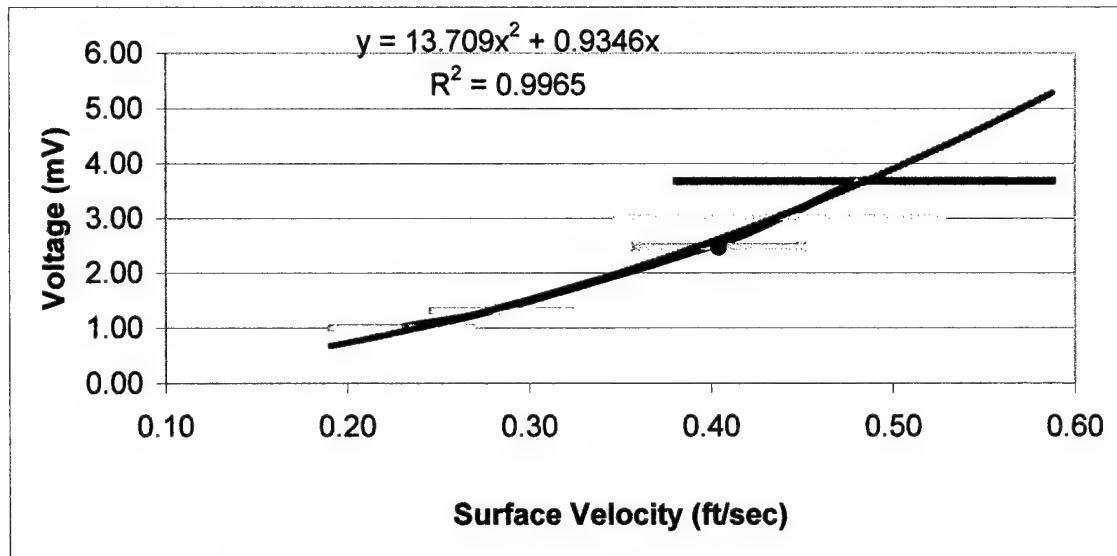
Meter #	x^2 Coefficient	x Coefficient	Constant	R^2
1 Bottom	13.709	0.9346	0	0.9965
2 Bottom	5.0318	0.492	0	0.9996
3	1.6824	2.1518	0	0.9774
4	4.5361	-1.7202	0	0.9812
5 Top	4.2119	0.8544	0	0.9885
5 Bottom	5.5628	0.5828	0	0.9898
7	2.3409	2.9764	0	0.9758
8	12.597	-8.1953	1.464	0.9994

Table 4.1 Design #1 Meter Calibration Best Fit Polynomial Coefficients and R^2 Values

4.1.2 Response Reproducibility

After calibrating the design #1 meters, an experiment was performed to test meter reproducibility performance. A calibration curve for a design #1 double strain gage meter was experimentally determined on July 1, 1999 (Day 1). Figure 4.3 shows the Day 1 curves of both the top and bottom meters with the fitted 2nd order polynomials. The top strain gage meter was the second meter that required a polynomial fit not through zero. A second set of points were taken on July 7, 1999 (Day 7). The Day 7 results are indicated in Figure 4.4 and 4.5 overlying the Day 1 results for the top and bottom meters, respectively.

The Day 7 results were correlated to the best fit polynomial regression calculated to match the Day 1 results (see Table 4.2). The Day 7 results correlate relatively close to the polynomial regression for both meters with the top meter being extremely good. The last individual point for Day 7 effected the R^2 value significantly since it varied substantially from the best fit Day 1 polynomial regression. Further calculation were done in Appendix B to determine if any regions of the best fit polynomial regression line

were less adequate in describing the meters' velocity vs voltage relationship. The early regions of both curves were not as accurate on an individual point scale.

Top: $y = 34.472x^2 - 14.488x + 1.5591$ Bottom: $y = 9.8787x^2 - 0.6044x$
$R^2 = 0.9961$ $R^2 = 0.9944$
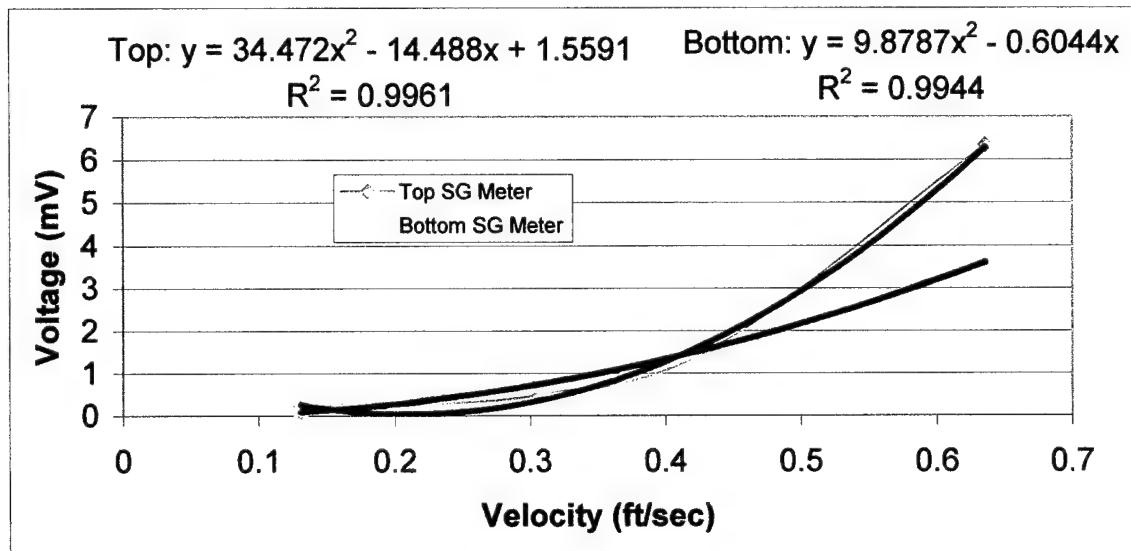
Figure 4.3 Repeatability Experiment: Day 1 Calibration Graph for Double Gage Meter
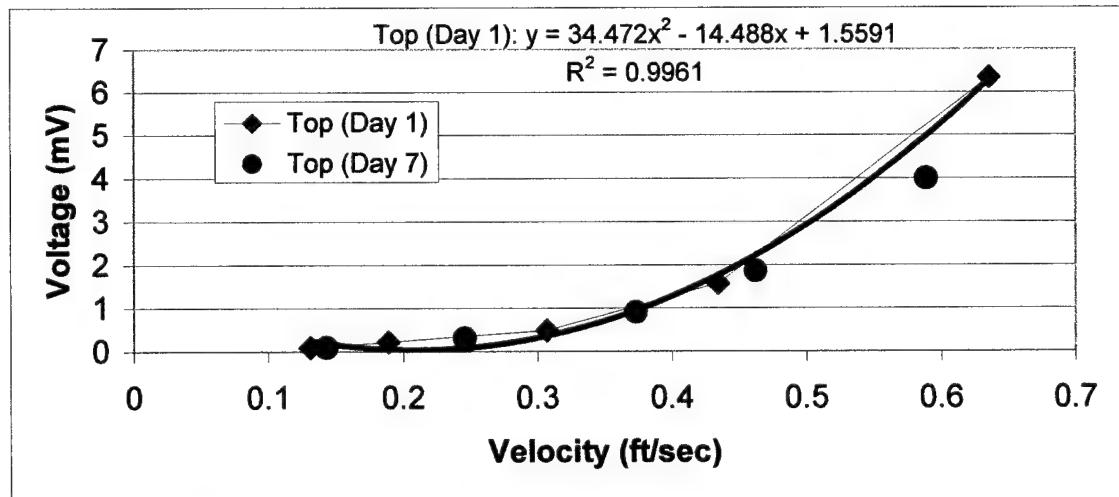
Figure 4.4 Day 7 Top Meter Results Overlaid on Day 1 Top Meter Graph
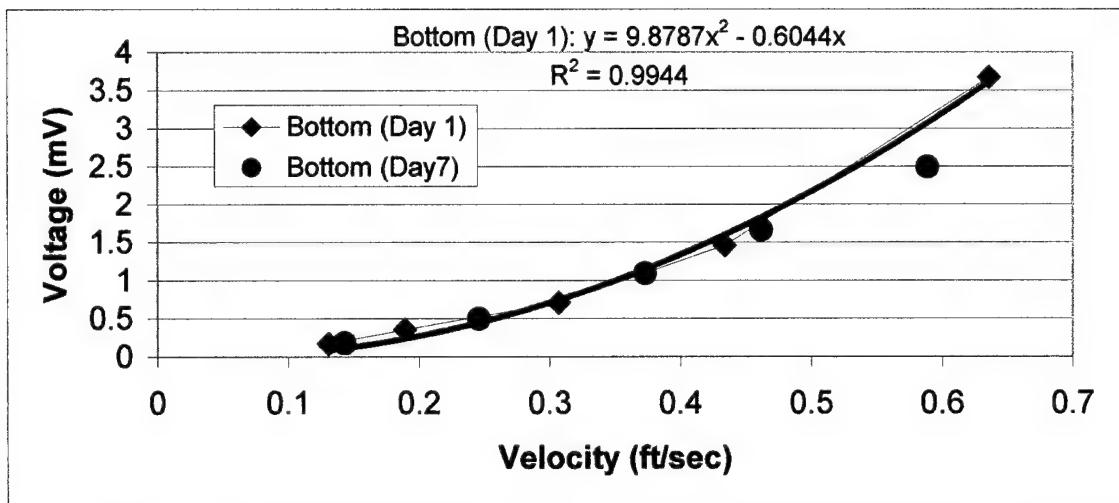
Figure 4.5 Day 7 Bottom Meter Results Overlaid on Day 1 Bottom Meter Graph

Meter Identification	R^2
Day 1 Top	0.9961
Day 1 Bottom	0.9944
Day 7 Top	0.9979
Day 7 Bottom	0.8903

Table 4.2 R^2 Values for Day 1 and Day 7 Correlated to Day 1's Polynomial Regression

4.1.3 Effect of Neck Thickness

Calibration trials were conducted with different aluminum neck thicknesses. Neck thickness was varied from the design standard of 0.006" to 0.003" on the bottom meter calibrated as strain gage meter 1. The results indicated better sensitivity at lower flows relative to the majority of the other meters, but the durability of this thickness of aluminum is limited. The neck separated from the paddle after limited usage just as experienced in a previous trial. The thickness of 0.006" for the neck was used throughout the rest of the experiments.

4.1.4 Effect of Paddle Depth

The velocity profile will change as a function of depth in a stream or calibration

channel. The velocity decreases with depth as the bed drag produces an increasing effect

with depth. An experiment was conducted using two separate design 1 single gage

meters at two different heights from the bed in the calibration channel. Figure 4.6 shows

a graph of the results. The meters' responses are very similar at the two depths but
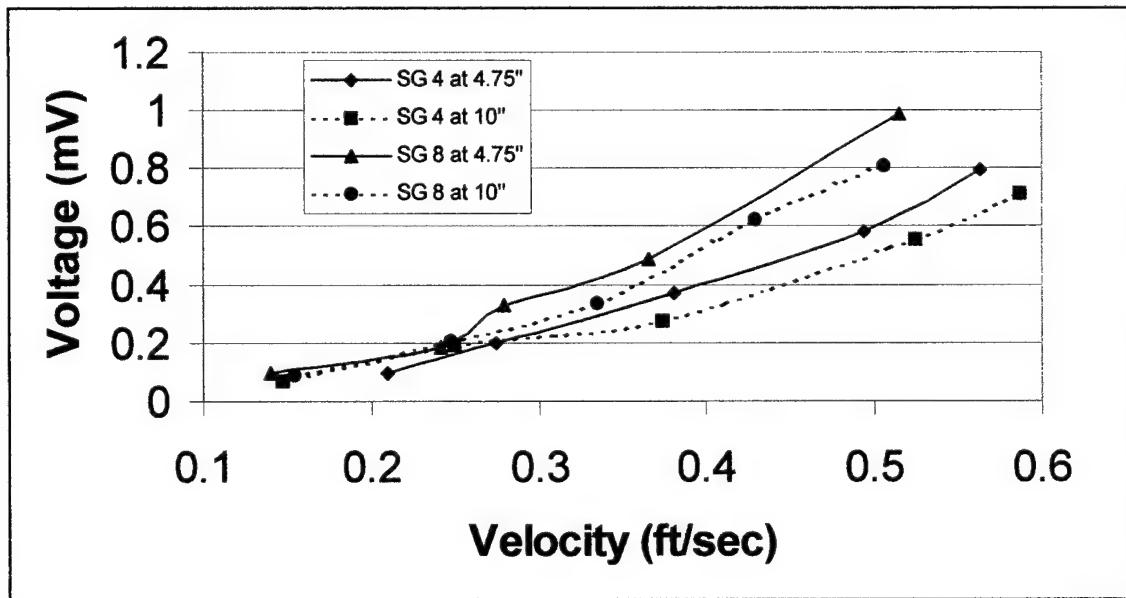
Figure 4.6 Comparison of Two Single Strain Gage Meters at 2 Calibration Channel
Heights

still vary from each other even at the same height. This result highlights the need to

calibrate individual meters (see section 4.2.1). The results of these graphs indicate that

the velocity is very similar in the calibration channel but that the meters are sufficiently

sensitive to record the expected decrease in velocity with proximity to the channel bed

4.1.5 Zero Set for Meters

During the calibration experiments, the zeroing of the calibration meter seemed to

often change more significantly with increased flows. This seems to be due to an

extremely long relaxation time for the aluminum neck to return to its original state, which

may be partially due to the wax and silicon coating resisting the aluminum's tendency to

return to its original state. In extreme instances, small permanent deformation of the

aluminum from excessive stress was observed. This effect, when the aluminum bends

close to its elastic limit or yield point, can limit the range of this meter. Due to slight

fluctuations (noise) of the meter's zero value, the meters are limited below very low

flows that provide responses <0.1 mV. Each meter has a unique low flow limitation

based on its overall neck thickness and the inherent limitations of the noise to signal ratio

of the hardware, which is illustrated in the various calibration graphs in Appendix A.

Further effects of the higher flow rates could not be determined due to the limited range

of flows possible in our calibration channel.

4.1.6 Effect of Gage Size

Trials were conducted to determine if there were any benefits or drawbacks to

increasing the size of the strain gage to cover more of the area of the aluminum neck. A

meter using 0.25" strain gages was placed on the bottom of the double strain gage meter

6 and tested in the calibration channel. The results were compared to meter 1's response

in the repeatability test (see Figure 4.7). The effect of varying the strain gage size from

0.125" to 0.25" is not overwhelming and much of the observable effect may be attributed
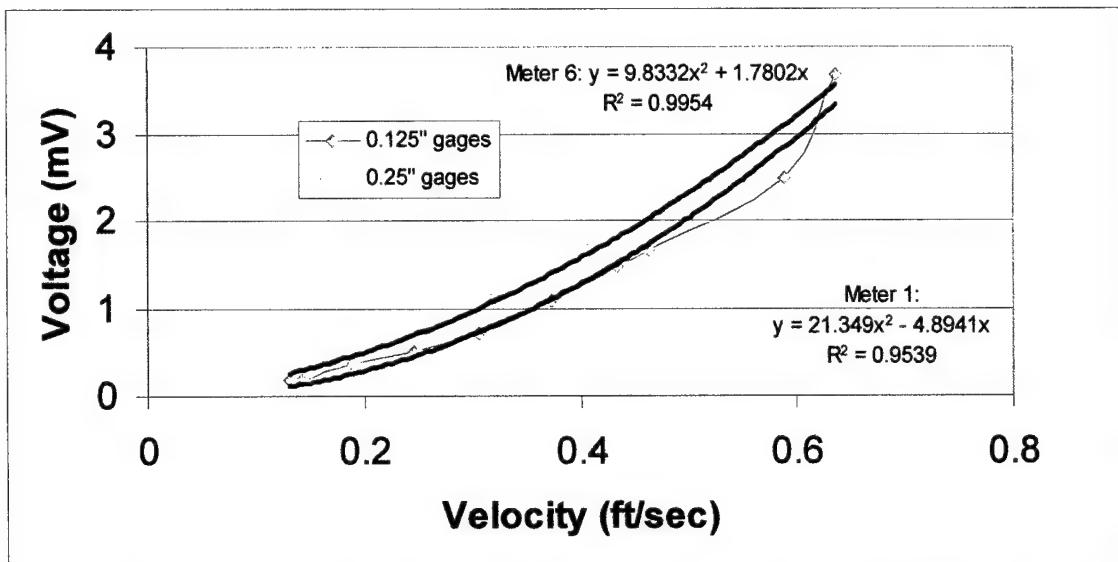
Figure 4.7 Comparison of Top Strain Gage Meters with the Varied Strain Gage Lengths

to the inherent differences between meters (see calibration results in section 4.1.1).

However, if anything, there is slightly more sensitivity when the size is increased as

evidenced by the higher voltage response to the same stress (velocity) applied.

4.1.7 Design #1 Limitations

Design #1 limited us on paddle size as the only way to increase the paddle size was to

increase its length. This had already caused major concern on the July field trial since the

water height was very shallow in several areas across the stream, which made placement

of the meters difficult. If the paddle length is increased, it accesses a wider range of

velocities, which decreases with depth. Since the change in velocity with depth is

nonlinear, then the assumption that placing the paddle centroid at the desired depth (for

use of a particular coefficient) accesses that depth's velocity becomes more untenable as

the paddle length increases. In addition, it is time consuming and an error prone exercise

to position paddles at prescribed fractional depths in a natural watercourse.

After the July field trial and further experiments, the design was modified to determine if improvements to the initial design were possible. A major modification would allow for varying paddle widths and heights. A second desirable modification would allow velocity measurement just below the surface of the stream to avoid the correct depth issue. The major concern with this design was that knowledge of a near-surface velocity coefficient to multiply against the measured velocity is variable especially in shallow depths and areas with vegetation.

4.2 Design #2 Meter

4.2.1 Meter Calibration

The design #2 meters were calibrated in the flume (section 3.5), and the results are listed in Appendix E. A single curve calibration was not possible as found for the design #1 meters, but a good fit was achieved for all meters with a best fit polynomial through zero. The initial calibration data range for the meters 1 and 2 used in the field trial (see later) at $J^2 8$ did not extend far enough so three more data points were added to each and their calibration graphs were extended (Appendix F).

4.2.2 Torque/Normal Stress (causing torque on the neck) Trials

Experiments were done to measure the extent of strain in the horizontal direction versus the vertical direction. The design of the paddle and neck was intended to minimize the potential for significant strain in the horizontal direction as compared to the vertical. In this experiment, a vertical and horizontal strain gage were both attached to the front and back side of the neck of two meters. An initial calibration test connecting all four gages in a full wheatstone bridge circuit was conducted. Next, half bridge circuit

connections with only the vertical or horizontal strain gages attached were conducted. The results of full and half bridge circuit tests are shown in Figures 4.9 and 4.10 for two separate meters. The vertical half bridge and the full bridge calibration curves are very similar indicating that the bending is almost entirely in the vertical direction and that the design does not suffer from signal noise generated from the velocity forces in the horizontal direction.

4.2.3 Paddle Size and Shape Effect

Paddle size variations were expected to impact the force that bends the neck. Therefore, variations in paddle area were expected to have an impact on the sensitivity to flows. The force of the water should impact a larger paddle more significantly. Figures 4.11 and 4.12 are the results of testing two meters with different paddle sizes. The three paddle sizes were 1.5" x 4" (6 in^2), 2" x 4.5" (9 in^2), and 2"x 6" (12 in^2). Both diagrams show a definite improvement in sensitivity from the 6 in^2 paddle to the 9 in^2 or the 12 in^2 paddles but very little improvement from the 9 in^2 to the 12 in^2 paddles.

It does appear that there is a maximum area, maybe also a maximum height and length, above which the meter sensitivity is only minimally improved. Potential influences for this limitation may include the weight of the paddle or when the water is shed off the paddle, a layer is created that minimizes the force of the water on the paddle (a shedding effect) (15).

Variation of response for paddles with the same surface area, but different heights and therefore, different centroids, was examined. Figure 4.8 shows the calibration curves for the same meter with two different paddle geometries but the same areas. The paddle

geometries are 1.5" x 4" (6 in^2) and 2" x 3" (6 in^2). From the plots, the paddle that is 2"

high is bent more than the 1.5" high paddle under the same stream velocity since it

provides a higher output voltage. This implies that in the same flow, the paddle with the

greater height can be more sensitive to similar flow rates. Further study needs to be

conducted to determine if this effect is caused by surface drag caused by the float altering

the near surface velocity profile or by some other phenomena.
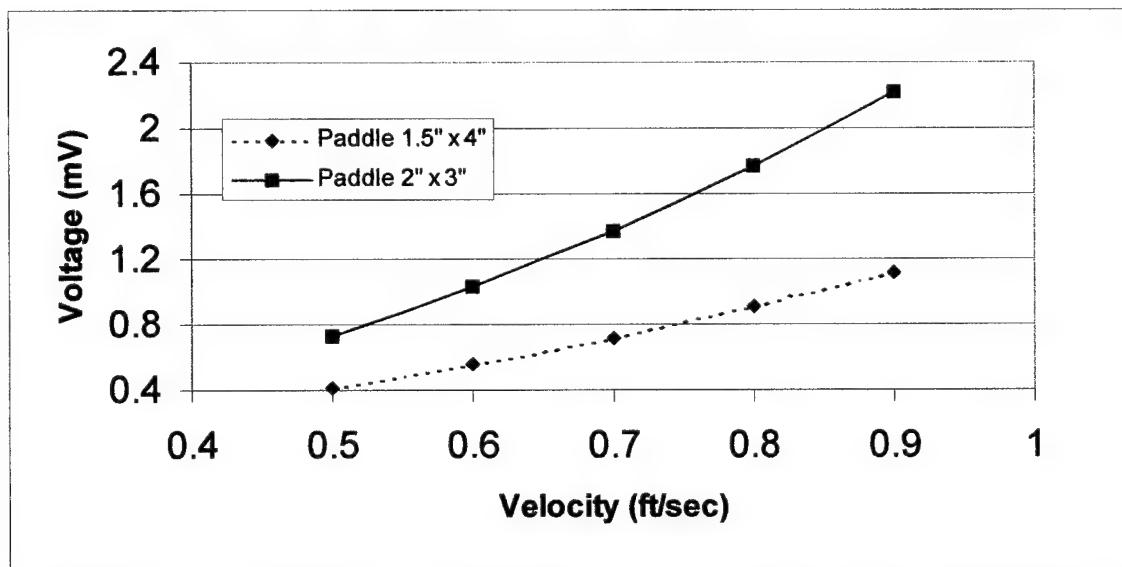
Figure 4.8 Design #2 Strain Gage Meter 2, Variable Height Paddle Comparison Graph
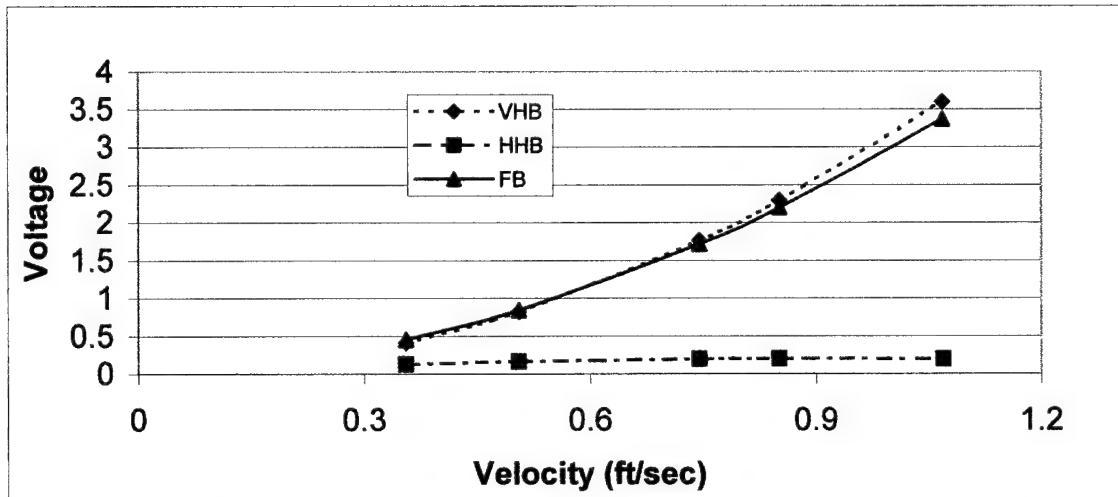
Figure 4.9 Meter 1 w/ Vertical and Horizontal Strain Gages and 2" x 6" Paddle
Comparison; VHB (Vertical Strain Gages in a Half Bridge Circuit), HHB (Horizontal
Strain Gages in a Half Bridge Circuit), and FB (Both Vertical and Horizontal Strain
Gages in a Full Bridge Circuit)
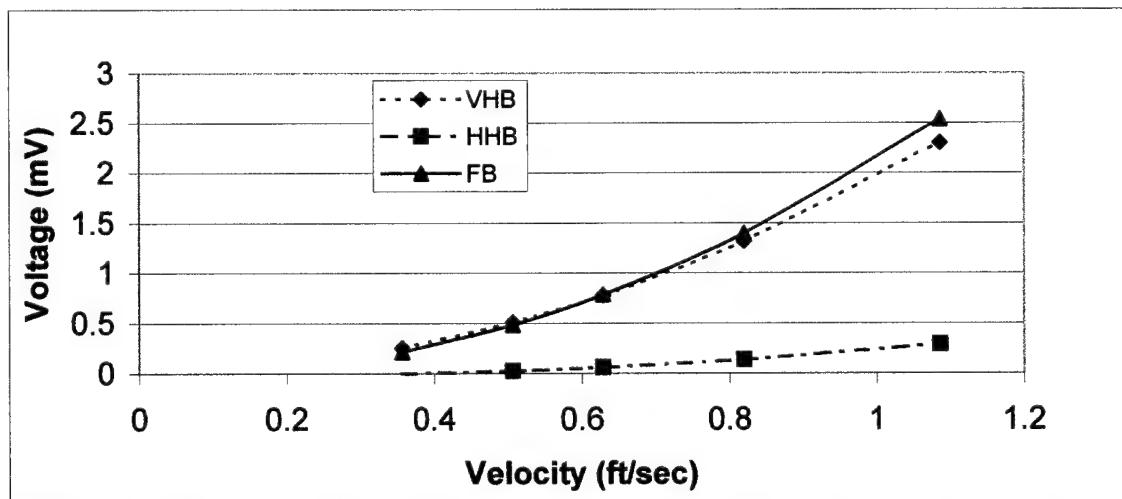
Figure 4.10 Meter 2 w/ Vertical and Horizontal Strain Gages and 1.5" x 4" Paddle
Comparison; VHB (Vertical Strain Gages in a Half Bridge Circuit), HHB (Horizontal
Strain Gages in a Half Bridge Circuit), and FB (Both Vertical and Horizontal Strain
Gages in a Full Bridge Circuit)
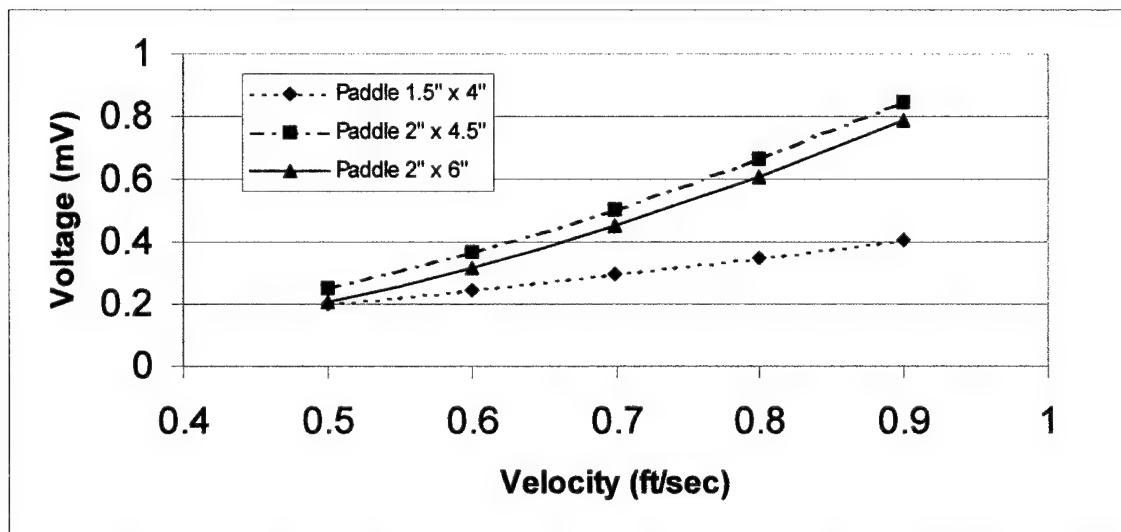
Figure 4.11 Design #2 Strain Gage Meter 1, Paddle Comparison Graph
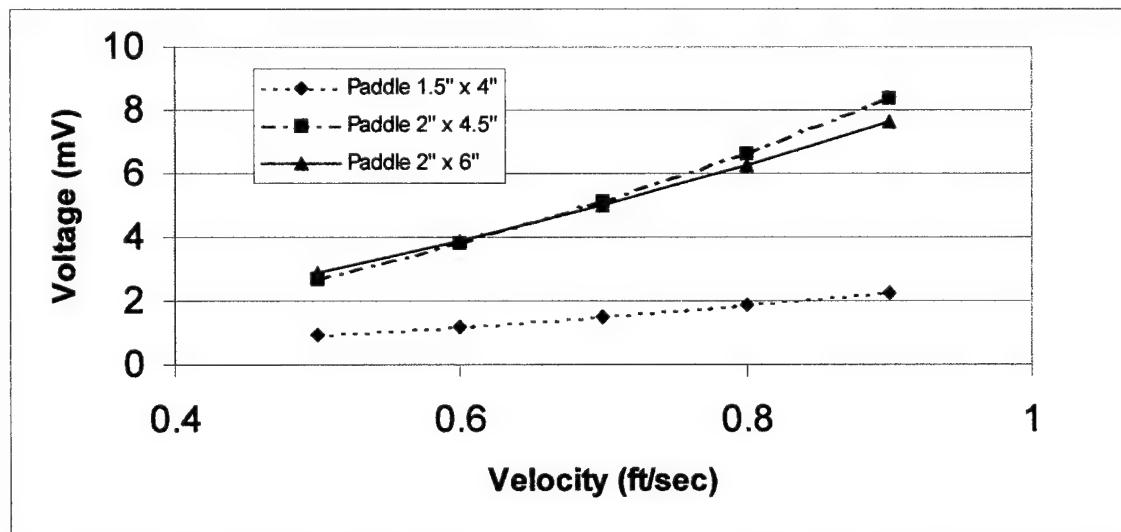
Figure 4.12 Design #2 Strain Gage Meter 3, Paddle Comparison Graph

4.2.4 Meter Protection

In a stream, the strain gage meters need protection to help shed off floating debris. In the first design, the sides of the supporting structure provided some protection. During the July and December trials, there was very little debris snagged by the paddles. The wires attaching the meter to the computer station set up onshore collected moss and algae, which had to be removed occasionally during the December trip. These wires should normally be suspended above the water for future tests.

The design #2 meter could benefit from additional protection so experiments were done to verify the effects of sidewalls on the meters. The sidewalls were attached to the styrofoam structure and kept 5" apart and equal distances from the two paddle sizes used. The area between the paddle and the sidewall for the 3" wide paddle was 1" but for the 4" paddle, it was 0.5". The sidewalls extended 4" down and were 8" long and 1/16" thick. The results of the two comparative calibration studies between a meter with sidewalls and without are shown in Figures 4.13 and 4.14. It does appear that there is increased sensitivity for the wider paddle as its response (voltage) is higher to a set force (velocity) when sidewalls are present. This would imply that the shedding of water on the sides by the paddle is restricted by a 0.5" side clearance but essentially unrestricted by a 1" clearance for the flow conditions tested.
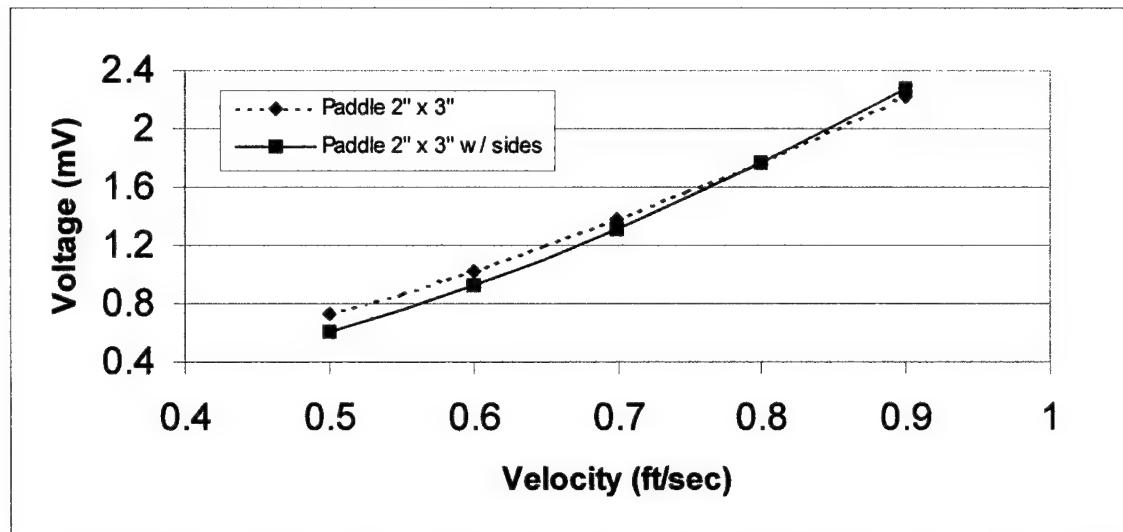
Figure 4.13 Design #2 Strain Gage Meter 2 w/ and w/o Sidewall Comparison Graph
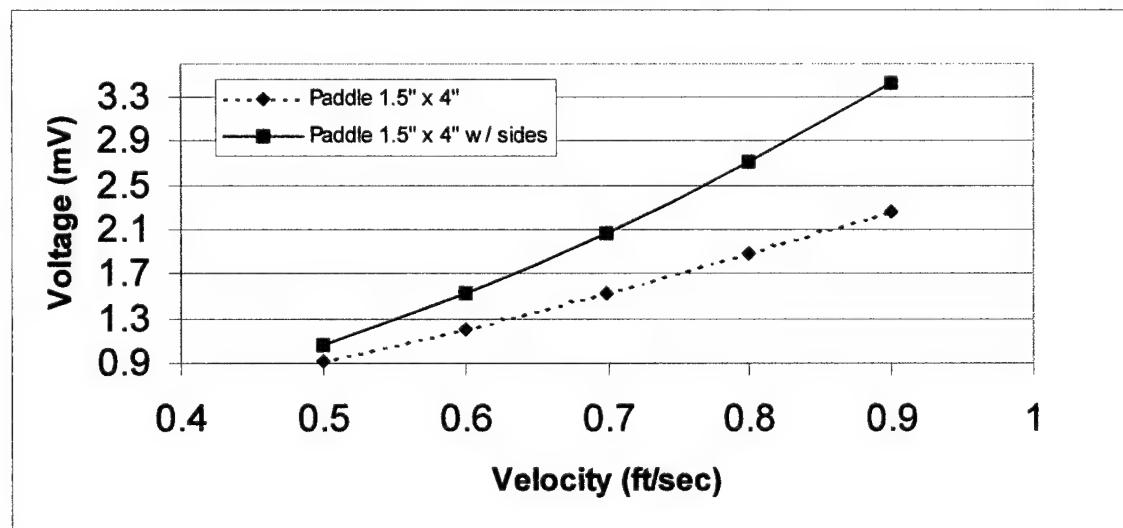
Figure 4.14 Design 2 Strain Gage Meter 3 w/ and w/o Sidewall Comparison Graph

4.3 Field Trials

4.3.1 June 1999 Field Trial

The initial field test of design #1 was in June. Cursory inspection of the results in the field did indicate that flow changes trended as expected with variation in stream stage. However, it was realized later when calibrating the flow meters that a software parameter needed to be changed to provide useful data. In the LabVIEW software, the default value for the DAQ board analog channels must be set for nonreferenced single-ended inputs for use with our selected strain gage board (16 and 17). Due to the oversight, the initial test results were deemed invalid and are not mentioned further.

4.3.2 July 1999 Field Trial

The second trip on July 22, 1999 provided more useful results in field testing design #1 at Pinal Creek. This field trip included a bromide tracer study, which provided a limited comparison set for the flow meter data. Appendix C lists the results of the bromide study conducted by Roger Koelsch from the U of A Hydrology Department (18). Due to problems with the stream profile during this trip, the meter locations were moved to about 30 feet downstream of the previously defined and studied $J^2 8$ stream location. Figure 4.15 shows the cross-sectional area where the strain gage meters were placed at the new site. The zero level in this figure corresponds to the water level height at 1603 on July 22 before the flood. The standard plan for the meters was to place two meters in the main channel region, 1 in the shallow, less vegetative region and 1 in the vegetative region. In this trial due to the stream profile, four meters, with 1 double gage meter covering the main channel, were located across the stream at the location downstream of

$J^2$8. A cross-sectional region upstream of $J^2$7.5 was also monitored during this trip but the cross-sectional area was not evaluated prior to a storm event occurrence, which significantly altered the stream bed profile, making the $J^2$7.5 data usefulness limited.

One of the major problems with the design in this field trip experiment was that the water depth was very shallow (6" or less) in several areas across the stream so placement of the meters was limited. Meters 4 and 8 neck/paddle areas were not completely submerged at the $J^2$8 site. When calibrating these meters, the neck/paddle areas were not completely submerged to minimize variation of the force due to dissimilar paddle areas exposed between the calibration and field trials. Appendix D shows an example calculation used to determine the strain gage meters' flow estimation for the $J^2$8 transect. Table 4.3 lists the results of the strain gage data, the bromide tracer study and the USGS Inspiration Dam results.

Design 1 Meter Flow Rate/Time	Bromide Tracer Study/Time	USGS Inspiration Dam Flow Data/Time
2.9 ft^3·s^{-1}/1603	2.38-2.84 ft^3·s^{-1}/1612	2.4 ft^3·s^{-1}/1530*
2.8 ft^3·s^{-1}/1830	2.38-2.84 ft^3·s^{-1}/1718	2.4 ft^3·s^{-1}/2000*

* Recorded Flow rates at Inspiration Dam did not change over this timeframe

Table 4.3 Flow Rate Comparison Results for July 22 Field Trial
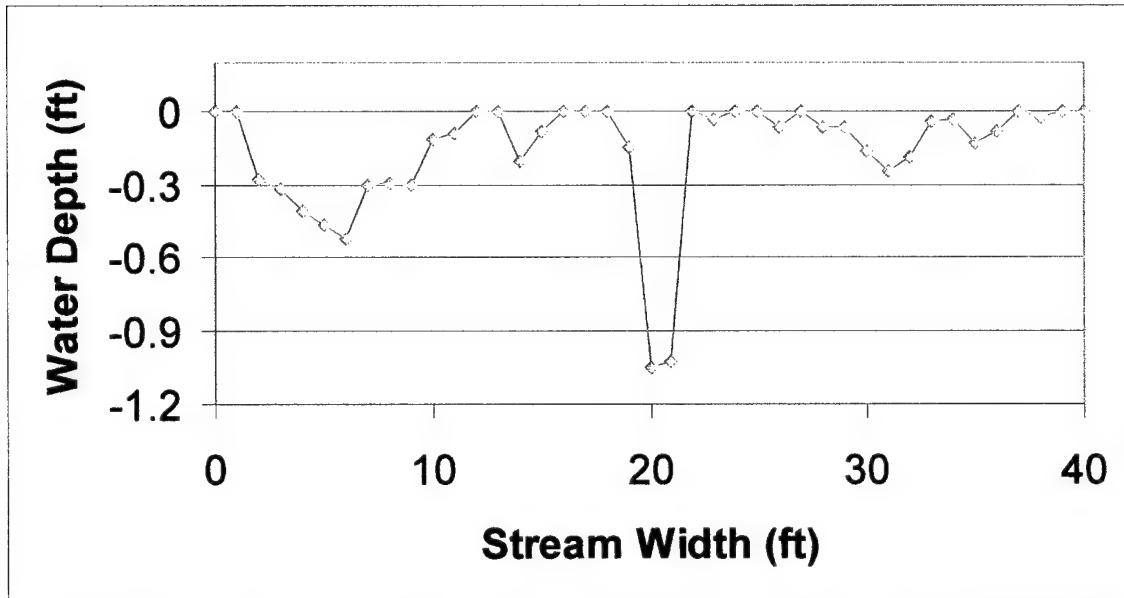
Figure 4.15 Cross Sectional Area Just Below $J^2 8$ Location at 1603 on July 22

4.3.3 December 1999 Field Trial

The next field trial, testing the design #2 flow meters, was conducted at Pinal Creek on December 15, 1999. The flow was significantly higher than the previous trips. A metals removal treatment plant was operational and the plant effluent was now being introduced to the stream and increased the flow significantly. This field experiment also included a comparison of the flow meter data versus a bromide tracer study.

Four meters were spread out across both the $J^2 8$ and $J^2 7.5$ transects with two in the main zone and two in the lower flow (shallow and/or vegetative) zones. The field data calculations are similar to the July field trial except that the design #2 meters measure surface velocity in a stream. The applicable coefficient for fractional mean velocity is very sensitive to depth changes for shallow streams (<0.5 ft) and to changes in vegetation density. Appendix D shows an example calculation used to determine the strain gage

meters' flow estimation for both $J^27.5$ and J^28 except that the coefficient used for the meters in the main channel and non-vegetative regions was 0.8 (19), and a very rough estimate coefficient for the shallow vegetation regions of 0.5 was used. The coefficient is expected to be low in the vegetation area but more studies need to be done to determine if it is possible to assign coefficients under a variety of depths and vegetative conditions.

An example of the water depth and meter's output voltage, V_o, is given in Table 4.4. It was done to see if the relationship between the flow meters and the water level height at J^28 on December 15 is easily discernible. The values appear relatively constant over the 4 hours illustrated but the flow rate shifts indicated by the water height are not readily discernible from the meters' output voltage. The estimated error in measuring from the stage tube to the water during these studies is $^{+/-}1/16$" so stage changes of 1/16" or less are insignificant. Evaluation of the Table 4.4 results suggests that the coefficient of fractional mean velocity is relatively insensitive to the stage variations experienced in this time period. The flow at Inspiration Dam varied by 0.2 $ft^3 \cdot s^{-1}$ during this time period.

Time	Stream Stage Relative to Level at 1210 Hours	Meter 1 V_o (mV)	Meter 2 V_o (mV)	Meter 3 V_o (mV)
1210	0 inches	4.52	9.41	0.56
1315	+0.0625	4.73	9.69	0.69
1407	-0.25	4.96	8.99	0.62
1429	-0.1875	4.90	9.40	0.69
1504	+0.0625	4.80	8.9	0.64
1602	-0.0625	5.28	9.11	0.67

Table 4.4 Stream Height vs Meter Output Voltage

Appendix G lists the results of the bromide study for the December trip. There was significant sulfate interference during the IC analysis but due to consistent trends in the

sample analyses, the data is useful. Figures 4.16 and 4.17 show the cross-sectional areas

of the two chosen monitoring locations across the stream. Table 4.5 lists the results of

the strain gage data, the bromide tracer study and the USGS Inspiration Dam results.

Note that the meter in the densest vegetative zone for $J^2 7.5$ was accidentally broken

during sampling and no readings are recorded. The results from this vegetative region

should have been negligible. The measured flow rate for $J^2 8$ was too high. If just the two

main channel meters were used, 7.1 and 7.5 $ft^3 \cdot s^{-1}$ at 1400 and 1500, respectively, were

calculated. Also note, that the two outer area meters covered 75% of the water area but

much of this was stagnant. Thus, small errors in the mean velocities in these areas have

large impacts on the overall flow rate calculated. Hindsight indicates an insufficient

number of meters were utilized for the vegetated area and those used were not placed in

flows representative of the mean flow in this zone. It may be appropriate to neglect or

reconsider the approach in heavily vegetative areas, but further study is needed.

Design #2 Meter Flow Rate/Time	Bromide Tracer Study/Time	USGS Inspiration Dam Flow Data/Time
6.13 $ft^3 \cdot s^{-1}$ /1400 at $J^2 7.5$	6.72-7.31 $ft^3 \cdot s^{-1}$ /1356	7.0 $ft^3 \cdot s^{-1}$ /1345
6.88 $ft^3 \cdot s^{-1}$ /1500 at $J^2 7.5$	6.72-7.31 $ft^3 \cdot s^{-1}$ /1506	6.8 $ft^3 \cdot s^{-1}$ /1730
13.04 $ft^3 \cdot s^{-1}$ /1400 at $J^2 8$	6.72-7.31 $ft^3 \cdot s^{-1}$ /1356	7.0 $ft^3 \cdot s^{-1}$ /1345
13.66 $ft^3 \cdot s^{-1}$ /1500 at $J^2 8$	6.72-7.31 $ft^3 \cdot s^{-1}$ /1506	6.8 $ft^3 \cdot s^{-1}$ /1730

Table 4.5 Flow Rate For the December Field Trip as Measured by Three Different Methods
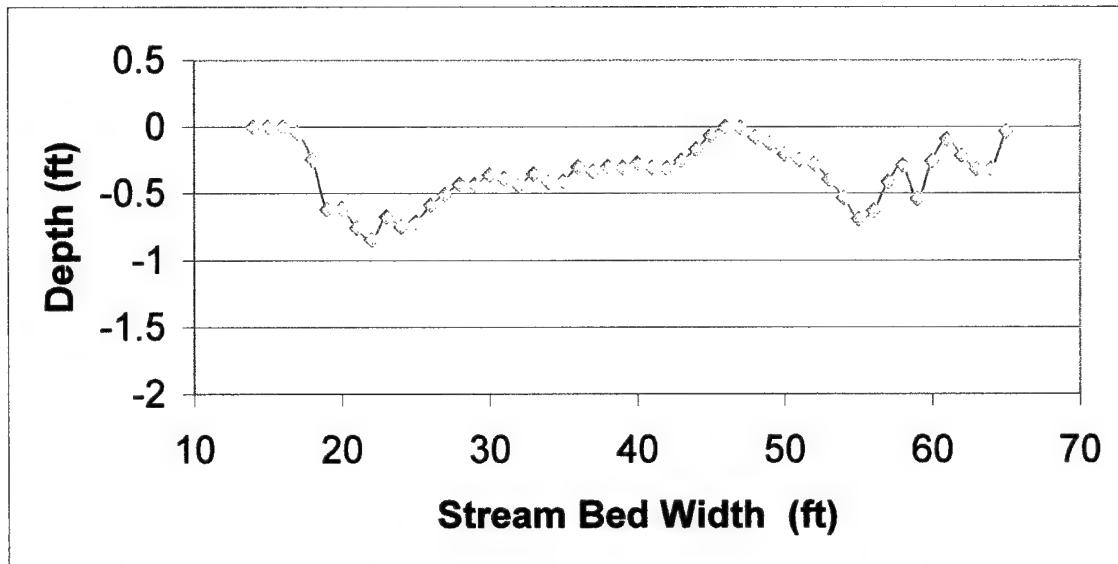
Figure 4.16 December Field Trip – $J^2$7 Cross-Sectional Stream Area (Zero depth corresponds to the freewater surface elevation at the time of survey)
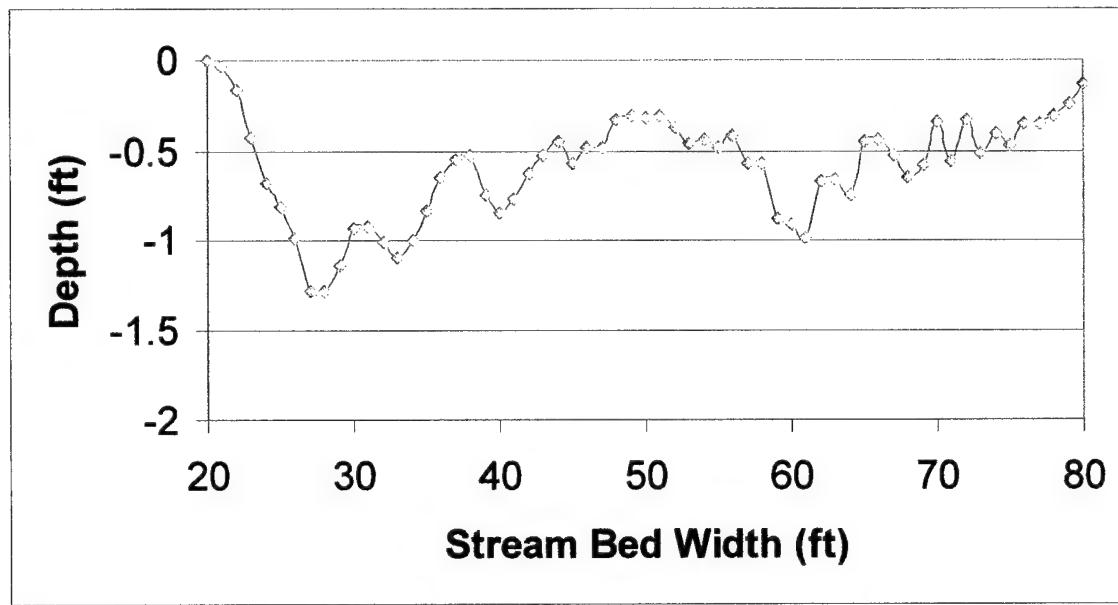
Figure 4.17 December Field Trip – $J^2$8 Cross-Sectional Stream Area (Zero depth corresponds to the freewater surface elevation at the time of survey)

4.4 Theoretical Experiments

Strain is related to the deformation of a material. Stress is related to the force applied to the material. Hooke's Law relates stress to strain by a constant called the "Modulus of Elasticity", E. This constant is different for unique materials. Aluminum has an $E = 10 \times 10^6$ psi (20). The neck of the flow meter may be considered to act as a cantilever beam since one end is fixed and the other free. The strain gages measure the deformation as the force of the flowing water on the paddle bends the neck.

The horizontal deformation of a cantilever beam is related to the force at the free end of the bending beam by the equation (21):

$$d = F * L^3 / (3 * E * I) \qquad \text{(Eqn 4-1)}$$

Where d is the horizontal deformation, F is the force on the free end of the beam, L is the total length of the bending area of the meter's neck and I is the moment of inertia for the neck and related to the neck thickness by the equation (22):

$$I = 1/12 * \text{neck thickness}^3 * \text{neck width} \qquad \text{(Eqn 4-2)}.$$

In this experiment, the horizontal deformation is related to voltage, and therefore, both are related to the force of the water in a stream by E.

For the calculations in this experiment, the direct force on the neck of the paddle caused by the passing water is assumed to be minimal compared to the force on the paddle caused by the water. Also, the force in the y–direction (vertical) is assumed to be negligible for the angle of neck bend and not further addressed. Two design # 2 meters, used previously as meters 2 and 3 in figures 4.8 and 4.12, were chosen due to their excellent sensitivities and that they already were tested with various paddle sizes.

The first experiment was to vary the horizontal deformation of each meter's neck and relate the deformation to output voltage. A calibration stand was built so that the neck of a meter could be bent to various degrees. A caliper quantified this change by measuring the horizontal deformation. This value could be measured while recording the corresponding output voltage from the strain gage circuit. Figures 4.18 and 4.19 show the horizontal deformation vs output voltage results for the two meters. Output voltage readings were stable, requiring one reading at each horizontal deformation increment.
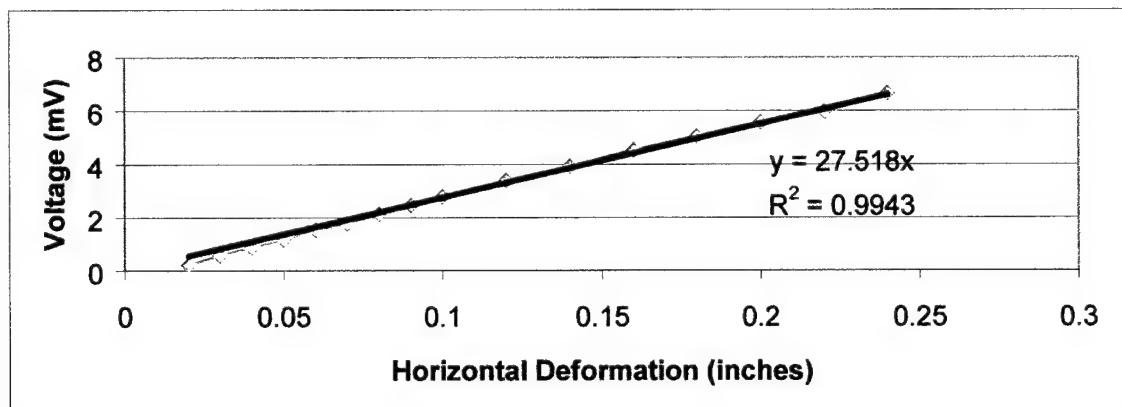
Figure 4.18 Horizontal Deformation vs Output Voltage for Meter 2 (see also Figure 4.8)
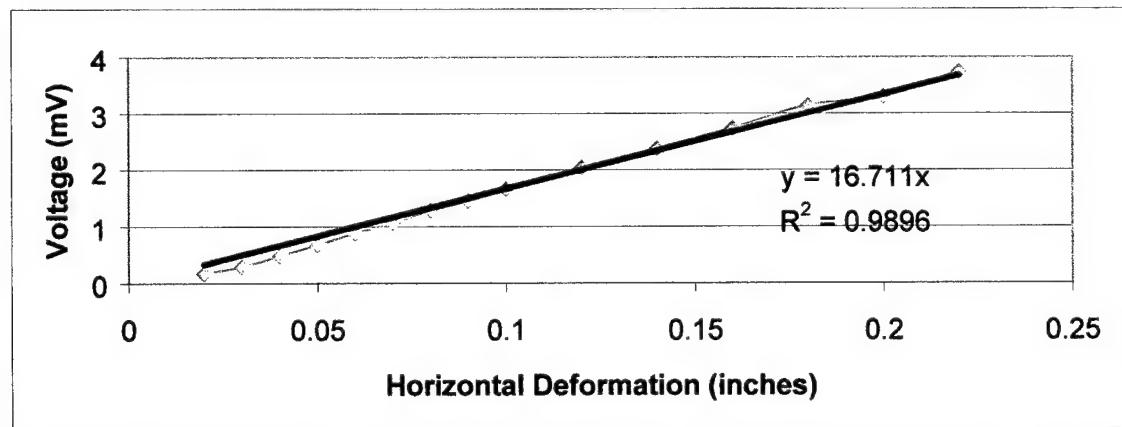
Figure 4.19 Horizontal Deformation vs Output Voltage for Meter 3 (see also Figure 4.12)

To determine the force on the neck, the water force on the paddle needs to be determined. The equation

$$F_x = C_D \text{ (drag coefficient)} * A(rea_x) * \rho \text{ (density of water) } * V(elocity)^2/2$$

was used to determine this force (23). The paddle area decreases with greater flow rates since the area is considered the silhouetted area that would be seen when looking at the paddle from the flow direction. The area changes as the paddle bends so a subscript x is added to remember that the height is altered to reflect the size reduction in the calculations. The drag coefficient used in the calculations was obtained from the literature (24). The paddle was considered a flat plate and the Reynolds Number was calculated based on the calculated velocity (from the calibration graph equation) of the stream and the height of the paddle.

After determining the force on the paddle for each horizontal deformation (output voltage) position, the resulting force on the end of the neck had to be resolved. This was possible assuming static equilibrium which means the summation of all forces and moments must equal zero. This implies that there is a force at the fixed end of the neck equal to the negative of the force on the paddle. There is also a bending moment at this position equal to the force of the paddle multiplied by the distance to the centroid of the paddle (= neck height + paddle height/2). Assuming that all the bending is in the neck (the paddle acts as a rigid plate) and applying translational equilibrium conditions of forces only, the force at the free end of the neck is equal to the negative force of the fixed end. This means that the force on the paddle is equivalent to the force on the free end of the neck.

The actual thickness of the necks of the meters are not easily measurable due to the varying thickness of protective coatings, adhesive, and attached strain gages under current construction methods. For this experiment, the total thicknesses, related as if it were all aluminum, of the two meter's necks were obtained by using equation 4-1 and understanding that $I = 1/12$ x neck thickness^3 x neck width. The horizontal deformation, output voltage, calculated force based on paddle size, and the two meters' average neck thicknesses are listed in Appendix J.

The composite neck thicknesses (aluminum plus gage, coatings and adhesives) of the two meters were approximately 0.028 and 0.019 inches (as aluminum equivalent). This implies that the same force applied to both meters would not provide the same horizontal deformation per equation 4-1, but varying the paddle sizes and geometries should not vary equivalent forces on each individual meter's neck. Figures 4-20 and 4-21 relate equivalent paddle forces to the output voltage from meters 2 and 3, respectively. The results indicate that there is a potential equivalent relationship between the forces of the varying paddle geometries on an individual meter. This relationship can be useful in reducing calibration time for each individual paddle variation and instead relating back to one force vs output voltage calibration curve for each meter.

The best fit lines in figures 4-20 and 4-21 are fitted by forcing a zero intercept as, ideally, when no force is applied, no deformation (voltage) should be observed. However, particularly for meter 3 (figure 4-21), the assumption of a zero intercept seems to be poor. A likely explanation for this behavior is that the gage, waterproof coatings and adhesives do not act elastically but experience some inelastic distortion and hence

retard the neck's return to zero when the force is removed. Although this construction

limitation is inevitable, it can be minimized by better standardizing the construction

procedure and materials.
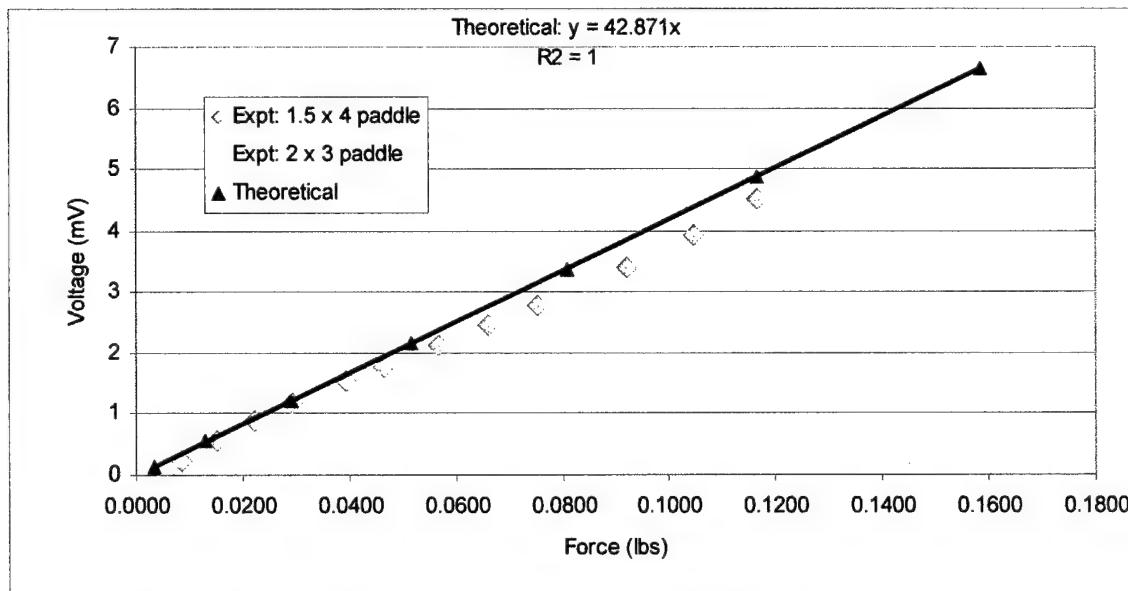
Figure 4.20 Force vs Voltage for Varying Paddle Geometries for Meter 2
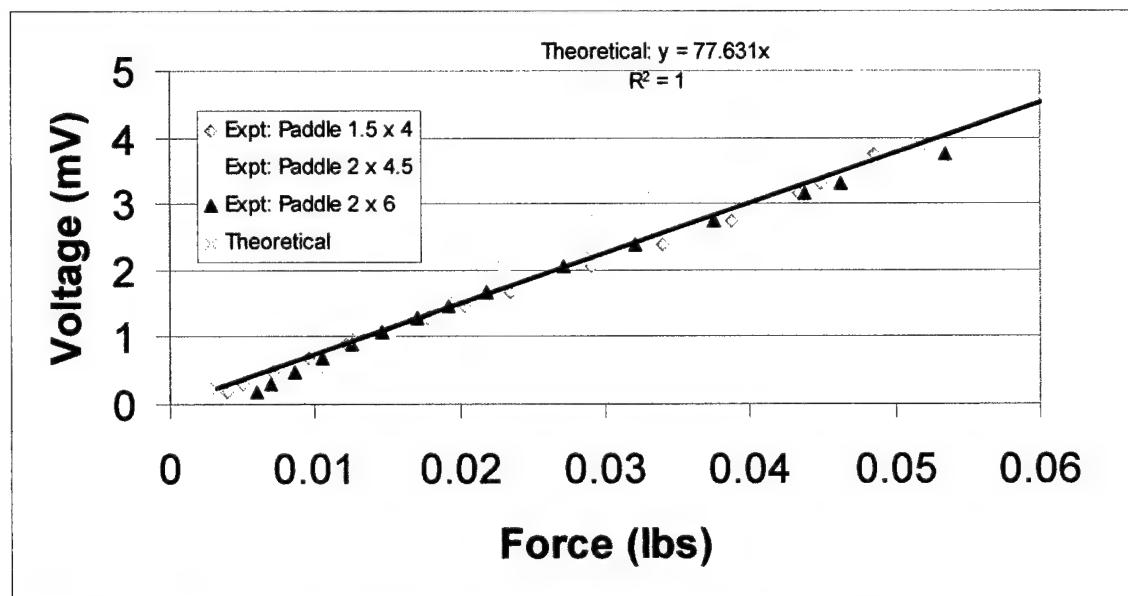
Figure 4.21 Force vs Voltage for Varying Paddle Geometries for Meter 3

CHAPTER 5. CONCLUSIONS

This study involved designing, constructing and testing flow meters using strain gage technology. The primary goals for the meter were to be portable and sensitive to low flows since current technology in these areas was inadequate. Two designs were tested. One measured velocity near the surface and the other measured subsurface velocity. Important factors when selecting a flow meter for use at a particular site is its accuracy and repeatability, its portability, its initial, operational, and maintenance costs, and its range. Studies were conducted to determine the ability of a strain gage meter to meet the selection criteria.

The accuracy and repeatability of the meter to measure velocity appears to be very good, definitely within +/- 10% (see section 4.1.2). The best fit calibration line is critical in ensuring this accuracy. The polynomial fit forced through zero seems to be the best and has strong potential for standardization. Further studies of meters using better adhesive are expected to decrease the error in repeated measurements and further confirm these findings. All of the design #2 meters had exceptional curves with this fit. Since the meter's accuracy in measuring velocity is very good, the accuracy of measuring flow rate at the low flows is only dependent on the technique applied. The design #1 meter arrangement is considered more reliable and accurate, but the design #2 meter is easier to use in field conditions. Further studies on determining coefficients for vegetative and shallow areas need to be conducted. Also, studies determining representative placement and the number of meters required across various cross-sectional lengths and vegetation zones would be useful.

The range of the meters is also of primary importance. The lower range of the majority of the meter appears to be near 0.2-0.3 ft/sec (see Appendix A and E). These levels are significantly below the propeller meter's minimum rate of 1.5 ft/sec and adequately covered the flow ranges at Pinal Creek except during the storm event when the meters' upper boundary for measurement was exceeded. The high range is still undetermined but smaller paddle sizes would have to be used since the elastic limit appeared to be close in a few of the meters that were calibrated near 1.5 ft/sec.

Both design #1 and design #2 meters are portable. Design #2 which floated on the surface was definitely easier to carry and setup. The initial cost of the complete system was about $6450, including computer and I/O hardware and software. Table 5.1 lists the major requirements and estimates their costs in studying the two stream locations at Pinal Creek.

Item	Quantity	Estimated Total Cost
Laptop Computer w/ I/O slot & 2 Batteries	1	$2500
LabVIEW software	1	$1300
Strain Gage Boards	2	$900
DAQ card and cable	1	$950
Strain Gage Meter	8	$800

Table 5.1 Low Flow Meter Design System Cost Estimates

The maintenance costs should be relatively small since there are no moving parts. Minor repair, i.e. soldering, readhering, applying protective coating, can be done at minimal cost. Protective carrying cases would be useful to minimize the jostling of the meters when being transported. This would definitely improve the meter's life

expectancy and keep maintenance costs down. The fatigue life of a meter still needs to be determined to assess the life expectancy of the gages. Operational costs are also small since the only ongoing cost is recharging the batteries. To assist in this, the laptop computer was shutdown between hourly readings. With this method, one battery lasted over 12 hours while operating four meters at each of two locations. Under current construction methods, a calibration channel is required, but if neck thicknesses between meters were consistent, a single calibration curve might be sufficient for the life expectancy of the meter.

This strain gage meter technology can measure velocity in a stream and appears to have the capability to be very accurate with good repeatability. Its low range is a definite improvement over current portable meters. The cost is fairly high to setup initially (although incremental cost of additional meters is only about $100) but comparable to other types of portable meters that might be used in an environmental field study. Both design #1 and design #2 meters look promising for measuring flow in low flow rate streams. More research needs to be done on the mean velocity coefficients appropriate for various depths and vegetative densities and the impact of measurements in the virtually stagnant vegetative side reaches in a stream.

REFERENCES

(1) Herschy, R.W.; *Streamflow Measurement*; Elsevier Applied Science, Pub., NY, 1985.

(2) U.S. Department of the Interior; *Water Measurement Manual, A Water Resources Technical Publication*; U.S. Government Printing Office: Denver, 1997, p. 4-3.

(3) Lee, J.K.; *Vegetative Resistance to Flow;* USGS, http://sflwww.er.usgs.gov/metadata/ sflwww/jklmet.html, 2000

(4) Cheremisinoff, N.P.; *Applied Fluid Flow Measurement*; Marcel Dekker, Inc., NY, 1979.

(5) Yen B,C.; Hydraulic *Resistance in Open Channels*, chapter in <u>Channel Flow Resistance: Centennial of Manning's Formula</u>; Yen, B.C. (Ed.); Water Resources Publications, Littleton, CO, 1991.

(6) U.S. Department of the Interior; *Water Measurement Manual, A Water Resources Technical Publication*; U.S. Government Printing Office: Denver, 1997, p. 4-12.

(7) Murdoch, Tom; Cheo, Martha; *Streamkeeper's Field Guide, Watershed Inventory and Stream Monitoring Methods*; The Adopt –A-Stream Foundation: Everett, WA 1999, p. 107.

(8) U.S. EPA; *Volunteer Stream Monitoring: A Methods Manual*; http:// www.epa.gov /OWOW/monitoring/volunteer/stream/vms51.html, 2000.

(9) U.S. Department of the Interior; *Water Measurement Manual, A Water Resources Technical Publication*; U.S. Government Printing Office: Denver, 1997, p. 13-1.

(10) U.S. Department of the Interior; *Water Measurement Manual, A Water Resources Technical Publication*; U.S. Government Printing Office: Denver, 1997, p. 13-1.

(11) U.S. Department of the Interior; *Water Measurement Manual, A Water Resources Technical Publication*; U.S. Government Printing Office: Denver, 1997, p. 10-2.

(12) U.S. Department of the Interior; *Water Measurement Manual, A Water Resources Technical Publication*; U.S. Government Printing Office: Denver, 1997, p. 10-26.

(13) Roland, Paul A., *The use of strain gauges to measure low velocity fluid flow*, Rev. Sci. Instrum., Vol 67, No. 6, June 1996, 2410-2414.

(14) U.S. EPA; *Volunteer Stream Monitoring: A Methods Manual*; http:// www.epa.gov /OWOW/monitoring/volunteer/stream/vms51.html, 2000.

(15) Montes, S.; *Hydraulics of Open Channel Flow*; ASCE Press, Inc., Reston, VA, 1988.

(16) National Instruments; *LabVIEW, QuickStart Guide*; National Instruments Corporation: Austin, TX 1999, p. 3-10.

(17) National Instruments; *DAQ, SC-2043-SG User Manual*; National Instruments Corporation: Austin, TX 1996, p. 2-1.

(18) Koelsch, R.S.; Unpublished Data; Department of Hydrology and Water Resources, University of Arizona, 1999.

(19) Murdoch, Tom; Cheo, Martha; *Streamkeeper's Field Guide, Watershed Inventory and Stream Monitoring Methods*; The Adopt –A-Stream Foundation: Everett, WA 1999, p. 112.

(20) Beer, Ferdinand P.; Johnston, Jr., E. Russell, *Mechanics of Materials*, McGraw-Hill Inc.: New York , 1981, p. 584.

(21) Mechanical Engineering and Applied Mechanics, University of Pennsylvania, Fall 1999 Semester, *Experiment #2: Strain Gage, Installation and Evaluation, Background*; http:// www.seas.upenn.edu/~meam247/fall/straingage/Straingage_main.htm, 1999.

(22) Roberson, John A.; Crowe, Clayton T.; *Engineering Fluid Mechanics*, John Wiley & Sons, Inc.: New York,1997, p. A-15.

(23) Roberson, John A.; Crowe, Clayton T.; *Engineering Fluid Mechanics*, John Wiley & Sons, Inc.: New York,1997, p. 431.

(24) Roberson, John A.; Crowe, Clayton T.; *Engineering Fluid Mechanics*, John Wiley & Sons, Inc.: New York,1997, p. 433.

Appendix A: Design #1 Meter Calibration Graphs
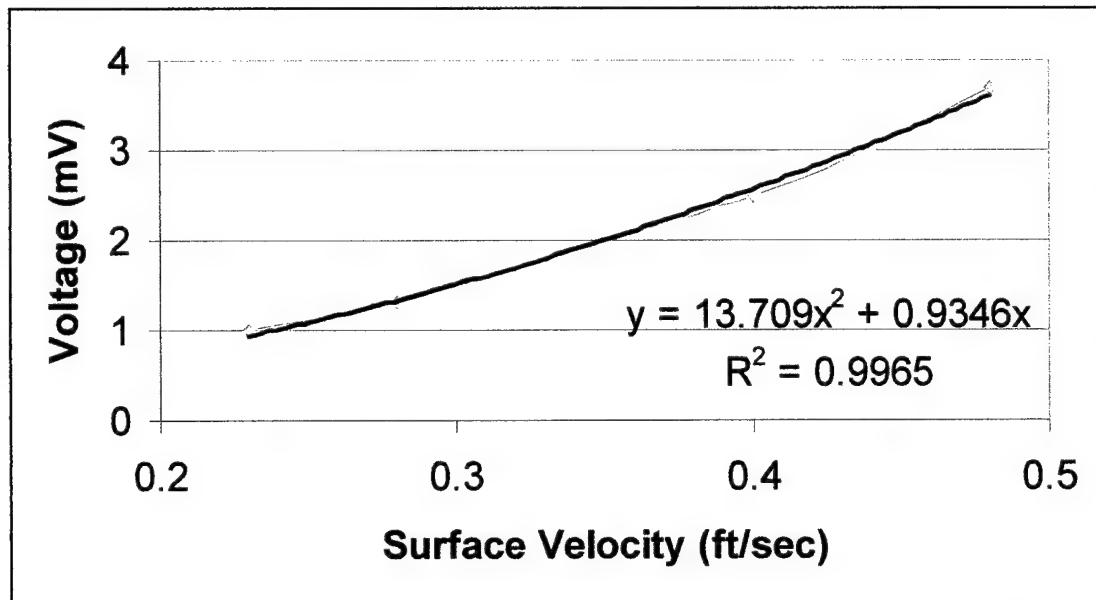
Figure A.1 Design #1 Double Strain Gage Meter 1, Bottom Paddle Calibration Plot
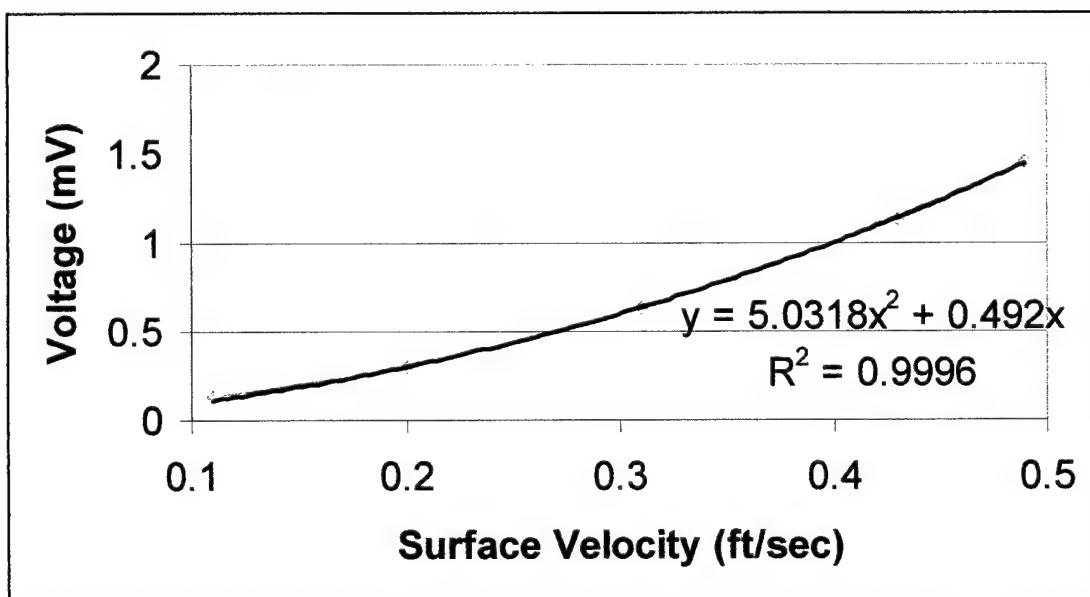
Figure A.2 Design #1 Double Strain Gage Meter 2, Bottom Paddle Calibration Plot
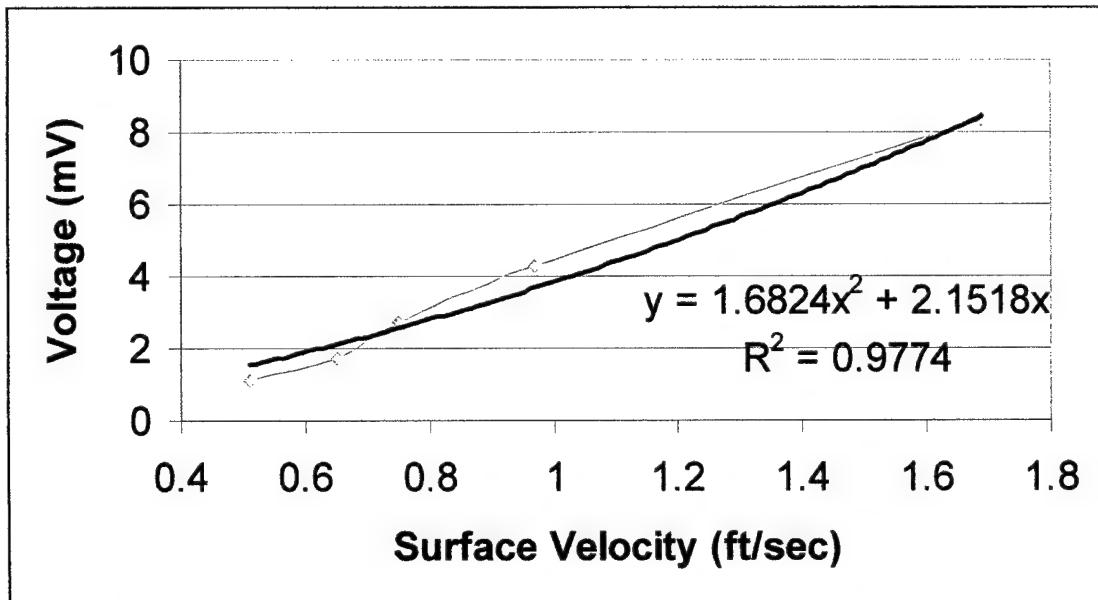
Figure A.3 Design #1 Single Strain Gage Meter 3, Calibration Plot
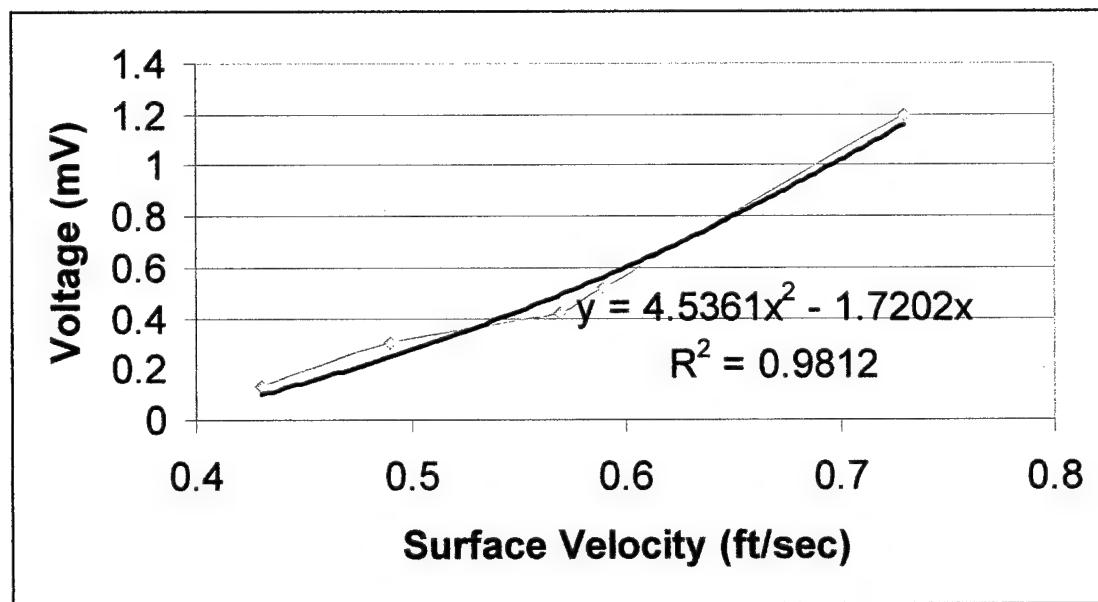
Figure A.4 Design #1 Single Strain Gage Meter 4, Calibration Plot
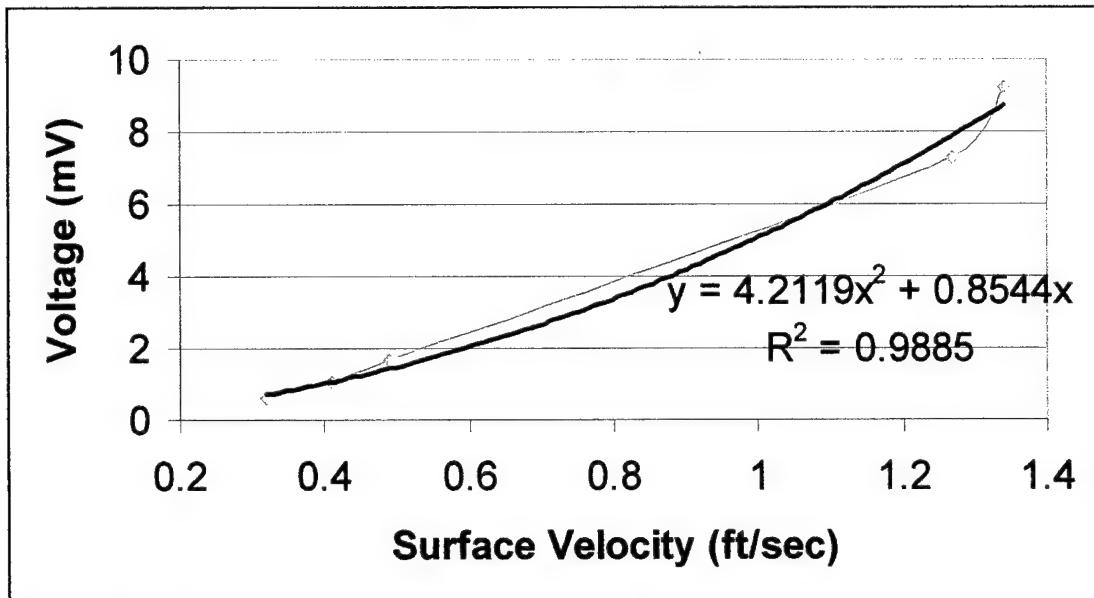
Figure A.5 Design #1 Double Strain Gage Meter 5, Top Meter Calibration Plot

$$y = 4.2119x^2 + 0.8544x$$
$$R^2 = 0.9885$$
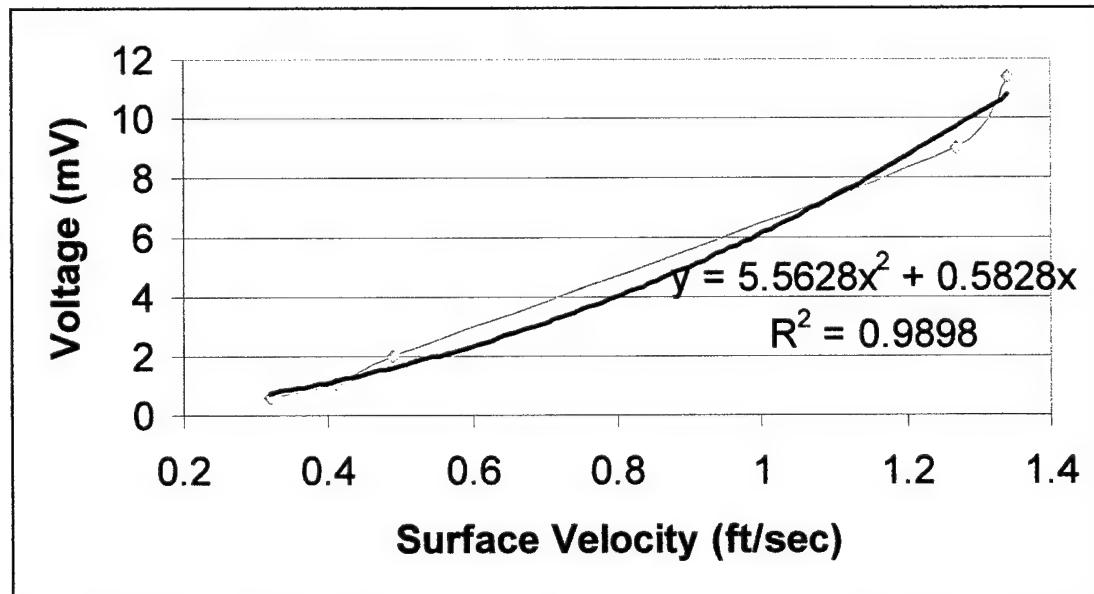
Figure A.6 Design #1 Double Strain Gage Meter 5, Bottom Meter Calibration Plot

$$y = 5.5628x^2 + 0.5828x$$
$$R^2 = 0.9898$$
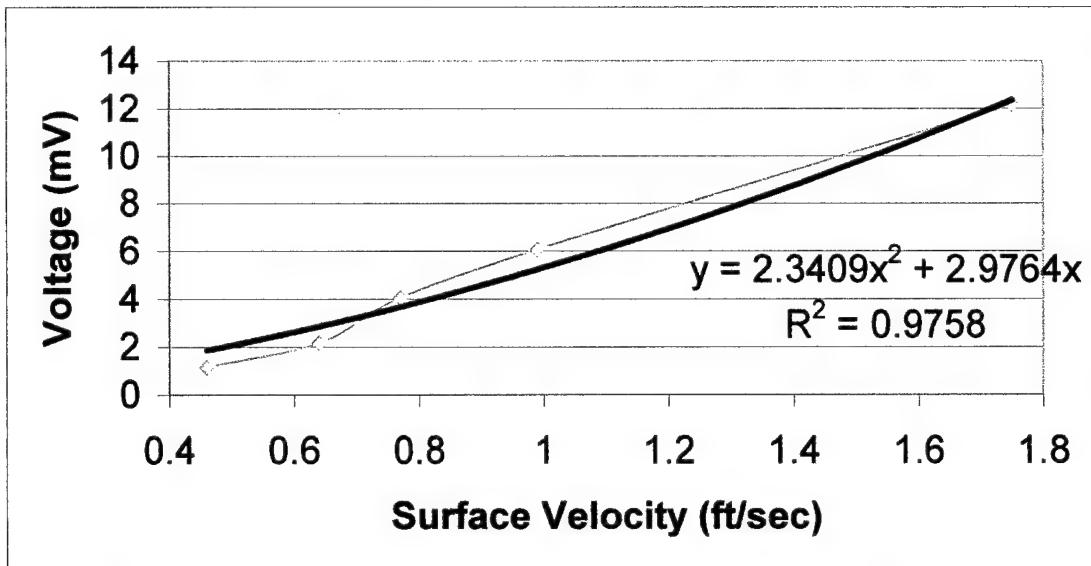
Figure A.7 Design #1 Single Strain Gage Meter 7, Calibration Plot

The chart shows Voltage (mV) vs Surface Velocity (ft/sec) with:
$y = 2.3409x^2 + 2.9764x$
$R^2 = 0.9758$
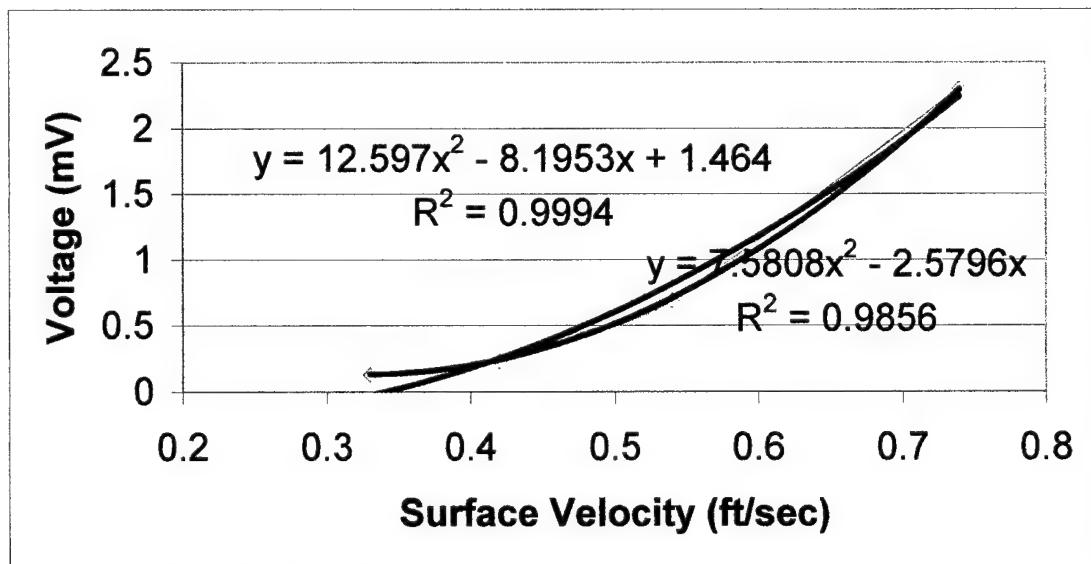
Figure A.8 Design #1 Single Strain Gage Meter 8, Calibration Plot

The chart shows Voltage (mV) vs Surface Velocity (ft/sec) with:
$y = 12.597x^2 - 8.1953x + 1.464$
$R^2 = 0.9994$

$y = 7.5808x^2 - 2.5796x$
$R^2 = 0.9856$

Appendix B: Repeatability Experiment: Point Error Response

Measured Voltage Reading	Measured Velocity Reading	Voltage Reading Based on Nonstandard Calibration Curve	% Error = Abs value $[(Volt_{calib}-Volt_{meas})/Volt_{calib}]*100$
0.095	0.143	.151	37.1%
0.31	0.246	0.195	59%
0.908	0.373	0.941	3.5%
1.86	0.462	1.92	3.1%
4	0.589	3.97	0.8%

Table B.1 Top Strain Gage Meter Repeatability Test Results w/ polynomial fit not through zero

Measured Voltage Reading	Measured Velocity Reading	Voltage Reading Based on Fig 8 Calibration Curve	% Error = Abs value $[(Volt_{calib}-Volt_{meas})/Volt_{calib}]$
0.182	0.143	0.116	56.9%
0.498	0.246	0.449	10.9%
1.09	0.373	1.15	5.2%
1.66	0.462	1.83	9.3%
2.49	0.589	3.07	18.9%

Table B.2 Bottom Strain Gage Meter Repeatability Test Results w/ Std Polynomial Fit

Measured Voltage Reading	Measured Velocity Reading	Voltage Reading Based on Fig 4.4 Calibration Curve	% Error = Abs value $[(Volt_{calib}-Volt_{meas})/Volt_{calib}]*100$
0.095	0.143	-0.276	134%
0.31	0.246	0.118	162%
0.908	0.373	1.29	29.5%
1.86	0.462	2.56	27.3%
4	0.589	5.01	20.2%

Table B.3 Top Strain Gage Meter Repeatability Test Results w/ polynomial fit through zero

Appendix C: Bromide Tracer Study at Pinal Creek – Jul 22, 1999 Time 1612-1718

Courtesy of: Roger Koelsch, U of A Hydrology Graduate Student

Location: Upstream of $J^2$7.5

Time	Ci (g/L)	Qi (mL/Min)	Cs (mg/L)	Qs (m^/s)	Comment
4	107	120	3.66	0.06212	
14	107	120	1.84	0.13169	Outlier, Not Averaged
26	107	120	3.71	0.06123	
44	107	120	3.22	0.07121	
58	107	120	3.05	0.07549	
			Average=	0.06751	or 2.38 $ft^3 \cdot s^{-1}$

Location: $J^2$7.5

Time	Ci (g/L)	Qi (mL/Min)	Cs (mg/L)	Qs (m^/s)	Comment
9	107	120	3.01	0.07657	
17	107	120	3.32	0.6892	
29	107	120	3.09	0.07443	
37	107	120	3.15	0.07291	
49	107	120	3.27	0.07005	
56	107	120	3.34	0.06848	
			Average=	0.07189	or 2.54 $ft^3 \cdot s^{-1}$

Location: $J^2$8

Time	Ci (g/L)	Qi (mL/Min)	Cs (mg/L)	Qs (m^/s)	Comment
11	107	120	2.5	0.09365	Plateau Not Reached, Not Averaged
20	107	120	2.85	0.08121	
31	107	120	2.88	0.0803	
40	107	120	2.9	0.0797	
52	107	120	2.87	0.0806	
61	107	120	2.87	0.0806	
			Average=	0.08048	or 2.84 $ft^3 \cdot s^{-1}$

C_i = Injection Conc. (Averaged Value)
Q_i = Injection Rate
C_s = Conc. In Stream
Q_s = Stream Flow Rate
C_b = Background Conc. (equals .215 mg/l)
Equation: $Q_s = (Q_i \cdot C_i)/(C_s - C_b)$

Appendix D: Design #1 Procedure for Flow Calculation of Field Data

Determine calibration curve for strain gage meters

Use Excel spreadsheet to determine water depth across stream's cross-sectional area

a) 1st Column: Use standard increments across stream starting from datum in feet

b) 2nd Column: Input height to top of depth gage from transit vertical level

c) 3rd Column: Input height from water to the top of depth gage at time t

d) 4th Column: Input transit vertical height to stream bed/ground

e) 5th Column: Calculate water depth at time t (=4th Column-3rd Column-2nd Column)

f) 6th Column: Average water depth between increment n and increment n+1 (=(5th Column$_n$+5th Column$_{n+1}$)/2)

g) 7th Column: Set negative average depths = 0 in situations were datum is several feet from water edge or sandbars

h) 8th Column: Determine water area in foot increments (= 6th Column * 1st Column)

i) 9th Column: Assign water area to applicable meter used in cross-sectional area

j) 10th- 13th Column: Assuming 4 meters used, list area assigned to meters 1-4 in columns 10-13, respectively

k) Bottom of 10th –13th Columns: Add total water area to be applied to each individual meter

Use corresponding voltage from field data for each meter at time t

Calculate surface velocity using calibration equations for each meter

Determine average velocity by multiplying coefficient of 0.9 x surface velocity

Multiply each individual meter's average velocity by the area determined in k) of excel spreadsheet to determine the total $ft^3 \cdot s^{-1}$ for each meter (For double gage meters, split the area from k) in two and multiply each meter by the split value and add for total $ft^3 \cdot s^{-1}$ for the meter)

Add the total $ft^3 \cdot s^{-1}$ for each meter to get a single total value for the stream at time t

Appendix E: Design #2 Meter Calibration Graphs

$$y = 3.6409x^2 - 0.9331x$$
$$R^2 = 0.9914$$
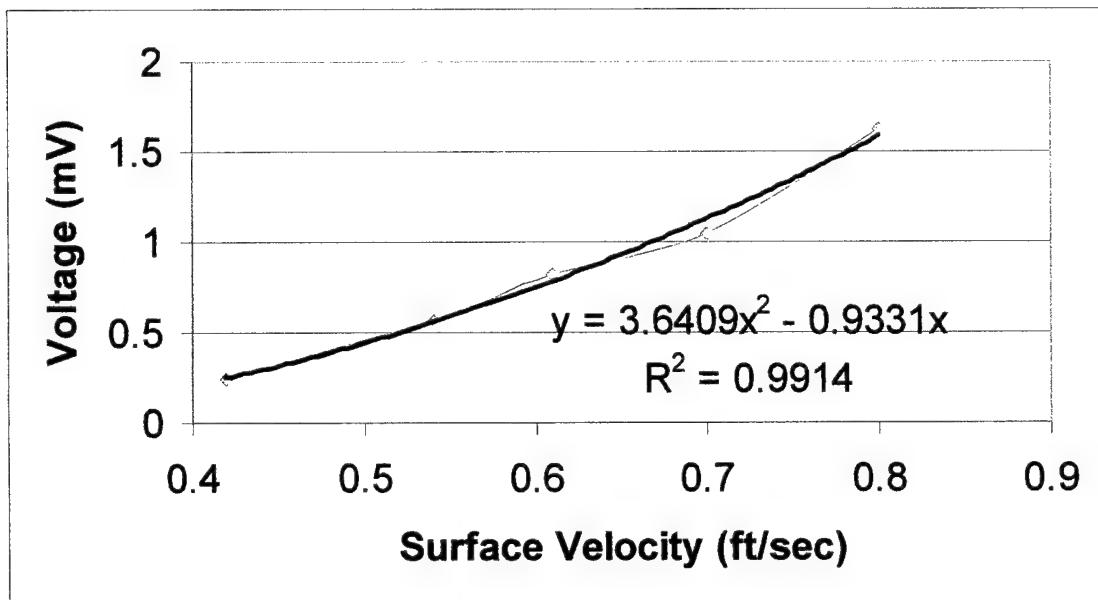
Figure E.1 Design #2 Strain Gage Meter 2 ($J^2$7.5), Calibration Plot

$$y = 3.5609x^2 + 0.1312x$$
$$R^2 = 0.9987$$
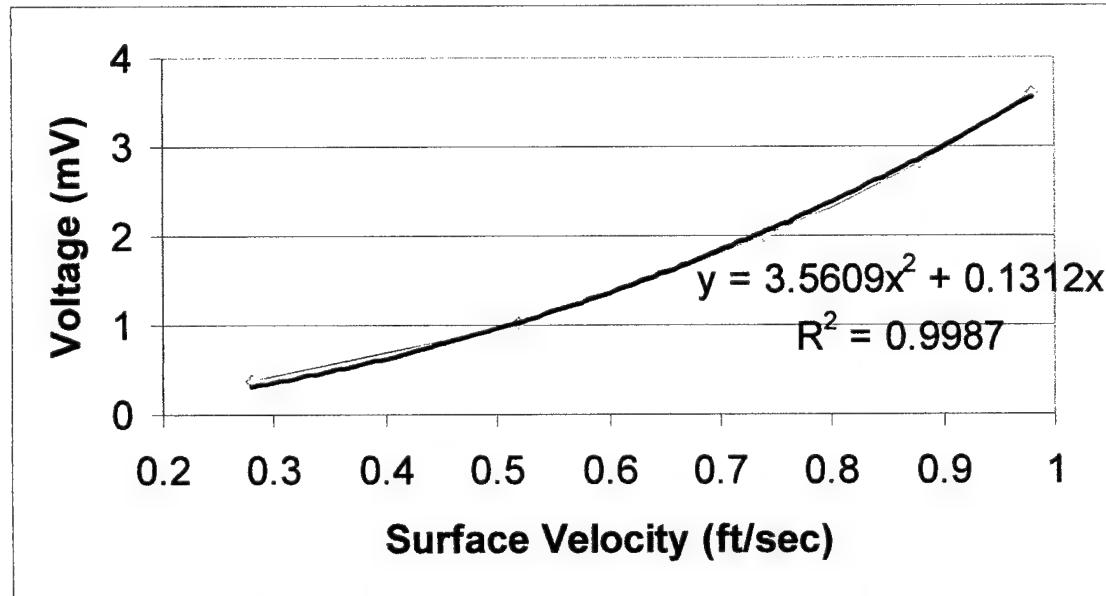
Figure E.2 Design #2 Strain Gage Meter 3 ($J^2$7.5), Calibration Plot
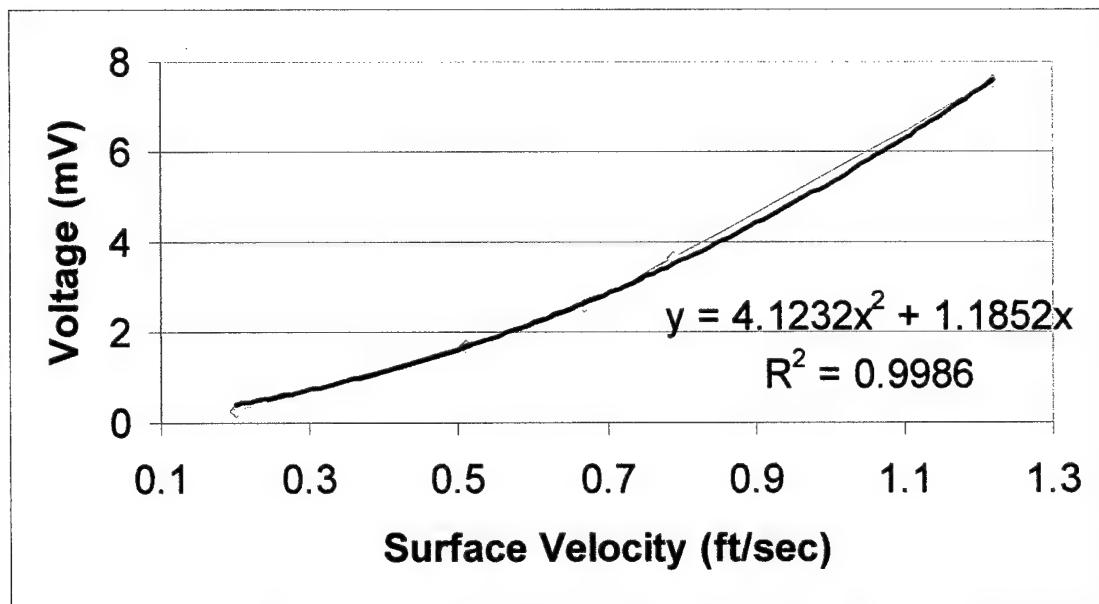
Figure E.3 Design #2 Strain Gage Meter 4 ($J^2$7.5), Calibration Plot

The plot shows Voltage (mV) on the y-axis (0 to 8) versus Surface Velocity (ft/sec) on the x-axis (0.1 to 1.3), with equation:

$$y = 4.1232x^2 + 1.1852x$$
$$R^2 = 0.9986$$
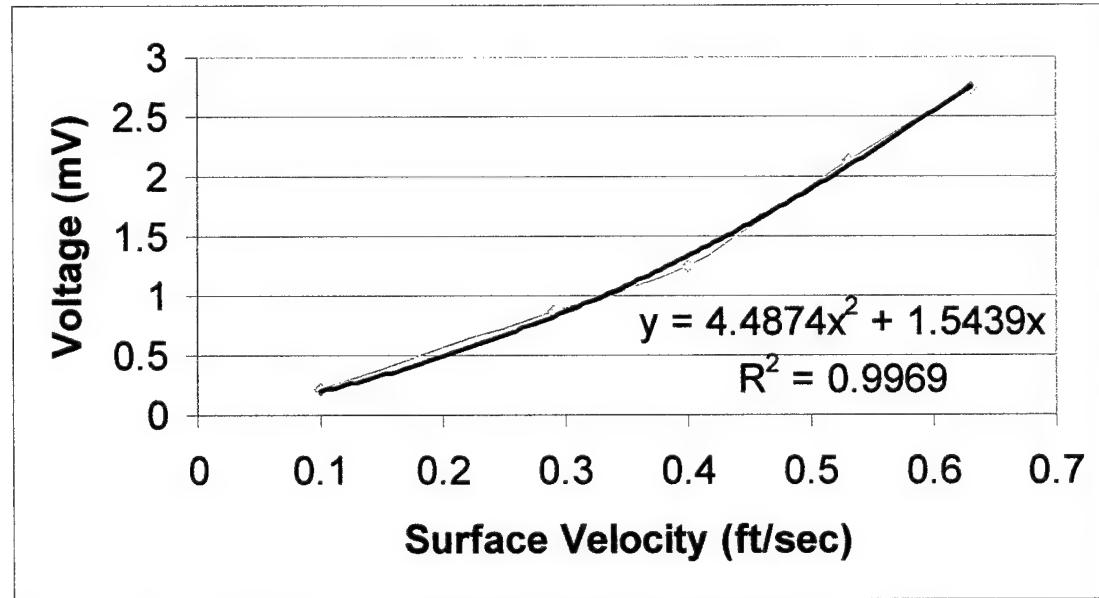
Figure E.4 Design #2 Strain Gage Meter 1 ($J^2$8), Calibration Plot

The plot shows Voltage (mV) on the y-axis (0 to 3) versus Surface Velocity (ft/sec) on the x-axis (0 to 0.7), with equation:

$$y = 4.4874x^2 + 1.5439x$$
$$R^2 = 0.9969$$
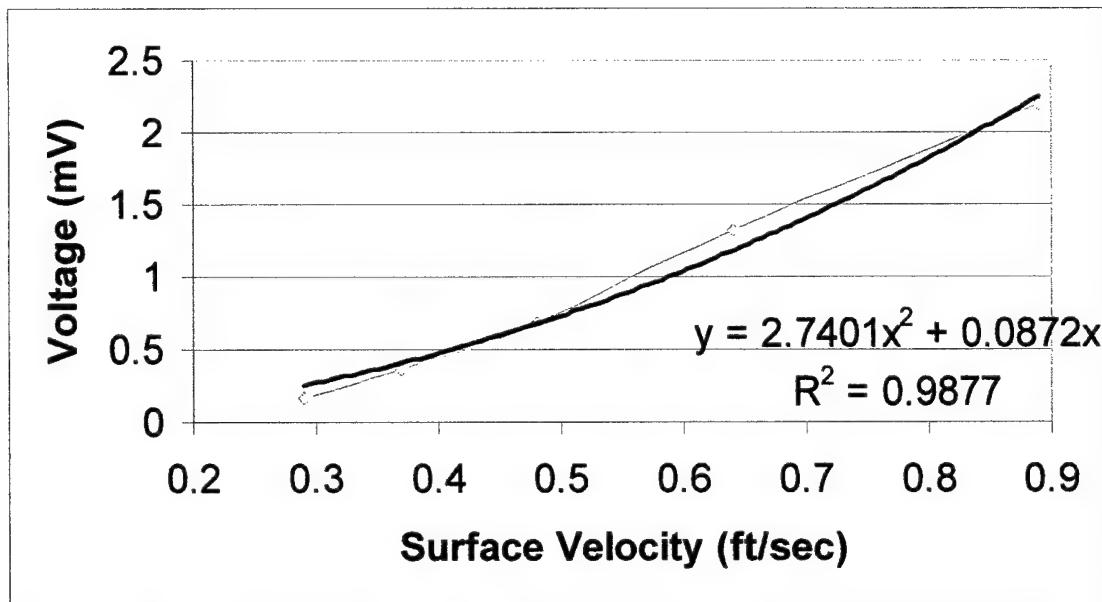
Figure E.5 Design #2 Strain Gage Meter 2 ($J^2$8), Calibration Plot
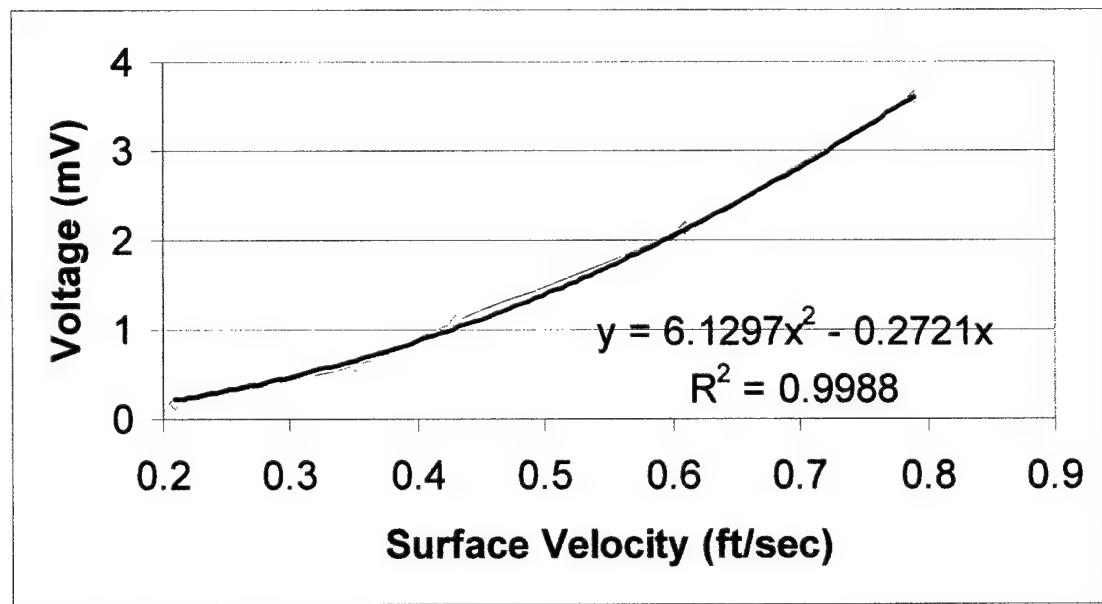
Figure E.6 Design #2 Strain Gage Meter 3 ($J^2$8), Calibration Plot
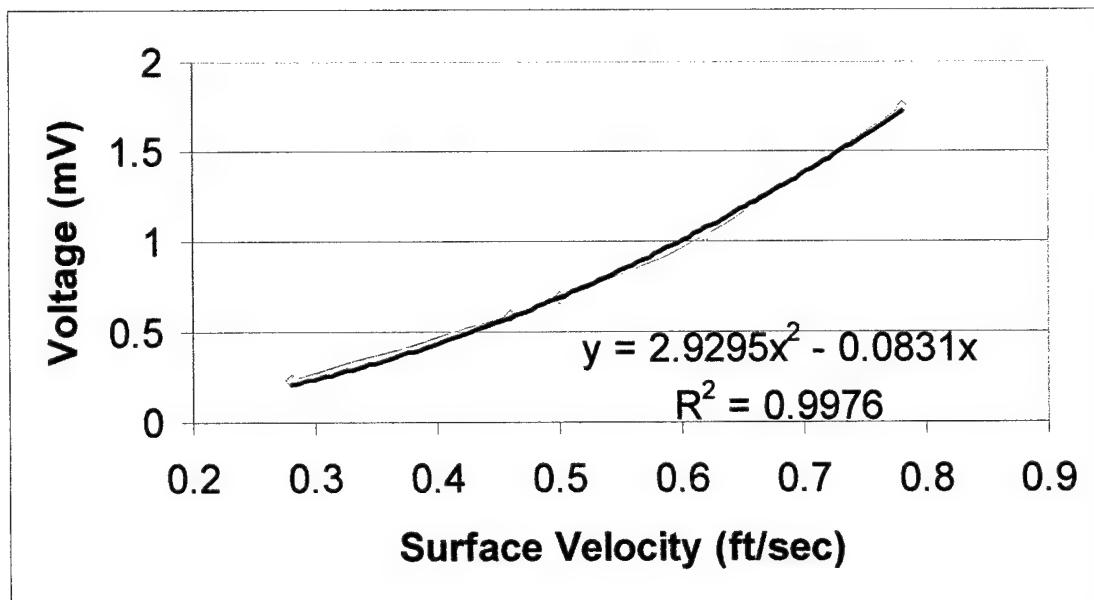
Figure E.7 Design #2 Strain Gage Meter 4 ($J^2$8), Calibration Plot

Appendix F: Design #2 Meter Calibration Extension Curves for Meters 1 and 2

$$y = 2.5099x^2 + 2.689x$$
$$R^2 = 0.9763$$
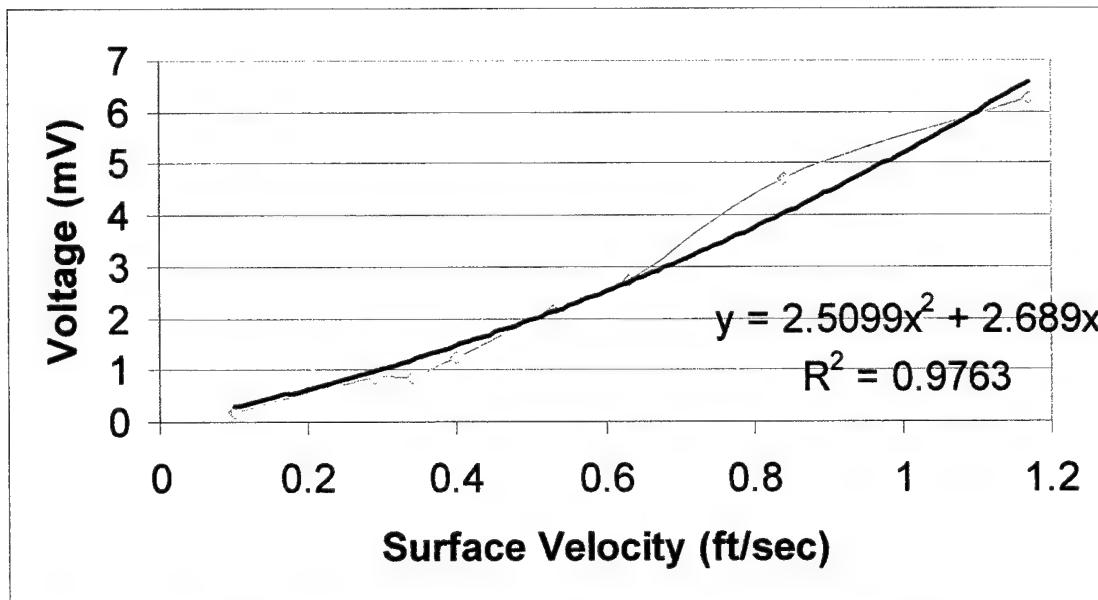
Figure F.1 Design #2 Strain Gage Meter 1 ($J^2$8), Calibration Extension Plot

$$y = 3.3179x^2 - 0.2238x$$
$$R^2 = 0.9963$$
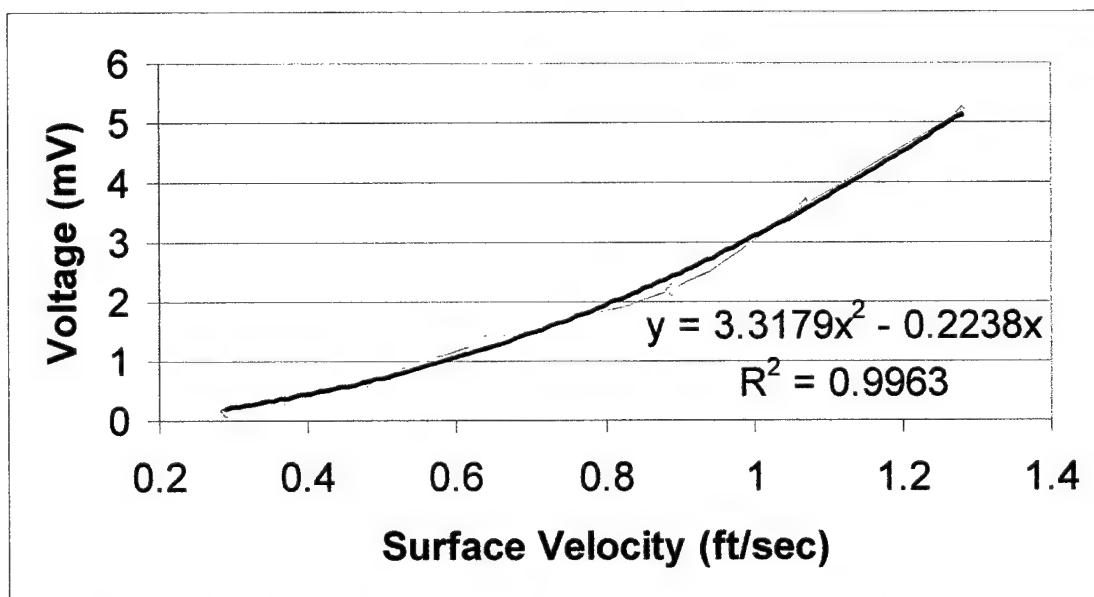
Figure F.2 Design #2 Strain Gage Meter 2 ($J^2$8), Calibration Extension Plot

Appendix G: Bromide Tracer Study at Pinal Creek – Dec 15, 1999 Time 1356-1506

Source Concentration Measured: 118.5 mg/l and 116.5 mg/l (Average 117.5 mg/l)
Background Bromide Concentration: ~0mg/l

Location: Upstream of $J^2 7.5$

Time	Ci (g/L)	Qi (mL/min)	Cs (mg/L)	Qs (m^3/s)
10	117.5	256.7	2.28	0.221
15	117.5	256.7	2.46	0.204
20	117.5	256.7	2.38	0.211
25	117.5	256.7	2.47	0.204
30	117.5	256.7	2.84	0.177
35	117.5	256.7	2.16	0.233
40	117.5	256.7	2.71	0.186
45	117.5	256.7	2.68	0.188
50	117.5	256.7	2.44	0.206
55	117.5	256.7	2.74	0.184
60	117.5	256.7	2.59	0.194
65	117.5	256.7	2.67	0.188
			Average	**0.200**
				or 7.04 $ft^3 \cdot s^{-1}$

Location: $J^2 7.5$ — Average — Values Taken at 3 Points Across Stream

Time	Ci (g/L)	Qi (mL/min)	Cs (mg/L)	Qs (m^3/s)	Pt 1	Pt 2	Pt 3
10	117.5	256.7	2.243333	0.224	2.75	2.32	1.66
15	117.5	256.7	2.303333	0.218	2.69	2.37	1.85
20	117.5	256.7	2.333333	0.215	2.77	2.37	1.86
25	117.5	256.7	2.416667	0.208	2.8	2.39	2.06
30	117.5	256.7	2.546667	0.197	2.83	2.55	2.26
35	117.5	256.7	2.506667	0.201	2.92	2.48	2.12
40	117.5	256.7	2.47	0.204	2.86	2.41	2.14
45	117.5	256.7	2.46	0.204	2.85	2.39	2.14
50	117.5	256.7	2.47	0.204	2.83	2.43	2.15
55	117.5	256.7	2.356667	0.213	2.78	2.26	2.03
60	117.5	256.7	2.42	0.208	2.81	2.36	2.09
65	117.5	256.7	2.43	0.207	2.72	2.42	2.15
70	117.5	256.7	2.643333	0.190	3.11	2.66	2.16
			Average	**0.207**			
				or 7.31 $ft^3 \cdot s^{-1}$			

Location: J²8			Average		Values Taken at 3 Points Across Stream		
Time	Ci (g/L)	Qi (mL/min)	Cs (mg/L)	Qs (m^3/s)	Pt 1	Pt 2	Pt 3
10	117.5	256.7	2.396667	0.210	2.3	2.57	2.32
15	117.5	256.7	2.553333	0.197	2.54	2.65	2.47
20	117.5	256.7	2.66	0.189	2.71	2.73	2.54
25	117.5	256.7	2.736667	0.184	2.82	2.74	2.65
30	117.5	256.7	2.76	0.182	2.83	2.79	2.66
35	117.5	256.7	2.773333	0.181	2.86	2.77	2.69
40	117.5	256.7	2.773333	0.181	2.86	2.82	2.64
45	117.5	256.7	2.74	0.184	2.84	2.75	2.63
50	117.5	256.7	2.716667	0.185	2.83	2.69	2.63
55	117.5	256.7	2.65	0.190	2.78	2.65	2.52
60	117.5	256.7	2.596667	0.194	2.73	2.59	2.47
65	117.5	256.7	2.553333	0.197	2.66	2.55	2.45
70	117.5	256.7	2.483333	0.202	2.65	2.44	2.36
			Average	**0.190**			
				or 6.72			
				ft³·s⁻¹			

Ci = Injection Conc. (Averaged Value)
Qi = Injection Rate
Cs = Conc. In Stream
Qs = Stream Flow Rate
Cb = Background Conc. (equals .215 mg/l)
Equation: Qs = (Qi*Ci)/(Cs-Cb)

The bromide analysis was conducted on a Dionex Model 500 IC on Feb 9, 2000. All stream samples were very high in sulfate. This sulfate peak area interfered with the bromide peak area. The area under the bromide peak was manually adjusted to neglect the sulfate interference. An example of the bromide peak area, manually adjusted, is found in Figure G.1. The sulfate peak area varied throughout the analysis but the bromide results remained relatively constant as expected with a constant feed source. Figures G.2-G.4 show the bromide results at each sampling point over the test period.

Sample Analysis Report

Sample Name : J7 55-1
Data File Name : C:\PEAKNET\DATA\KEVIN\KEVINBR3_054.DXD

Method File Name : c:\peaknet\method\kevin\kevin.met
Date Time Collected : 2/9/00 10:20:15 PM
System Operator : Kevin

Peak Information : All Peaks

Peak #	Component Name	Retention Time	Amount (ppm)	Peak Area	Peak Height
1	flouride	2.35	0.00	386906	70397
2	chloride	3.30	0.00	7227681	1049197
3	sulfate	4.28	0.00	117255116	7900389
4	bromide	5.60	2.78	124413	14568
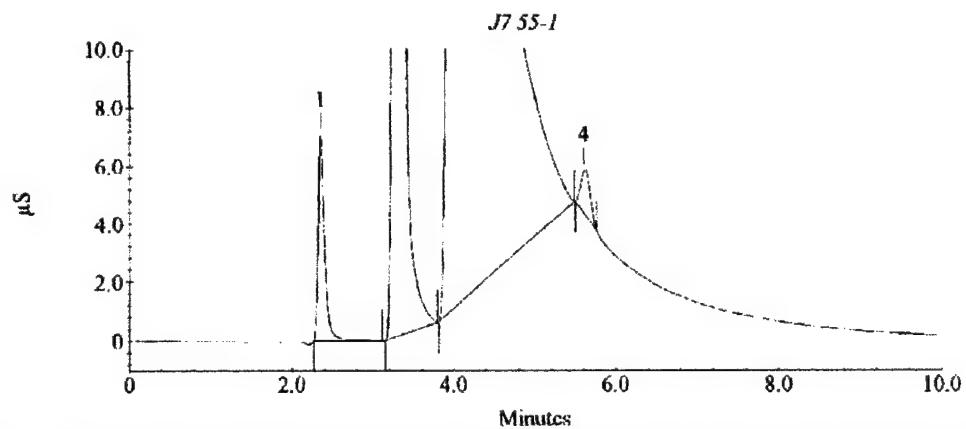
Figure G.1 Example of Bromide Tracer Study Results
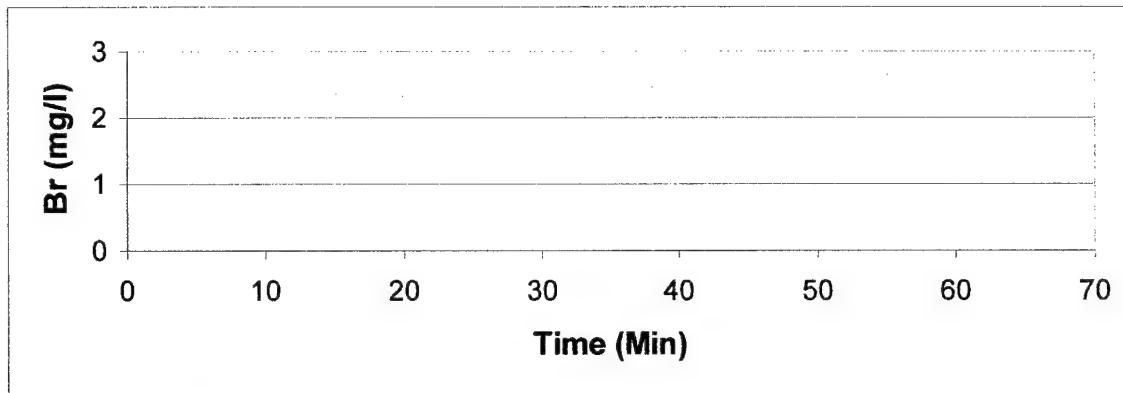
Figure G.2 Bromide Concentrations at Location Upstream of $J^2 7.5$
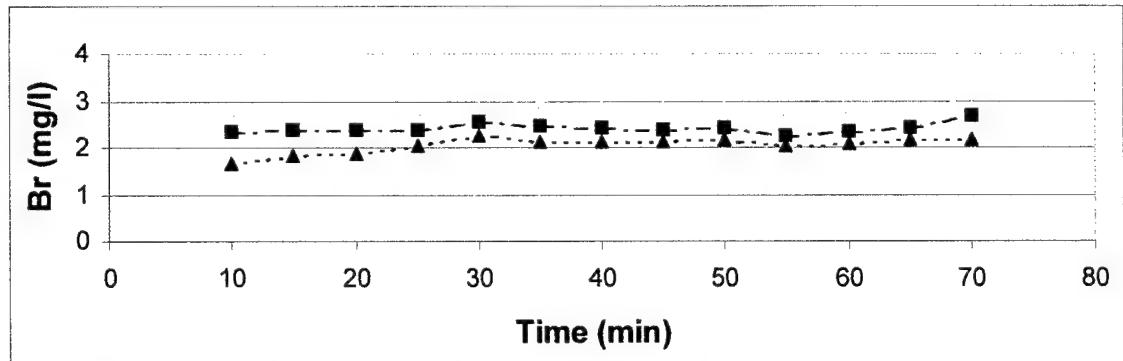
Figure G.3 Bromide Concentrations Taken at 3 Points Across $J^2 7.5$ Location
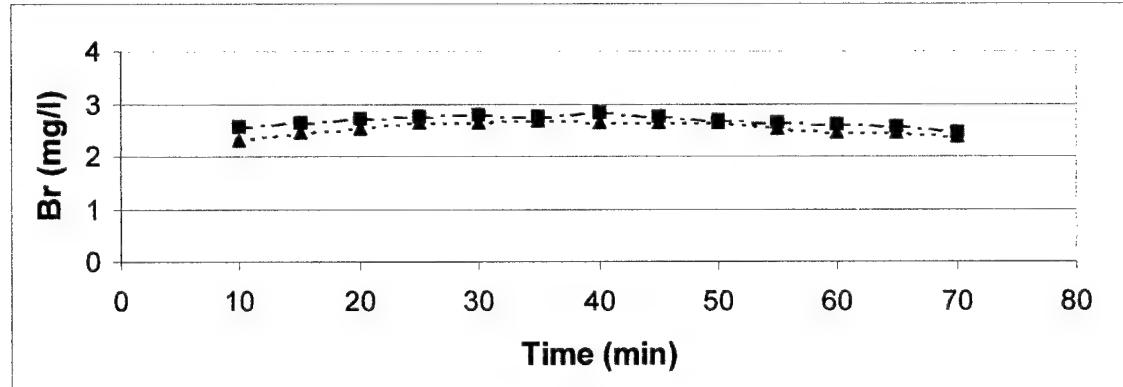
Figure G.4 Bromide Concentrations Taken at 3 Points Across $J^2 8$ Location

Appendix H: Calibration Curves for Design #2 Meters with Combinations of Vertical and Horizontal Full or Half Bridge Circuits

H.1 Full Bridge Circuits Calibration Curves
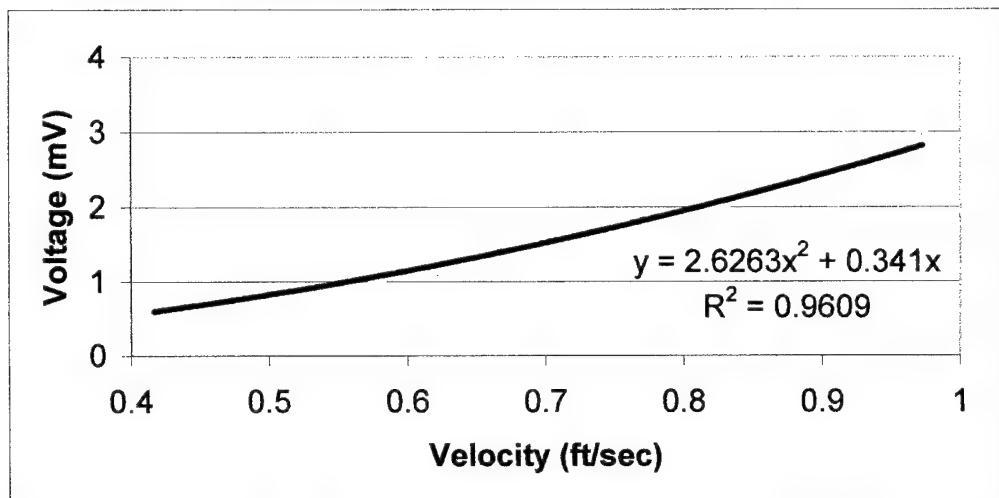
Figure H.1 Meter 1 w/ Vertical and Horizontal Strain Gages and 2" x 6" Paddle

The equation shown on the figure:
$$y = 2.6263x^2 + 0.341x$$
$$R^2 = 0.9609$$
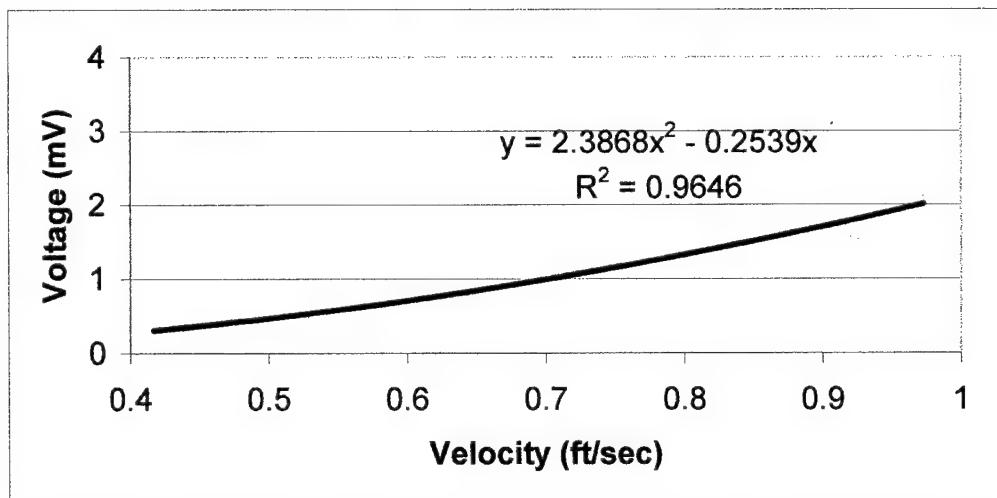
Figure H.2 Meter 2 w/ Vertical and Horizontal Strain Gages and 1.5" x 4" Paddle

The equation shown on the figure:
$$y = 2.3868x^2 - 0.2539x$$
$$R^2 = 0.9646$$

H.2 Horizontal Half Bridge Circuit Calibration Curves

$$y = -0.248x^2 + 0.4479x$$
$$R^2 = 0.7195$$
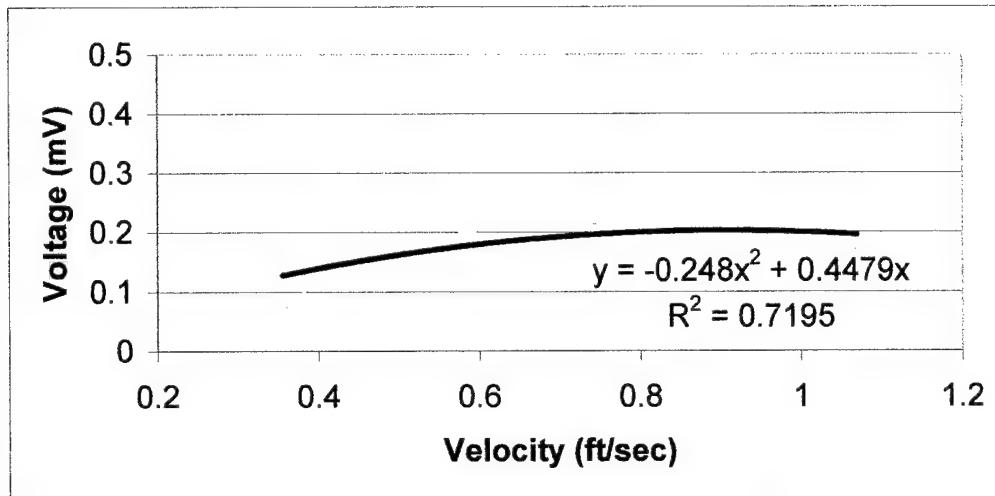
Figure H.3 Meter 1 w/ Vertical and Horizontal Strain Gages and 2" x 6" Paddle; Only Horizontal Strain Gages Connected in Half Bridge Circuit

$$y = 0.3782x^2 - 0.1431x$$
$$R^2 = 0.993$$
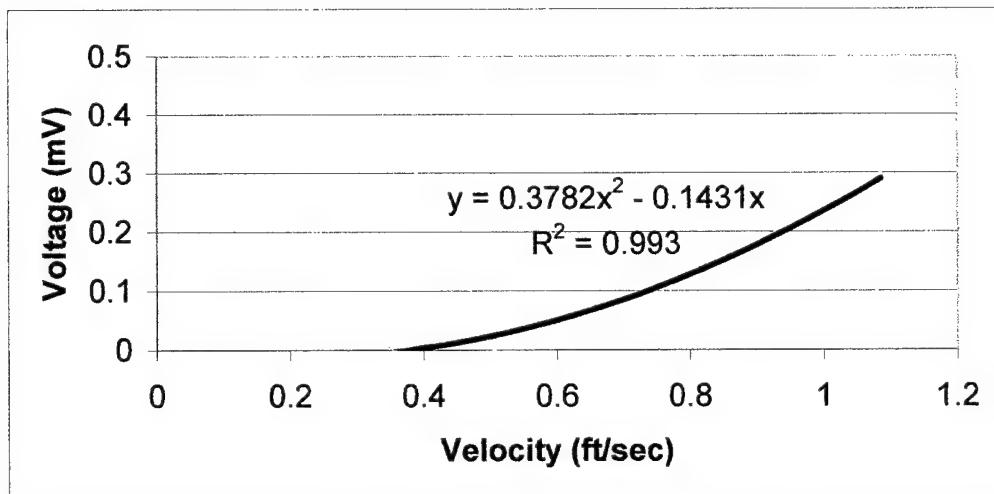
Figure H.4 Meter 2 w/ Vertical and Horizontal Strain Gages and 1.5" x 4" Paddle; Only Horizontal Strain Gages Connected in Half Bridge Circuit

H.3 Vertical Half Bridge Circuits Calibration Curves
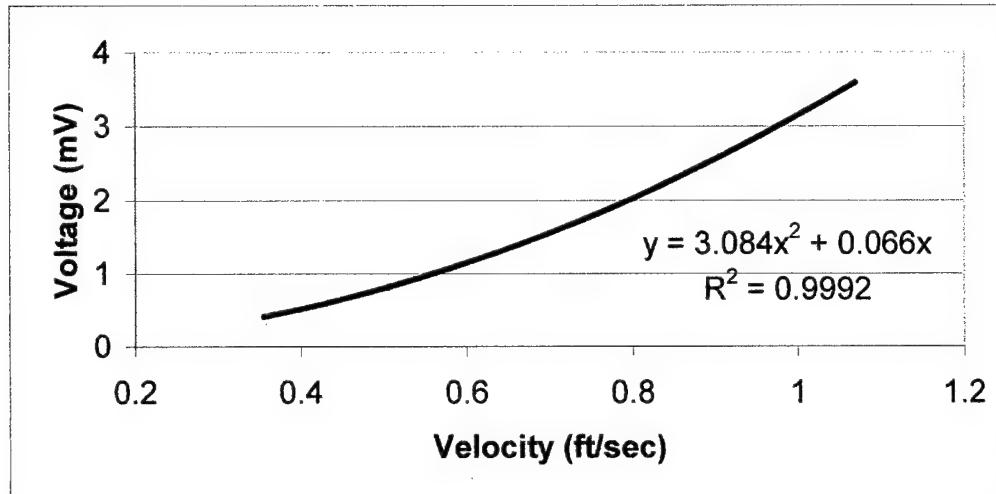
Figure H.5 Meter 1 w/ Vertical and Horizontal Strain Gages and 2" x 6" Paddle; Only
Vertical Strain Gages Connected in Half Bridge Circuit
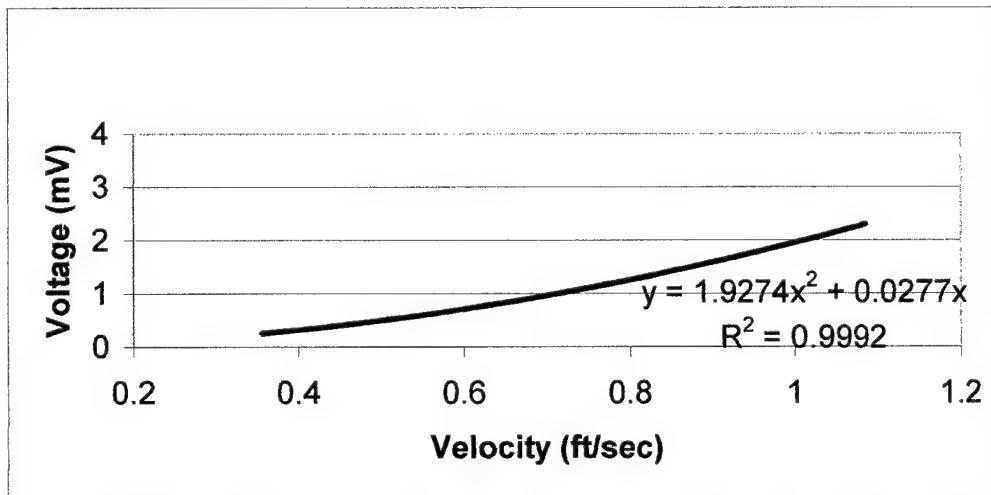
Figure H.6 Meter 2 w/ Vertical and Horizontal Strain Gages and 1.5" x 4" Paddle; Only
Vertical Strain Gages Connected in Half Bridge Circuit

Appendix I: Paddle Size Comparison Calibration Graphs

I.1 Variation of Paddle Height
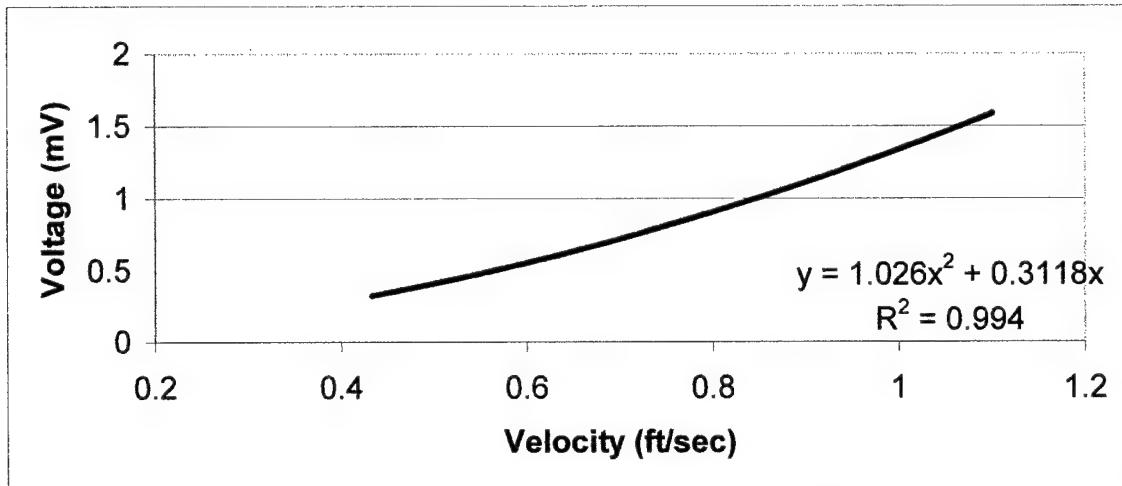
Figure I.1 Design #2 Strain Gage Meter 2 w/ 1.5" x 4" Paddle Calibration Plot

$$y = 1.026x^2 + 0.3118x$$
$$R^2 = 0.994$$
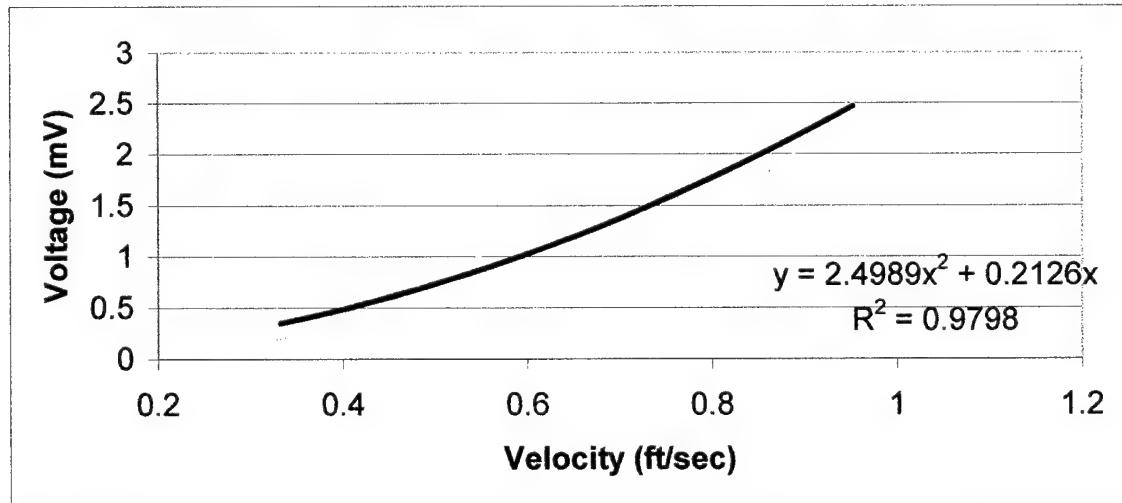
Figure I.2 Design #2 Strain Gage Meter 2 w/ 2" x 3" Paddle Calibration Plot

$$y = 2.4989x^2 + 0.2126x$$
$$R^2 = 0.9798$$

I.2 Paddle Area Variations
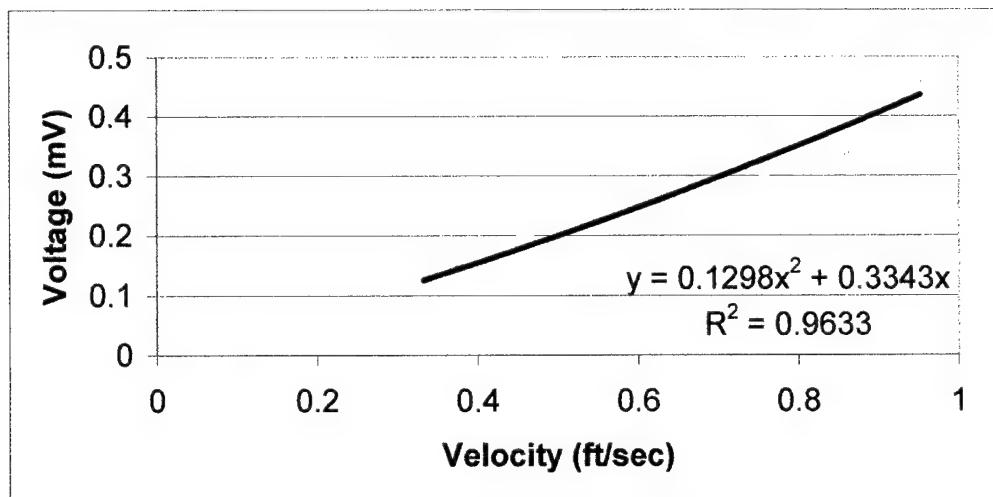
Figure I.3 Design #2 Strain Gage Meter 1 w/ 1.5" x 4" Paddle Calibration Plot

$y = 0.1298x^2 + 0.3343x$

$R^2 = 0.9633$
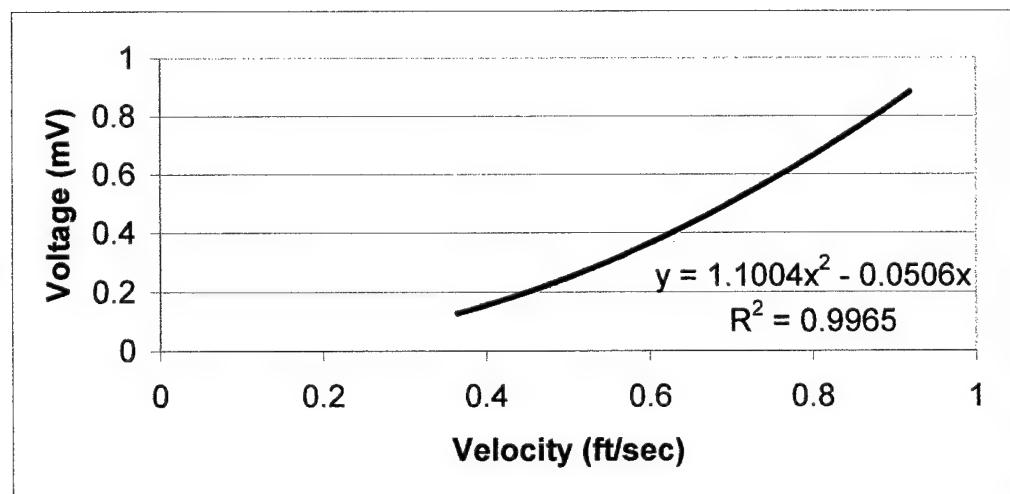
Figure I.4 Design #2 Strain Gage Meter 1 w/ 2" x 4.5" Paddle Calibration Plot

$y = 1.1004x^2 - 0.0506x$

$R^2 = 0.9965$
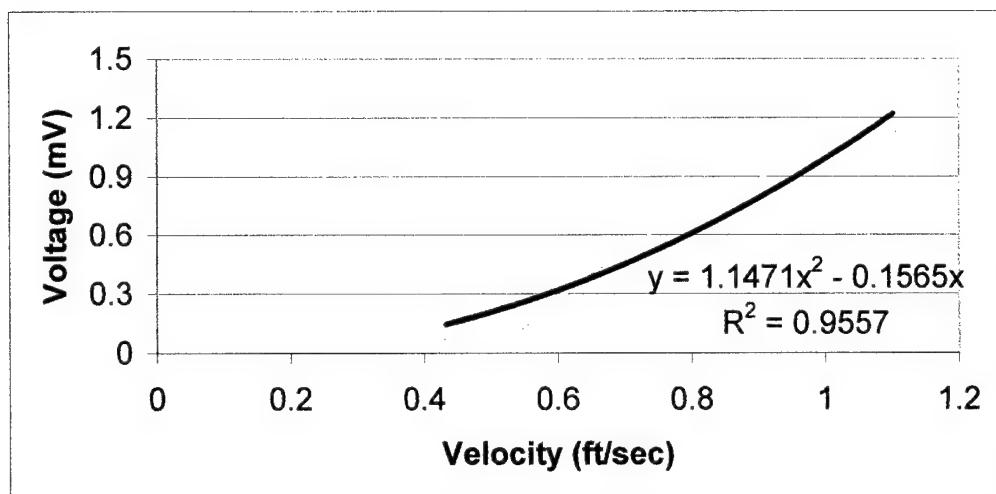
Figure I.5 Design #2 Strain Gage Meter 1 w/ 2" x 6" Paddle Calibration Plot

The plot shows Voltage (mV) versus Velocity (ft/sec) with the fitted curve $y = 1.1471x^2 - 0.1565x$ and $R^2 = 0.9557$.
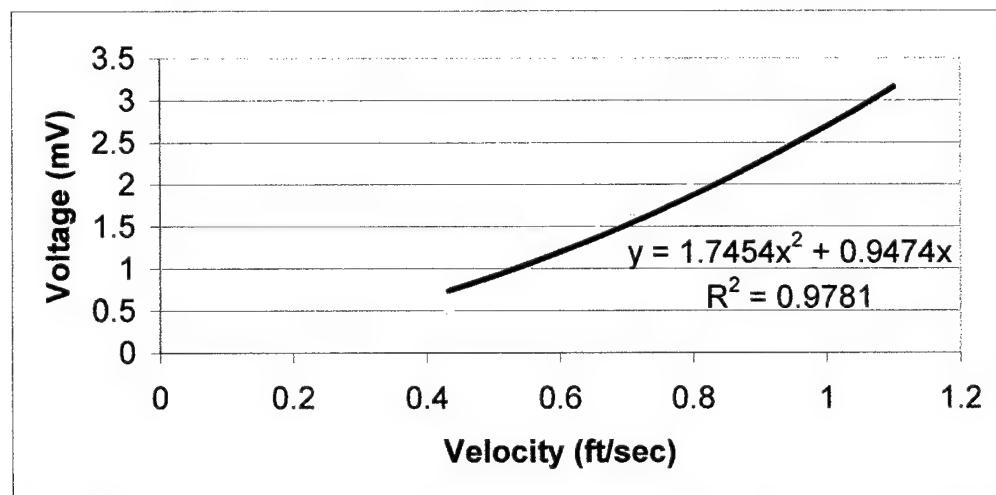
Figure I.6 Design #2 Strain Gage Meter 3 w/ 1.5" x 4" Paddle Calibration Plot

The plot shows Voltage (mV) versus Velocity (ft/sec) with the fitted curve $y = 1.7454x^2 + 0.9474x$ and $R^2 = 0.9781$.
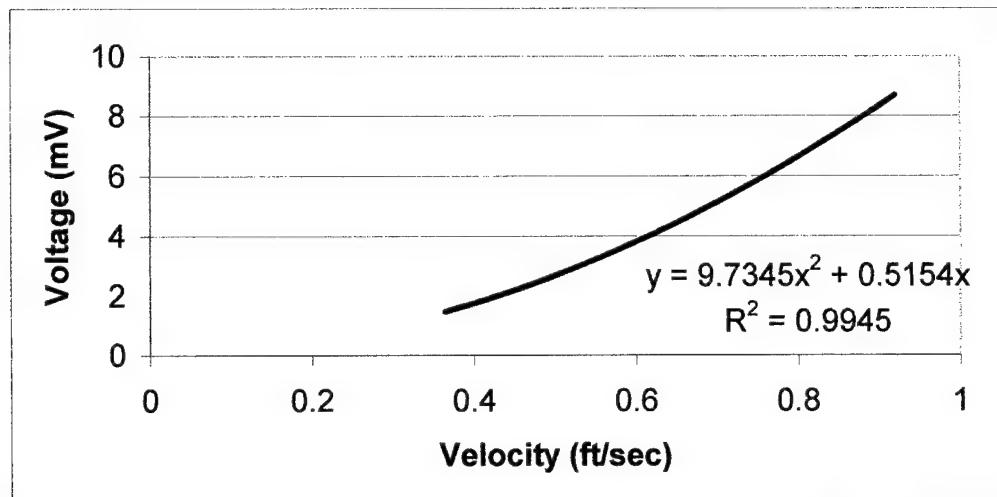
Figure I.7 Design #2 Strain Gage Meter 3 w/ 2" x 4.5" Paddle Calibration Plot

The first plot shows Voltage (mV) versus Velocity (ft/sec) with the fitted equation:

$$y = 9.7345x^2 + 0.5154x$$
$$R^2 = 0.9945$$
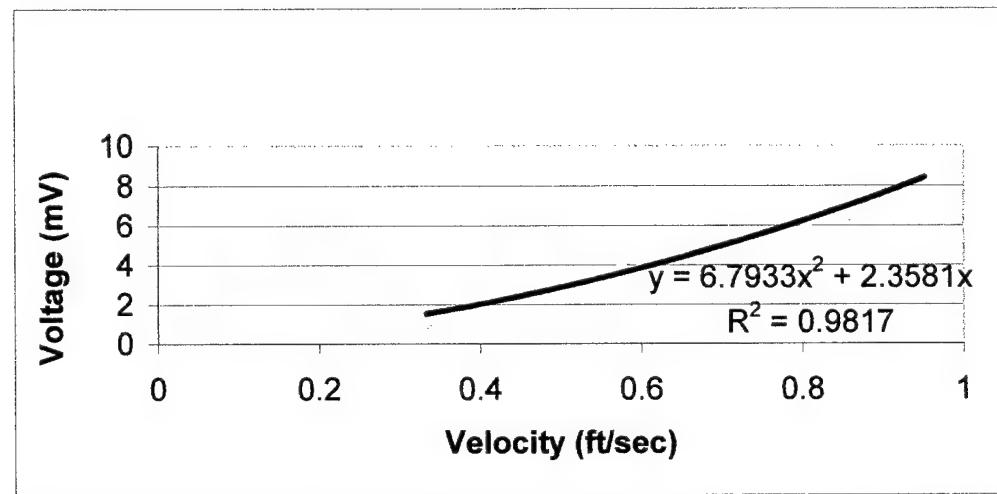
Figure I.8 Design #2 Strain Gage Meter 3 w/ 2" x 6" Paddle Calibration Plot

The second plot shows Voltage (mV) versus Velocity (ft/sec) with the fitted equation:

$$y = 6.7933x^2 + 2.3581x$$
$$R^2 = 0.9817$$

I.3 Side Wall Calibration Comparisons
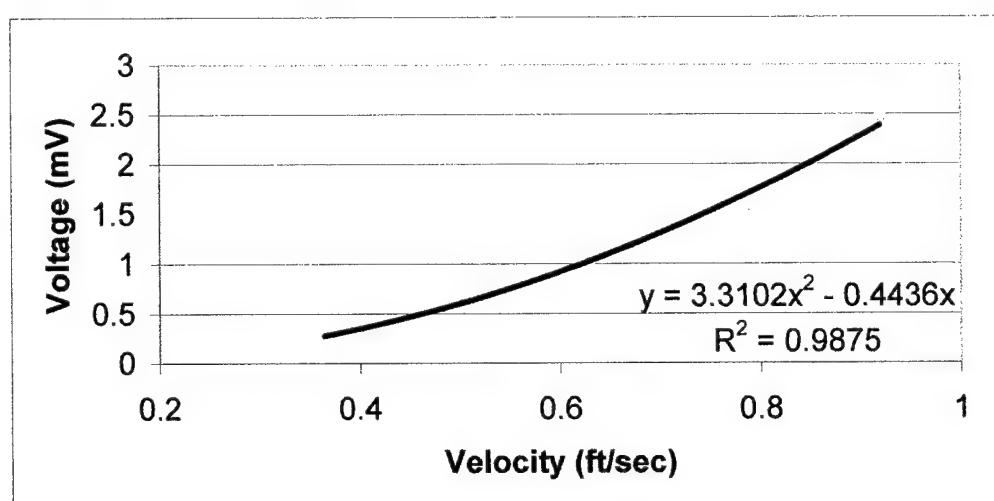
Figure I.9 Design #2 Strain Gage Meter 2 and 2" x 3" Paddle with Side Walls

The equation shown on the chart is $y = 3.3102x^2 - 0.4436x$ with $R^2 = 0.9875$.
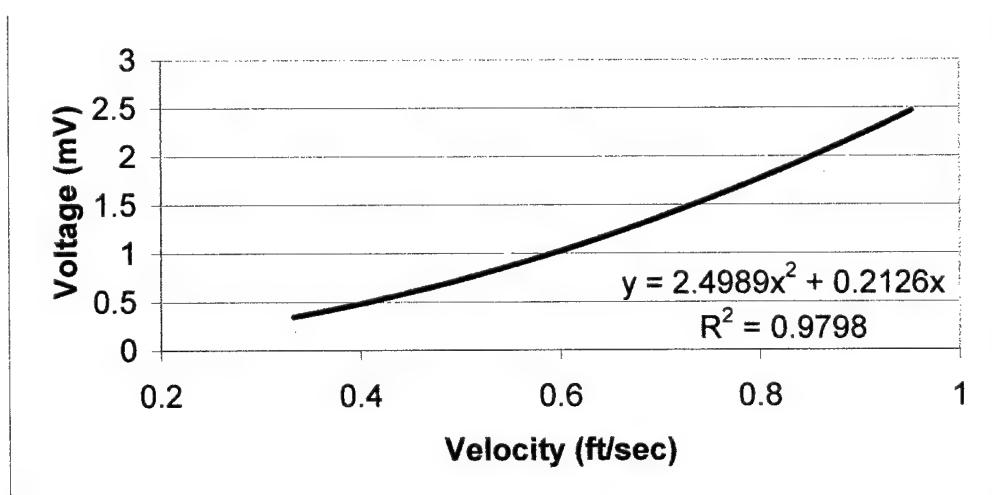
Figure I.10 Design #2 Strain Gage Meter 2 and 2" x 3" Paddle with No Side Walls

The equation shown on the chart is $y = 2.4989x^2 + 0.2126x$ with $R^2 = 0.9798$.
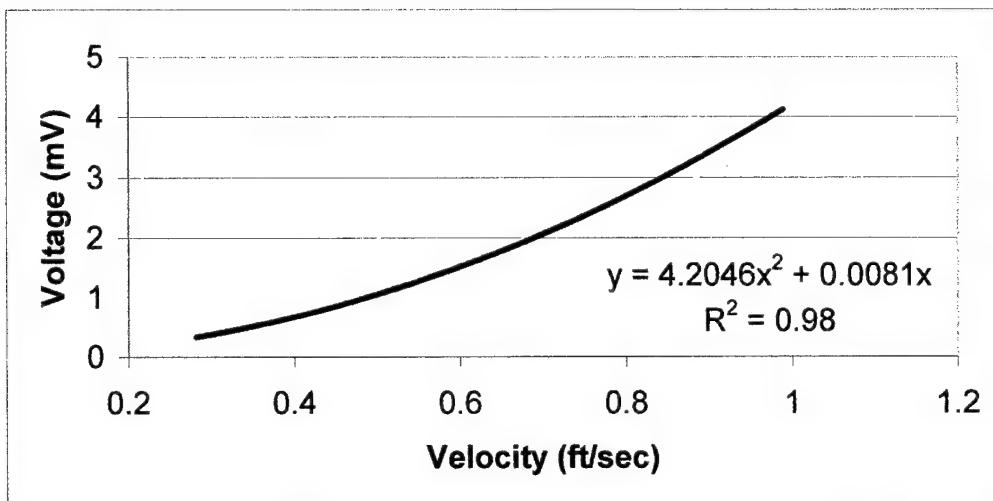
Figure I.11 Design #2 Strain Gage Meter 3 and 1.5" x 4" Paddle with Side Walls
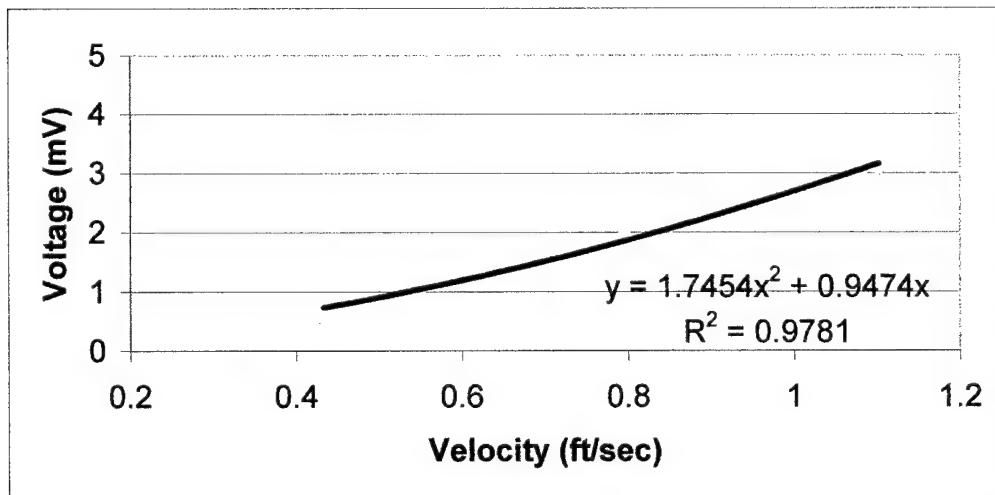
Figure I.12 Design #2 Strain Gage Meter 3 and 1.5" x 4" Paddle with No Side Walls

Appendix J

Vo	Horiz Deform	Length	dl/L	Angle	Calc Vel	Paddle Ht	P. Width	P. Area (sq in)	P.A. (sq ft)	Reynolds #	Drag Coef
0.22	0.02	0.75	0.027	1.53	0.326	1.50	4	6.00	0.042	3.33E+03	2
0.57	0.03	0.75	0.040	2.29	0.434	1.50	4	6.00	0.042	4.44E+03	2
0.88	0.04	0.75	0.053	3.05	0.524	1.50	4	5.99	0.042	5.36E+03	2
1.17	0.05	0.75	0.067	3.81	0.604	1.50	4	5.99	0.042	6.18E+03	2
1.53	0.06	0.75	0.080	4.57	0.698	1.50	4	5.98	0.042	7.12E+03	2
1.78	0.07	0.75	0.093	5.33	0.758	1.49	4	5.97	0.041	7.74E+03	2
2.14	0.08	0.75	0.107	6.09	0.841	1.49	4	5.97	0.041	8.56E+03	2
2.46	0.09	0.75	0.120	6.84	0.908	1.49	4	5.96	0.041	9.24E+03	2
2.78	0.1	0.75	0.133	7.59	0.970	1.49	4	5.95	0.041	9.85E+03	2
3.39	0.12	0.75	0.160	9.09	1.074	1.48	4	5.92	0.041	1.09E+04	2
3.91	0.14	0.75	0.187	10.57	1.147	1.47	4	5.90	0.041	1.15E+04	2
4.52	0.16	0.75	0.213	12.04	1.215	1.47	4	5.87	0.041	1.22E+04	2
5.04	0.18	0.75	0.240	13.50	1.258	1.46	4	5.83	0.041	1.25E+04	2
5.56	0.2	0.75	0.267	14.93	1.287	1.45	4	5.80	0.040	1.27E+04	2
5.96	0.22	0.75	0.293	16.35	1.299	1.44	4	5.76	0.040	1.28E+04	2
6.65	0.24	0.75	0.320	17.74	1.302	1.43	4	5.71	0.040	1.27E+04	2

Table J.1 Meter 2, Paddle 1.5"x4", Theoretical Results

Appendix J

Water Density	Force(x) on Paddle	Mod of Elasticity	thickness (=ft)	t (inches)
1.94	0.0086	1.00E+07	0.00200	0.024029
1.94	0.0152	1.00E+07	0.00212	0.025407
1.94	0.0222	1.00E+07	0.00218	0.026185
1.94	0.0294	1.00E+07	0.00223	0.026719
1.94	0.0392	1.00E+07	0.00231	0.027664
1.94	0.0463	1.00E+07	0.00231	0.027776
1.94	0.0568	1.00E+07	0.00237	0.028438
1.94	0.0661	1.00E+07	0.00240	0.02877
1.94	0.0754	1.00E+07	0.00242	0.029013
1.94	0.0920	1.00E+07	0.00243	0.029177
1.94	0.1045	1.00E+07	0.00241	0.028918
1.94	0.1167	1.00E+07	0.00239	0.028694
1.94	0.1243	1.00E+07	0.00235	0.028181
1.94	0.1293	1.00E+07	0.00230	0.027565
1.94	0.1310	1.00E+07	0.00223	0.026818
1.94	0.1305	1.00E+07	0.00217	0.026021

Table J.1 Meter 2, Paddle 1.5"x4", Theoretical Results

Vo	Horiz Deform	Length	dl/L	Angle	Calc Vel	Paddle Ht	P. Width	P. Area (sq in)	P.A. (sq ft)	Reynolds #
0.22	0.02	0.75	0.027	1.53	0.315	2.00	3	6.00	0.042	4.30E+03
0.57	0.03	0.75	0.040	2.29	0.445	2.00	3	6.00	0.042	6.08E+03
0.88	0.04	0.75	0.053	3.05	0.551	2.00	3	5.99	0.042	7.52E+03
1.17	0.05	0.75	0.067	3.81	0.641	2.00	3	5.99	0.042	8.74E+03
1.53	0.06	0.75	0.080	4.57	0.742	1.99	3	5.98	0.042	1.01E+04
1.78	0.07	0.75	0.093	5.33	0.805	1.99	3	5.97	0.041	1.09E+04
2.14	0.08	0.75	0.107	6.09	0.884	1.99	3	5.97	0.041	1.20E+04
2.46	0.09	0.75	0.120	6.84	0.944	1.99	3	5.96	0.041	1.28E+04
2.78	0.1	0.75	0.133	7.59	0.994	1.98	3	5.95	0.041	1.35E+04
3.39	0.12	0.75	0.160	9.09	1.062	1.97	3	5.92	0.041	1.43E+04
3.91	0.14	0.75	0.187	10.57	1.091	1.97	3	5.90	0.041	1.47E+04

Table J.2 Meter 2, Paddle 2" x 3", Theoretical Experiment

Drag Coef	Water Density	Force(x) on Paddle	Mod of Elasticity	thickness (=ft)	t (inches)
2	1.94	0.0080	1.00E+07	0.00196	0.023501166
2	1.94	0.0160	1.00E+07	0.00216	0.025863152
2	1.94	0.0245	1.00E+07	0.00226	0.027073952
2	1.94	0.0332	1.00E+07	0.00232	0.027802867
2	1.94	0.0444	1.00E+07	0.00240	0.028827581
2	1.94	0.0521	1.00E+07	0.00241	0.028890957
2	1.94	0.0628	1.00E+07	0.00245	0.029409864
2	1.94	0.0715	1.00E+07	0.00246	0.029528649
2	1.94	0.0792	1.00E+07	0.00246	0.029492443
2	1.94	0.0900	1.00E+07	0.00241	0.0289655
2	1.94	0.0946	1.00E+07	0.00233	0.027976456

Table J.2 Meter 2, Paddle 2" x 3", Theoretical Experiment

Vo	Horiz Deform	Length	dl/L	Angle	Calc Vel	Paddle Ht	P. Width	P. Area (sq in)	P.A. (sq ft)	Reynolds #	Drag Coef
0.17	0.02	0.75	0.027	1.53	0.221	1.50	4	6.00	0.042	2.26E+03	2
0.29	0.03	0.75	0.040	2.29	0.251	1.50	4	6.00	0.042	2.57E+03	2
0.48	0.04	0.75	0.053	3.05	0.297	1.50	4	5.99	0.042	3.04E+03	2
0.68	0.05	0.75	0.067	3.81	0.344	1.50	4	5.99	0.042	3.51E+03	2
0.88	0.06	0.75	0.080	4.57	0.388	1.50	4	5.98	0.042	3.96E+03	2
1.07	0.07	0.75	0.093	5.33	0.428	1.49	4	5.97	0.041	4.37E+03	2
1.28	0.08	0.75	0.107	6.09	0.470	1.49	4	5.97	0.041	4.79E+03	2
1.45	0.09	0.75	0.120	6.84	0.503	1.49	4	5.96	0.041	5.12E+03	2
1.66	0.1	0.75	0.133	7.59	0.541	1.49	4	5.95	0.041	5.49E+03	2
2.04	0.12	0.75	0.160	9.09	0.604	1.48	4	5.92	0.041	6.11E+03	2
2.38	0.14	0.75	0.187	10.57	0.653	1.47	4	5.90	0.041	6.58E+03	2
2.74	0.16	0.75	0.213	12.04	0.699	1.47	4	5.87	0.041	7.01E+03	2
3.14	0.18	0.75	0.240	13.50	0.742	1.46	4	5.83	0.041	7.40E+03	2
3.3	0.2	0.75	0.267	14.93	0.757	1.45	4	5.80	0.040	7.50E+03	2
3.74	0.22	0.75	0.293	16.35	0.791	1.44	4	5.76	0.040	7.78E+03	2

Figure J.3 Meter 3, Paddle 1.5" x 4", Theoretical Experimetn

Water Density	Force(x) on Paddle	Mod of Elasticity	thickness (=ft)	t (inches)
1.94	0.0039	1.00E+07	0.00155	0.018544
1.94	0.0051	1.00E+07	0.00147	0.01764
1.94	0.0071	1.00E+07	0.00149	0.017934
1.94	0.0095	1.00E+07	0.00153	0.01834
1.94	0.0121	1.00E+07	0.00156	0.01871
1.94	0.0148	1.00E+07	0.00158	0.018974
1.94	0.0178	1.00E+07	0.00161	0.019314
1.94	0.0203	1.00E+07	0.00162	0.019406
1.94	0.0234	1.00E+07	0.00164	0.019657
1.94	0.0291	1.00E+07	0.00166	0.019879
1.94	0.0339	1.00E+07	0.00166	0.019877
1.94	0.0387	1.00E+07	0.00165	0.019859
1.94	0.0433	1.00E+07	0.00165	0.019832
1.94	0.0448	1.00E+07	0.00161	0.019361
1.94	0.0485	1.00E+07	0.00161	0.019265

Figure J.3 Meter 3, Paddle 1.5" x 4", Theoretical Experimetn

Vo	Horiz Deform	Length	dl/L	Angle	Calc Vel	Paddle Ht	P. Width	P. Area (sq in)	P.A. (sq ft)	Reynolds #	Drag Coef
0.17	0.02	0.75	0.027	1.53	0.271	2.00	4.5	9.00	0.062	3.70E+03	2
0.29	0.03	0.75	0.040	2.29	0.282	2.00	4.5	8.99	0.062	3.85E+03	2
0.48	0.04	0.75	0.053	3.05	0.300	2.00	4.5	8.99	0.062	4.09E+03	2
0.68	0.05	0.75	0.067	3.81	0.318	2.00	4.5	8.98	0.062	4.34E+03	2
0.88	0.06	0.75	0.080	4.57	0.336	1.99	4.5	8.97	0.062	4.58E+03	2
1.07	0.07	0.75	0.093	5.33	0.354	1.99	4.5	8.96	0.062	4.81E+03	2
1.28	0.08	0.75	0.107	6.09	0.373	1.99	4.5	8.95	0.062	5.06E+03	2
1.45	0.09	0.75	0.120	6.84	0.388	1.99	4.5	8.94	0.062	5.26E+03	2
1.66	0.1	0.75	0.133	7.59	0.406	1.98	4.5	8.92	0.062	5.50E+03	2
2.04	0.12	0.75	0.160	9.09	0.439	1.97	4.5	8.89	0.062	5.93E+03	2
2.38	0.14	0.75	0.187	10.57	0.469	1.97	4.5	8.85	0.061	6.29E+03	2
2.74	0.16	0.75	0.213	12.04	0.499	1.96	4.5	8.80	0.061	6.67E+03	2
3.14	0.18	0.75	0.240	13.50	0.532	1.94	4.5	8.75	0.061	7.07E+03	2
3.3	0.2	0.75	0.267	14.93	0.545	1.93	4.5	8.70	0.060	7.20E+03	2
3.74	0.22	0.75	0.293	16.35	0.581	1.92	4.5	8.64	0.060	7.61E+03	2

Figure J.4 Meter 3, Paddle 2" x 4.5", Theoretical Experiments

Water Density	Force(x) on Paddle	Mod of Elasticity	thickness (=ft)	t (inches)
1.94	0.0089	1.00E+07	0.00203	0.024324
1.94	0.0096	1.00E+07	0.00182	0.02183
1.94	0.0109	1.00E+07	0.00172	0.02065
1.94	0.0122	1.00E+07	0.00166	0.019944
1.94	0.0137	1.00E+07	0.00162	0.019475
1.94	0.0151	1.00E+07	0.00159	0.019118
1.94	0.0167	1.00E+07	0.00158	0.018923
1.94	0.0181	1.00E+07	0.00156	0.018675
1.94	0.0198	1.00E+07	0.00155	0.018591
1.94	0.0231	1.00E+07	0.00153	0.018411
1.94	0.0262	1.00E+07	0.00152	0.018227
1.94	0.0295	1.00E+07	0.00151	0.018147
1.94	0.0334	1.00E+07	0.00151	0.018178
1.94	0.0348	1.00E+07	0.00148	0.0178
1.94	0.0392	1.00E+07	0.00150	0.017941
		Average Thickness:	0.00161	0.01935

Figure J.4 Meter 3, Paddle 2" x 4.5", Theoretical Experiments

Vo	Horiz Deform	Length	d/L	Angle	Calc Vel	Paddle Ht	P. Width	P. Area (sq in)	P.A. (sq ft)	Reynolds #	Drag Coef
0.17	0.02	0.75	0.027	1.53	0.192	2.00	6	12.00	0.083	2.62E+03	2
0.29	0.03	0.75	0.040	2.29	0.207	2.00	6	11.99	0.083	2.83E+03	2
0.48	0.04	0.75	0.053	3.05	0.231	2.00	6	11.98	0.083	3.14E+03	2
0.68	0.05	0.75	0.067	3.81	0.255	2.00	6	11.97	0.083	3.47E+03	2
0.88	0.06	0.75	0.080	4.57	0.279	1.99	6	11.96	0.083	3.80E+03	2
1.07	0.07	0.75	0.093	5.33	0.301	1.99	6	11.95	0.083	4.10E+03	2
1.28	0.08	0.75	0.107	6.09	0.326	1.99	6	11.93	0.083	4.43E+03	2
1.45	0.09	0.75	0.120	6.84	0.346	1.99	6	11.91	0.083	4.69E+03	2
1.66	0.1	0.75	0.133	7.59	0.369	1.98	6	11.89	0.083	5.00E+03	2
2.04	0.12	0.75	0.160	9.09	0.412	1.97	6	11.85	0.082	5.56E+03	2
2.38	0.14	0.75	0.187	10.57	0.449	1.97	6	11.80	0.082	6.03E+03	2
2.74	0.16	0.75	0.213	12.04	0.487	1.96	6	11.74	0.081	6.50E+03	2
3.14	0.18	0.75	0.240	13.50	0.528	1.94	6	11.67	0.081	7.01E+03	2
3.3	0.2	0.75	0.267	14.93	0.544	1.93	6	11.59	0.081	7.18E+03	2
3.74	0.22	0.75	0.293	16.35	0.587	1.92	6	11.51	0.080	7.70E+03	2

Figure J.5 Meter 3, Paddle 2" x 6", Theoretical Experiment

Water Density	Force(x) on Paddle	Mod of Elasticity	thickness (=ft)	t (inches)
1.94	0.0060	1.00E+07	0.00178	0.021302
1.94	0.0069	1.00E+07	0.00163	0.019559
1.94	0.0086	1.00E+07	0.00159	0.019082
1.94	0.0105	1.00E+07	0.00158	0.018934
1.94	0.0125	1.00E+07	0.00158	0.018914
1.94	0.0146	1.00E+07	0.00158	0.018914
1.94	0.0171	1.00E+07	0.00159	0.019052
1.94	0.0192	1.00E+07	0.00159	0.019037
1.94	0.0219	1.00E+07	0.00160	0.019208
1.94	0.0271	1.00E+07	0.00162	0.019407
1.94	0.0320	1.00E+07	0.00162	0.019492
1.94	0.0375	1.00E+07	0.00164	0.019651
1.94	0.0438	1.00E+07	0.00166	0.019905
1.94	0.0462	1.00E+07	0.00163	0.019565
1.94	0.0535	1.00E+07	0.00166	0.019898

Average Thickness: 0.00162 0.01946

Figure J.5 Meter 3, Paddle 2" x 6", Theoretical Experiment

REPORT DOCUMENTATION PAGE

Public reporting burden for this collection of information is estimated to average 1 hour per response, including the time for reviewing instructions, searching existing data sources, gathering and maintaining the data needed, and completing and reviewing the collection of information. Send comments regarding this burden estimate or any other aspect of this collection of information, including suggestions for reducing this burden, to Washington Headquarters Services, Directorate for Information Operations and Reports, 1215 Jefferson Davis Highway, Suite 1204, Arlington, VA 22202-4302, and to the Office of Management and Budget, Paperwork Reduction Project (0704-0188), Washington, DC 20503.

1. AGENCY USE ONLY *(Leave blank)*	2. REPORT DATE 12.May.00	3. REPORT TYPE AND DATES COVERED THESIS

4. TITLE AND SUBTITLE
APPLICATION OF STRAIN GAGE TECHNOLOGY IN LOW FLOW STREAM MONITORING

5. FUNDING NUMBERS

6. AUTHOR(S)
CAPT BOERMA KEVIN L

7. PERFORMING ORGANIZATION NAME(S) AND ADDRESS(ES)
UNIVERSITY OF ARIZONA

8. PERFORMING ORGANIZATION REPORT NUMBER

FY00-157

9. SPONSORING/MONITORING AGENCY NAME(S) AND ADDRESS(ES)
THE DEPARTMENT OF THE AIR FORCE
AFIT/CIA, BLDG 125
2950 P STREET
WPAFB OH 45433

10. SPONSORING/MONITORING AGENCY REPORT NUMBER

11. SUPPLEMENTARY NOTES

12a. DISTRIBUTION AVAILABILITY STATEMENT
Unlimited distribution
In Accordance With AFI 35-205/AFIT Sup 1

12b. DISTRIBUTION CODE

13. ABSTRACT *(Maximum 200 words)*

14. SUBJECT TERMS	15. NUMBER OF PAGES
	16. PRICE CODE

17. SECURITY CLASSIFICATION OF REPORT	18. SECURITY CLASSIFICATION OF THIS PAGE	19. SECURITY CLASSIFICATION OF ABSTRACT	20. LIMITATION OF ABSTRACT